SECOND INTERIM SUMMARY REPORT
LEAD TELLURIDE BONDING AND SEGMENTATION STUDY

Covering period
November 1, 1966 - July 31, 1967

Contract No. NAS 5-9149

Prepared by
Tyco Laboratories, Inc.
Bear Hill
Waltham, Massachusetts 02154

for

National Aeronautics and Space Administration
Goddard Space Flight Center
Greenbelt, Maryland 20771

Tyco Laboratories, Inc.
Bear Hill
Waltham, Massachusetts 02154

Lead Telluride Bonding and Segmentation Study

Second Interim Summary Report

Covering period
November 1, 1966 - July 31, 1967

Contract No. NAS 5-9149

by

H. Bates
F. Wald
M. Weinstein

for

National Aeronautics and Space Administration
Goddard Space Flight Center
Greenbelt, Maryland 20771

SUMMARY

I. CONSTITUTIONAL INVESTIGATIONS

The basic constitutional principles of the systems Co-PbTe, Co-Sn-Te, Re-PbTe and Re-SnTe are presented. This concludes the basic investigations of the chemical compatibility between lead and tin telluride and elemental metals. The information gained is summarized from a fundamental viewpoint, and a method of estimating the reactivity of alloys is suggested.

II. Bonding Studies

1. High quality surface finishes on W and 3P contact surfaces do not significantly improve initial contact resistances; however, close dimensional control is necessary.

2. Hydrogen annealing at 820°C improves the bonding performance of 3P to tungsten; treatment below 600° was not found to affect the oxygen content of 3P elements.

III. COUPLE DESIGN, PREPARATION, AND TESTING

1. PbTe couples (3N and 3P) have been successfully prepared for life testing by simultaneous bonding to a common W shoe.

2. Segmented Si-Ge-PbTe couples were designed and prepared; preliminary measurements of efficiency were made. At a hot junction temperature of approximately 800°C, the maximum efficiency achieved has been approximately 7.6%, and the maximum power output, 2.10 watts per couple.

IV. COUPLE TEST DEVICES

1. A sixteen-station life test device for testing PbTe couples under operational conditions of gradient and load has been designed and constructed.

2. A test device for measurements of efficiency and electrical characteristics of segmented couples has also been constructed.

V. LIFE TESTING

1. Results of an 800-hour gradient life test of W-bonded 3N and 3P elements indicate the main source of degradation to be an increase in the resistance of the P elements and a decrease in their Seebeck voltage. Decreases in the Seebeck voltage of both legs contribute most heavily to the initial degradation of power; however, the rate of degradation had decreased sharply by the 800-hour point.

2. A second gradient life test during this period of bonded and unbonded 3P elements has reached 2600 hours. The presence of water vapor in the system has caused substantial increases in the contact resistance of most of the bonded elements. Decreasing Seebeck voltage remains the main source of degradation of the unbonded elements and those bonded elements which have remained low in resistance.

3. Isothermal life tests of bonded 3P elements at 525°C for 1000, 2000, and 3000 hours have revealed substantial increases in element resistance. These tests also indicated that initial contact resistance is not a reliable indicator of the performance of the contact during testing and that differences between batches of 3P material can substantially affect the life of the elements and contacts.

4. Life testing of W-bonded 3N and 3P elements showed minor changes in 3N bonded elements at 600°C for 4700 hours, but 3P elements decreased in resistance and most electrodes were oxidized to the point of destruction of the bond.

CONTENTS

CONTENTS (Cont.)

LIST OF ILLUSTRATIONS

LIST OF ILLUSTRATIONS (Cont.)

LIST OF ILLUSTRATIONS (Cont.)

LIST OF TABLES

LIST OF TABLES (Cont.)

I. INTRODUCTION

The widespread use of thermoelectric power generation has been anticipated for some years as the solution to a number of specialized power-supply problems. However, two major materials problems have hindered the application of thermoelectrics. The first is associated with the bulk material. Because of the predominantly covalent nature of most thermoelectric alloys, they tend to be weak and brittle. The presence of doping agents severely limits the use of thermal fabrication by casting because of segregation of the dopants, and thus a majority of commercially available thermoelements have been produced by powder metallurgical techniques. However, pressed and sintered compacts are usually porous to some extent and contain oxides and other particulate inclusions. Forces within the compacting die cause variations in density through the compact which can lead to discontinuous grain growth during sintering. It is not unusual for the internal pores to contain gases which, if they include oxygen, can cause oxidation during service.

Compounded with these problems is the second major difficulty of making satisfactory electrical and thermal contact to the thermoelement. A number of different approaches have been taken to provide low resistance, stable contacts to thermoelements under varying conditions of temperature, etc. These can be divided generally into methods which maintain contact mechanically, as by spring-loading, and those which employ an integral electrode, usually metallurgically bonded. The former add considerable size and complexity to the module system, while the latter, although more elegant and efficient, are most severely troubled by problems of material incompatibility. Among the important requirements for a suitable electrode is that it not react with the elements to produce low-melting phases, etc.; that the metal not be electrically active if it diffuses into the element; that the coefficient of expansion of the metal approximates that of the semiconductor element; and that it form a strong, low-resistance bond to the element. Some advantages can be gained by the use of a suitable intermediate braze which, most importantly, can provide a gradation

in properties between electrode and element. Once again, however, there are similar restrictions on the braze material if it is to provide a satisfactory bond.

This program comprises a study of the bonding of PbTe thermoelements to nonmagnetic electrodes, studies of the behavior of the elements and contacts at operational temperatures, a fundamental study of the compatibility of PbTe and SnTe with metals, and study and measurement of the physical and chemical characteristics of the PbTe thermoelements. Other aspects of the program include a study of the segmenting of Si-Ge thermoelements with PbTe and the design and construction of a sixteen couple life test station and a single couple apparatus for measurement of segmented couples.

The general aim of the program is to define the most appropriate system and process for the preparation of low-resistance, high strength bonds of nonmagnetic electrodes to PbTe alloys and to study the factors and processes involved in the degradation of thermoelements and contacts during extended service.

II. CONSTITUTIONAL INVESTIGATIONS

A. Introduction

The final constitutional studies on systems of lead and tin telluride with metals were concerned with the gross definition of the Co-PbTe, Co-SnTe, Re-PbTe, and Re-SnTe system. Establishment of the main constitutional features of these systems, together with some rather cursory compatibility tests of Co-Sn-Te braze + PbSnTe-thermoelement + Metal (W, Fe, Mo, Re), mark the end of the basic compatibility studies between lead and tin telluride and metals under the present contract.

B. Experimental Studies and Constitution

1. Co-PbTe

From thermal analysis and microstructural studies supplemented by X-ray investigations, the phase diagram presented in Fig. 1 has evolved.

Thus, cobalt is found to be stable with lead telluride, and the eutectic between the two does not melt unduly low with respect to temperatures encountered in lead telluride-based thermoelectric generators. The main constitutional features are a eutectic on the lead telluride side (Figs. 2, 3 and 4) and a monotectic, which was not further investigated, on the Co side (Fig. 5). The system resembles that of PbTe-Fe very much, except for the appreciably smaller monotectic region which leads to a much flatter slope of the liquidus-line from the eutectic towards the cobalt side.

Influences of PbTe on the transformation of Co have not been investigated. Furthermore, the solid solubility of Co in PbTe was not measured. However, it is expected to be small, since X-ray spectra of PbTe-Co mixtures did not show any detectable line shifts for PbTe.

A small deviation from true pseudobinary behavior is suspected, just as in the PbTe-Fe system, on the strength of microscopic observations which showed third phase inclusions; also, considerable scatter of the thermal results for the eutectic temperature was observed.

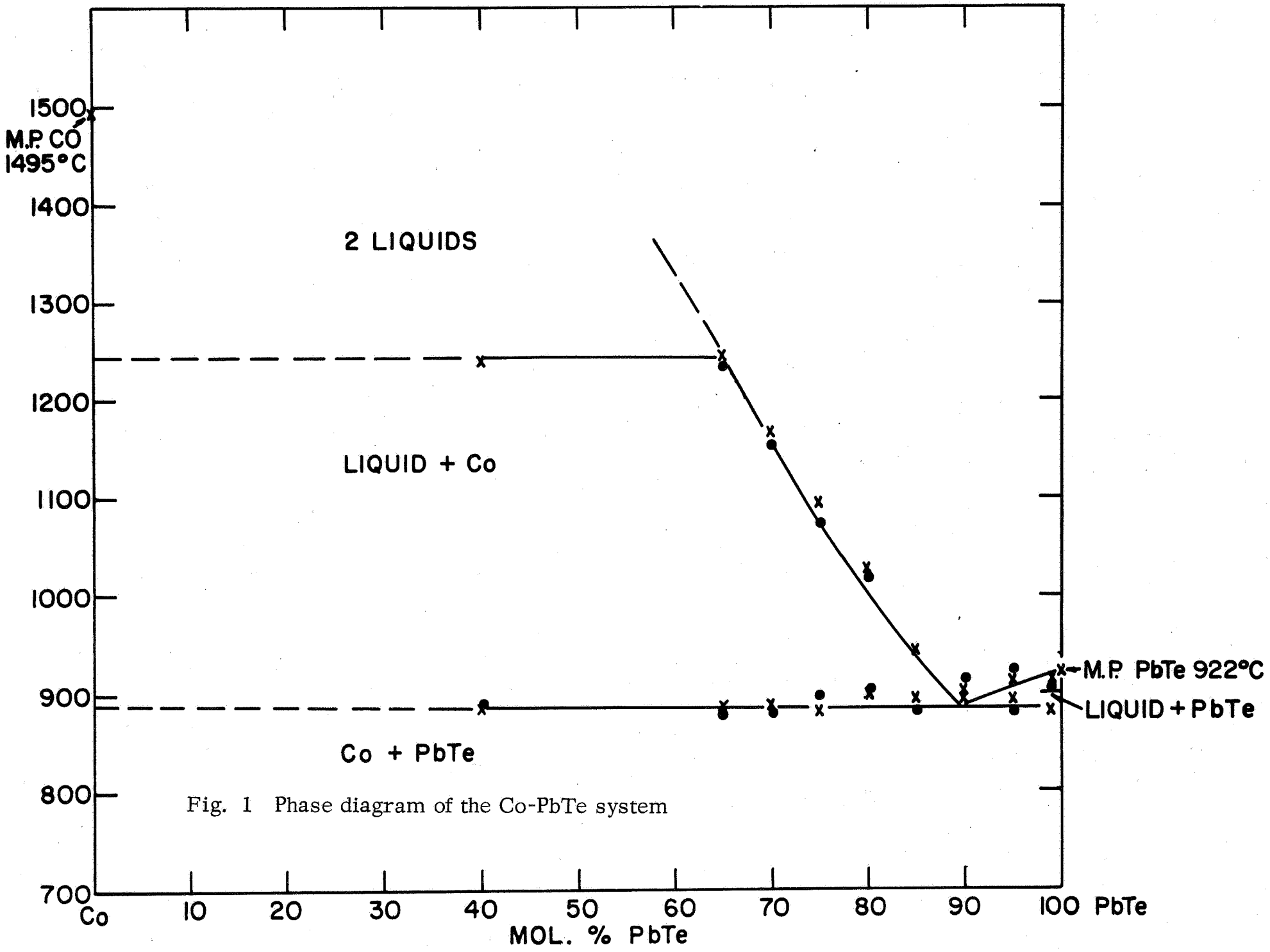

Fig. 1 Phase diagram of the Co-PbTe system

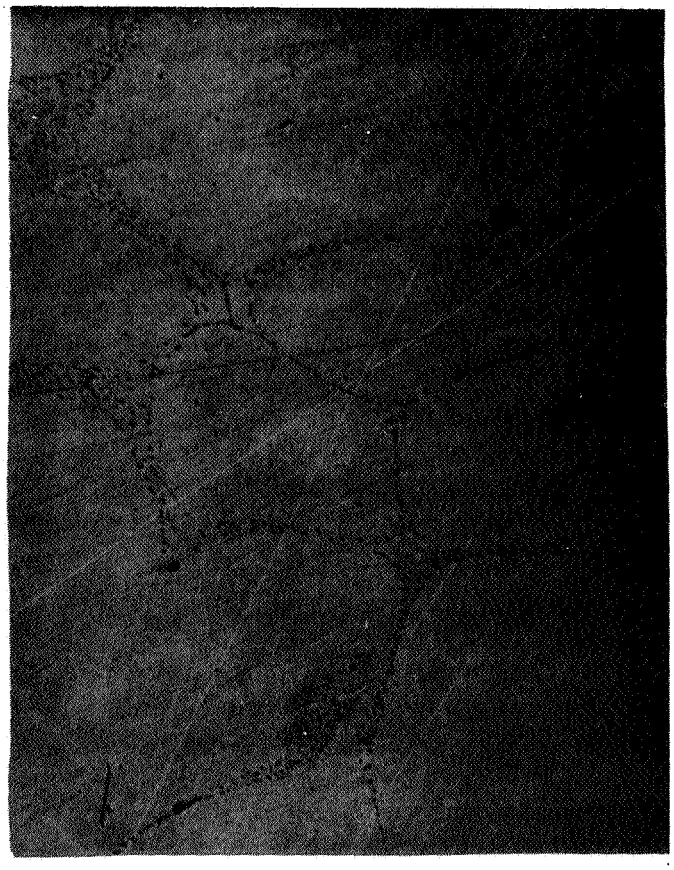

Fig. 2 99 mol % PbTe, 1 at % Co, as cast 350 X,
etched in dilute aqua regia,
primary crystals of PbTe + eutectic

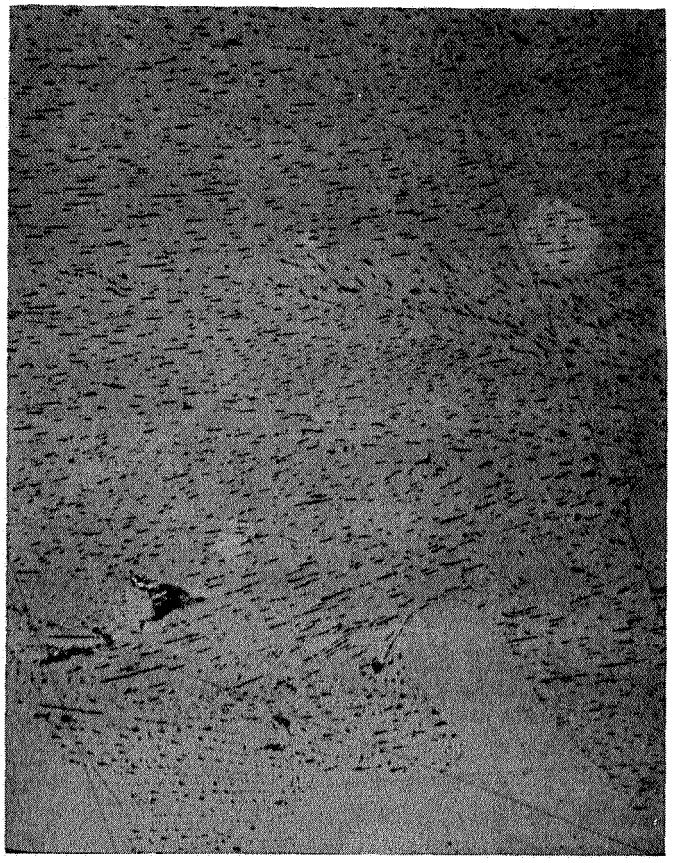

Fig. 3 90 mol % PbTe, 10 at % Co, as cast 250 X, etched in dilute aqua regia, almost completely eutectic structure, showing slight divorcement

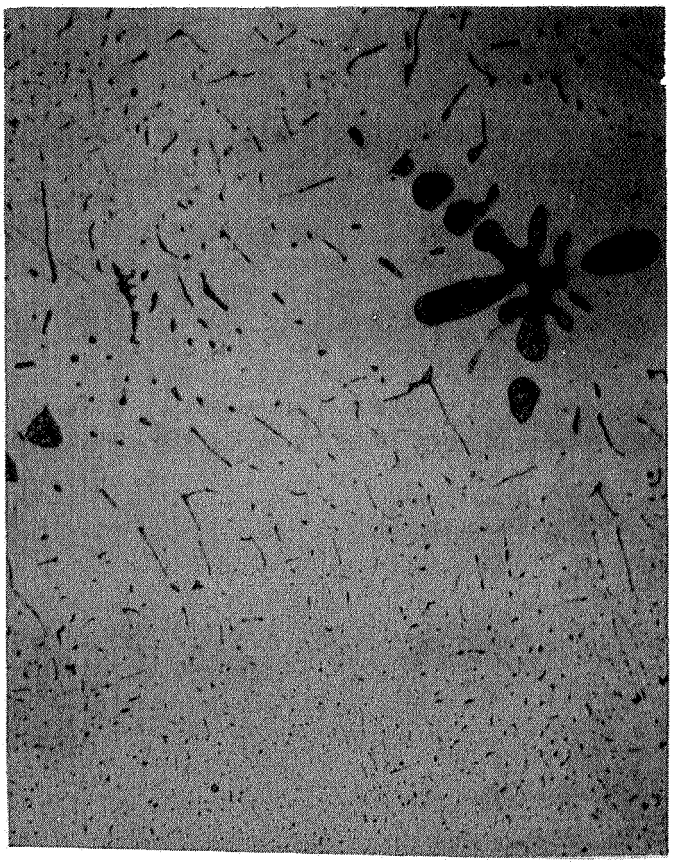

Fig. 4 75 mol % PbTe, 25 at % Co, as cast 250 X,
etched in dilute aqua regia,
primary crystals of Co in slightly divorced eutectic

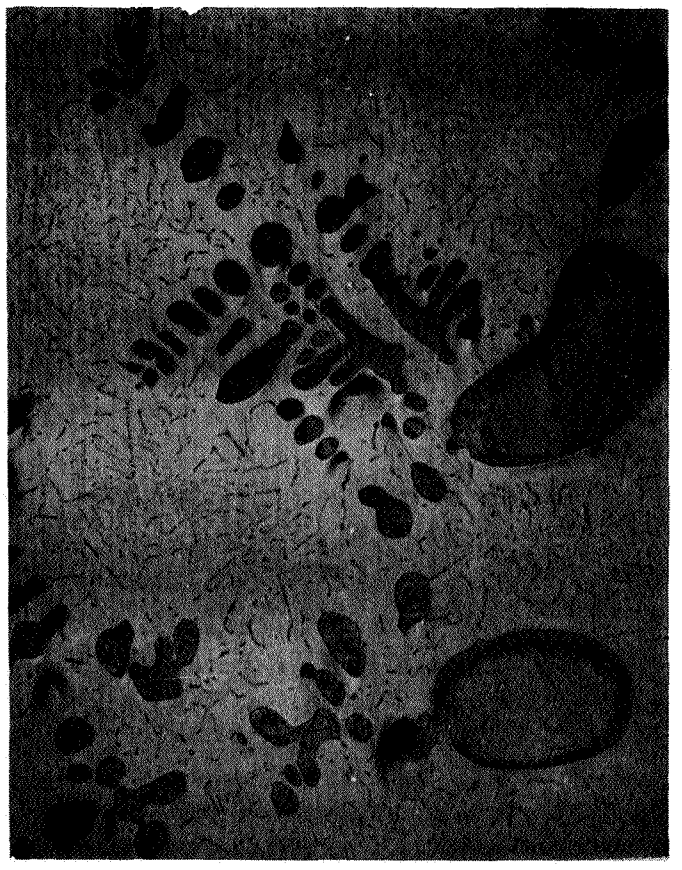

Fig. 5 40 mol % PbTe, 60 at % Co, as cast 300 X, etched in dilute aqua regia, monotectic globules and primary crystals of Co in divorced eutectic matrix

2. Co-SnTe

This system, which was first believed to be pseudobinary, must now be revised. Indeed, it proves to be of considerable complexity. So far, the pseudobinary systems CoTe-SnTe (Fig. 6) and Co_3Sn_2-SnTe (Fig. 7) have been identified, both of them being eutectic, with eutectic temperatures of 780° and 776°C respectively. Furthermore, it is believed that the Co_3Sn_2-CoTe system constitutes a solid solution series. However, it seems that at least some ordering or even compound formation must be assumed here, further complicating the whole matter. Nevertheless, all constituents seem to be metallic conductors or degenerate semiconductors, so that undesirable influences on the electrical properties of a junction containing Co are not to be expected.

Alloys lying on a line between SnTe and Co show two distinct sets of thermal effects. Between SnTe and the pseudobinary section Co_3Sn_2-CoTe, the terminal crystallization in all alloys occurs at 775°C with two more effects usually found at higher temperatures. Between Co_3Sn_2-CoTe and Co, a strong series of effects is found at 950°C, with some weaker ones at lower (750°C) or higher (1050°C) temperatures. Microstructures of alloys between SnTe and Co are shown in Figs. 8, 9 and 10.

The general outline of the ternary system as far as it can presently be deduced is shown in Fig. 11. More exact constitutional determinations, which are desirable, would have to start with a further elucidation of the binary constituent systems, since these are not yet completely investigated.

Nevertheless, it is obvious that Co reacts with SnTe and also that it would be, as far as its reaction products go, electrically neutral. Furthermore, the melting points of Co-Sn-Te alloys in certain concentration ranges possess values which are desirable for a brazing alloy for PbTe (PbTe-SnTe)-metal joints.

3. Re-PbTe

The lead telluride-rhenium system was investigated with three alloys. It is a degenerate eutectic system with a eutectic composition

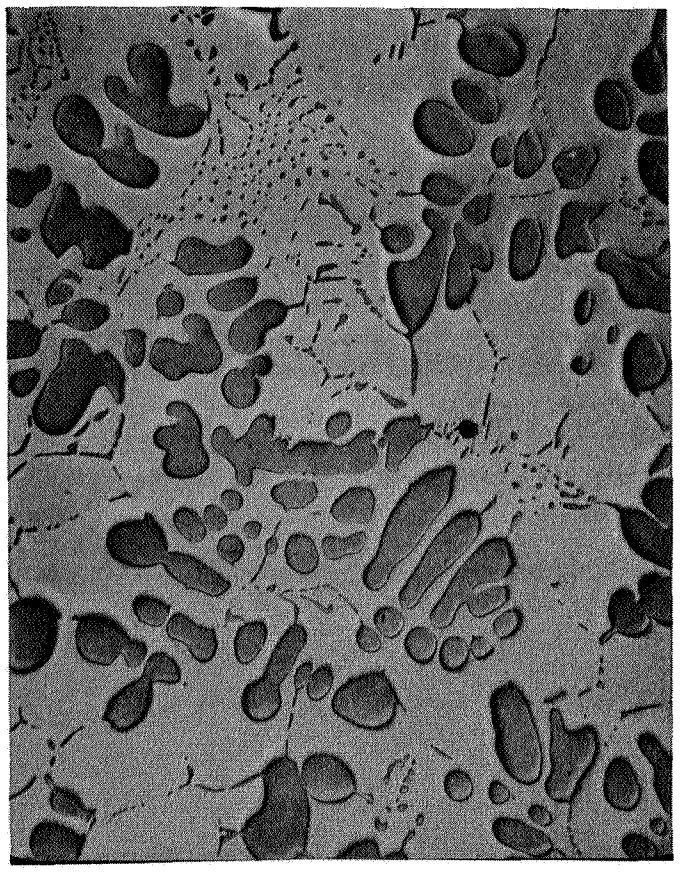

Fig. 6 75 mol % SnTe, 25 mol % CoTe, as cast 250 X,
etched in dilute aqua regia,
primary crystals in divorced eutectic matrix

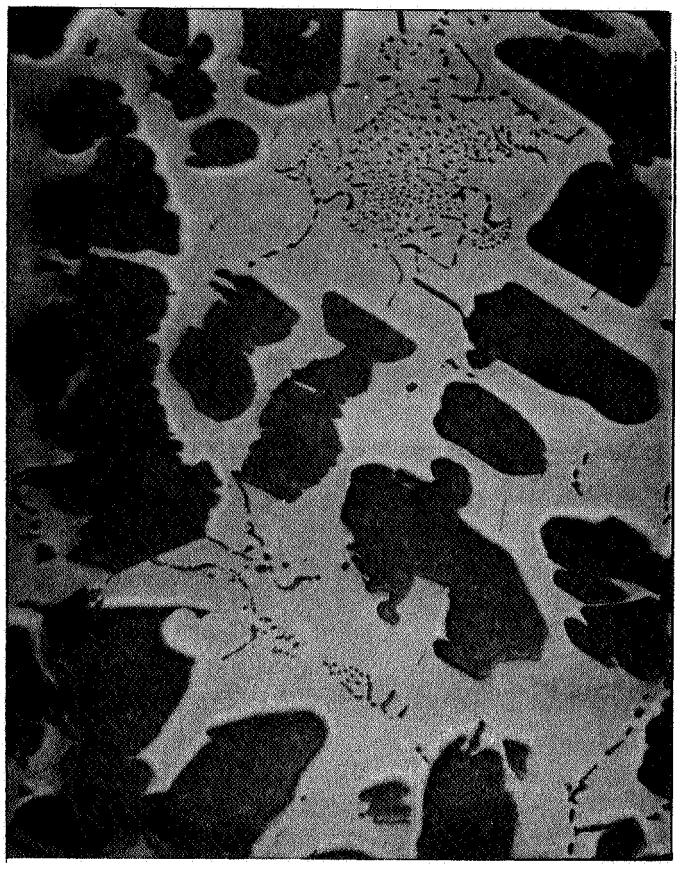

Fig. 7 75 mol % SnTe, 25 mol % Co_3Sn_2, as cast 250 X,
etched in dilute aqua regia,
primary crystals in divorced eutectic matrix

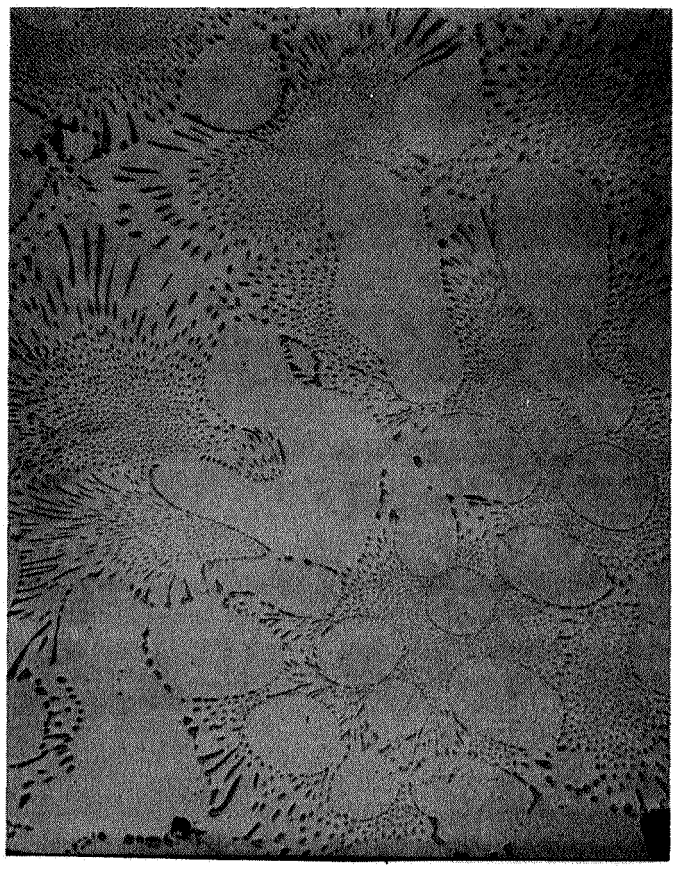

Fig. 8 90 mol % SnTe, 10 at % Co, as cast 250 X, etched in dilute aqua regia

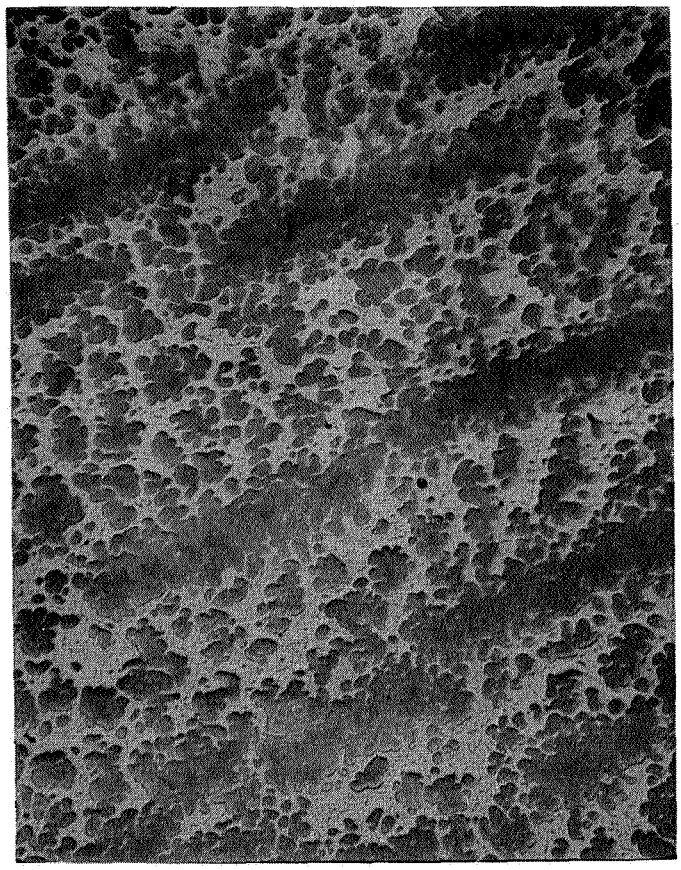

Fig. 9 45 mol % SnTe, 55 at % Co, as cast 250 X,
etched in dilute aqua regia,
Inhomogeneous solid solution is clearly visible

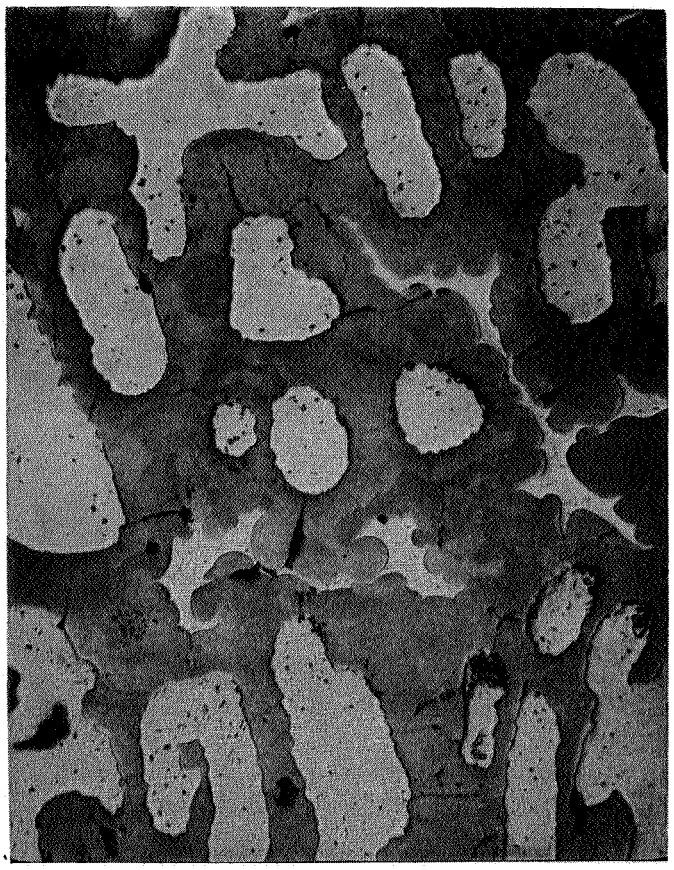

Fig. 10 20 mol % SnTe, 80 at % Co, as cast 250 X,
etched in dilute aqua regia,
Inhomogeneous solid solution is clearly visible

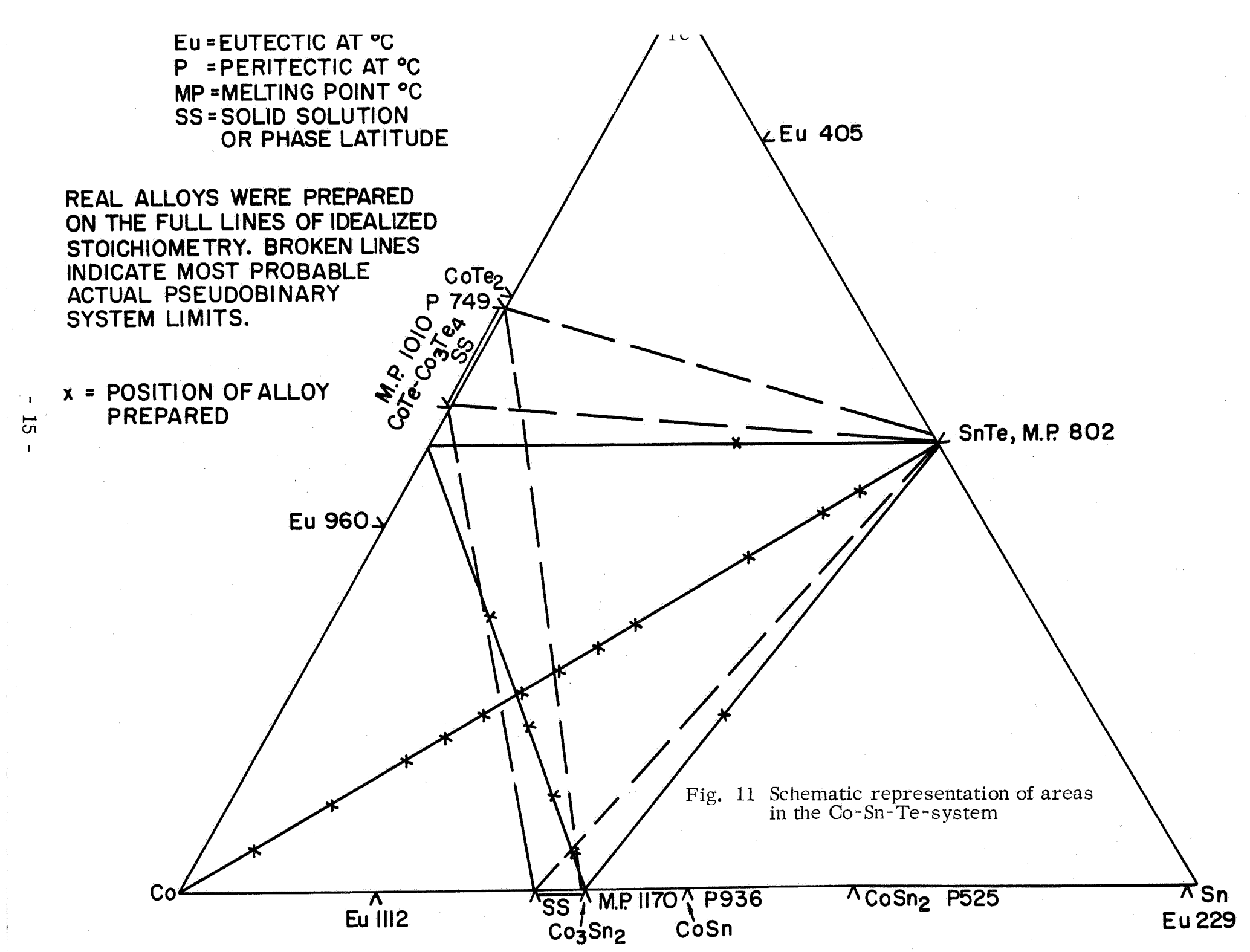

Fig. 11 Schematic representation of areas in the Co-Sn-Te-system

of less than 1 at % Re (Fig. 12). Furthermore, some globules of Re lead to the assumption that a monotectic reaction is also present in the system. The eutectic temperature was found at 919°C. No solubility of Re in PbTe could be detected.

4. Re-SnTe

This system, similar to that of Re-PbTe, appears as a degenerate eutectic (Fig. 13). The eutectic temperature was determined as 800°C. No solubility of Re in PbTe could be found, but monotectic behavior is quite likely here also.

5. The Use of Co-Sn-Te Alloys as Brazes for Thermoelectric Materials

Tin telluride itself was shown to be a quite effective brazing material for PbTe[1], but it had a number of disadvantages when used for PbSnTe. From the constitutional studies cited in II b, it seems that many of its disadvantages may be relieved by using alloys between SnTe and 10-40 at % Co as brazes. Such brazes consist basically of SnTe, CoTe, and Co_3Sn_2 although there may be solid solution or compound formation between the latter two. The alloys are nonmagnetic and have melting points falling into a desirable range for brazing.

It effectively wets Co, Fe, W, Re, and Mo, as well as PbTe and PbSnTe. No undesirable decreases in the solidus temperatures were noted in alloying trials of the above metals with the braze and thermoelectric materials. Although no actual brazing trials, electrical measurements, and life tests have been carried out, from a metallurgical standpoint this system constitutes one of the most promising possibilities at the present time.

C. Discussion

1. Estimation of Reactivity of Lead and Tin Telluride with Elemental Metals

In the First Interim Summary Report[2] on the present contract, it has been suggested that the reactivity of metals towards lead and tin

Fig. 12 95 mol % PbTe, 5 at % Re, as cast 250 X, etched in dilute aqua regia, partially dissolved piece of rhenium in lead telluride matrix

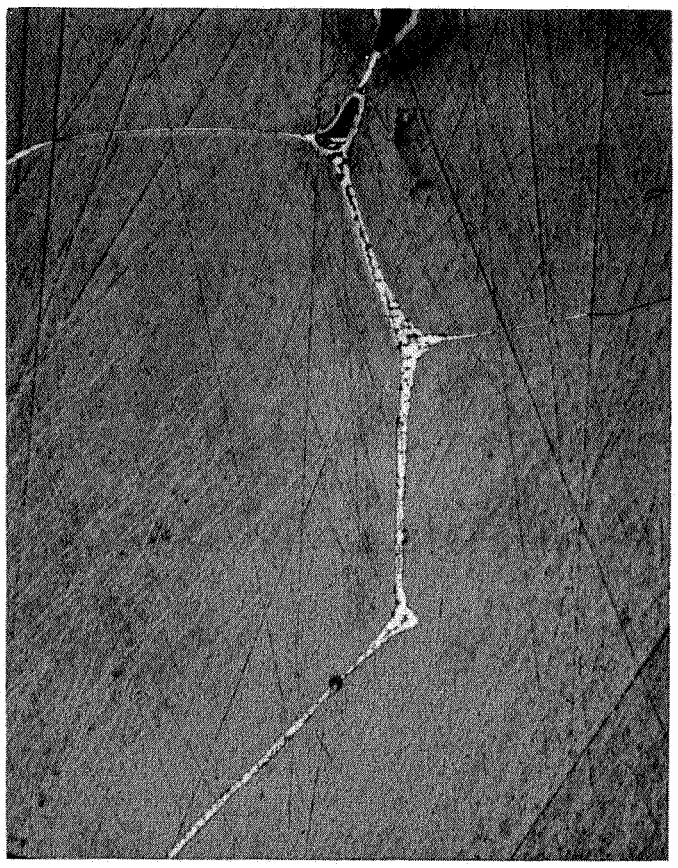

Fig. 13 90 mol % SnTe, 10 at % Re, as cast 250 X, etched in dilute aqua regia, degenerate SnTe-Re eutectic in the grain boundaries of SnTe

telluride may be estimated by comparing the heats of formation calculated from electronegativity differences.

The simplifying assumption used was to assign a valency of 2^- to Te, thus treating all compounds concerned as ionically bonded. The agreement of the estimated reactivities with those experimentally observed is remarkably good, despite the fact that it seems rather rash to treat most of the tellurides as ionic compounds, since it is well known that a large majority of them are more or less covalently bonded.

To recall all of the experimental findings[3], an outline of the periodic table is reproduced in which the border of the block of metals not reactive towards PbTe (and SnTe) is outlined (Table I). In addition, the electronegativities to be used for the present calculations are added. It is seen that the values for Cu, Ag, and Ni, as well as some other metals, have been adjusted from the previous table[2] in order to bring them in line with the experimental findings. This does not seem to be unreasonable, due to the fact that (a) these elements are situated on the right hand border of the reaction field, close to Te and (b) the bonding in their tellurides is rather peculiar. (Cu_2Te and Ag_2Te possess phase transformations at low temperatures, i. e. around 100-150°C with extreme transformation energies. NiTe-$NiTe_2$ is a continuous solid solution which changes from one structure to another.) Furthermore, we are still operating well within the spread of present day electronegativity estimation[4,5]. From the table as it now stands, one could predict that PbTe might be stable in the presence of Hg and Tl but SnTe would not. This point has not been tested.

Another point is that of the reactivity of Co, which does not react with PbTe but does with SnTe. First, it must be clear that metallic electronegativities of the same values as lead or tin constitute borderline cases. Secondly, in the case of Co, the reaction scheme is not straightforward. Coupled with the reaction

$$Co + SnTe \rightarrow CoTe + Sn$$

TABLE I

Elements Investigated for their Reactions with Lead and Tin Telluride Together with their Assigned Electronegativities.

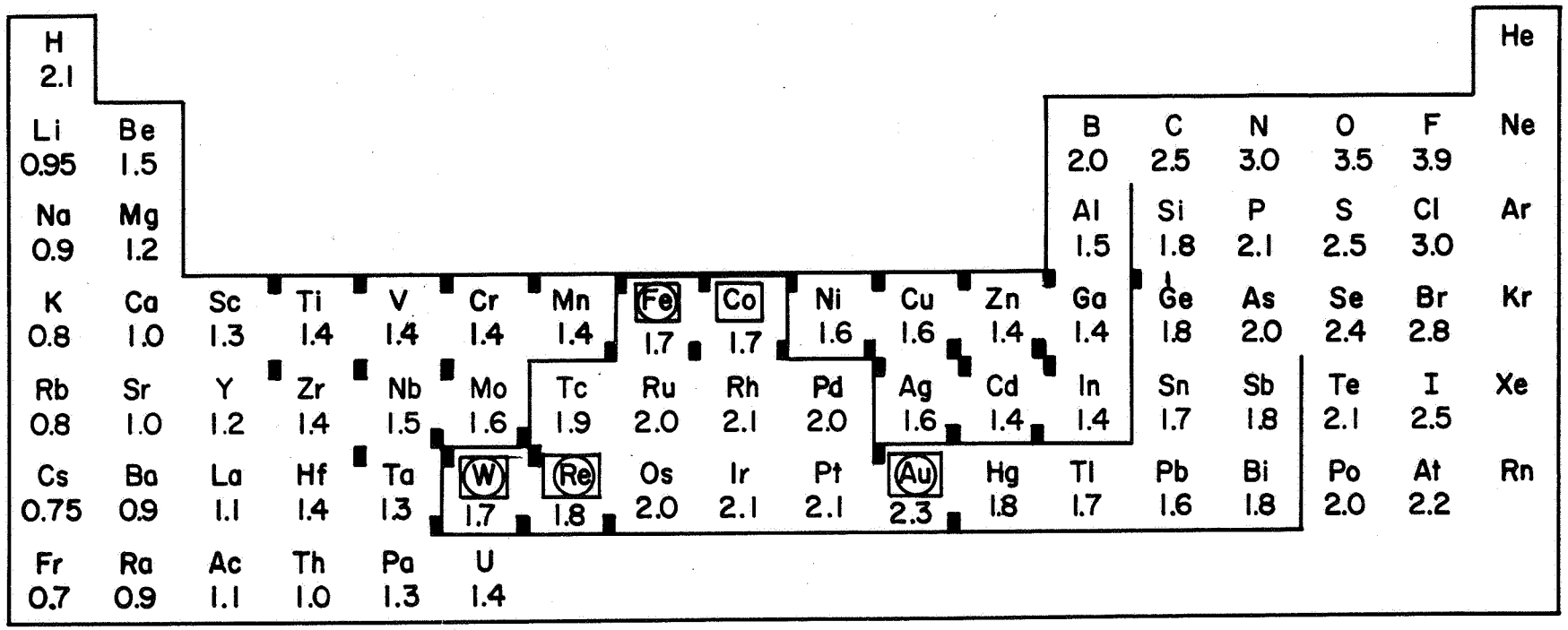

= Investigated with PbTe

= Investigated with SnTe

= Did not react with PbTe

= Did not react with SnTe

= Elements which should not react are inside box

is the second reaction: $Sn + 1\ 1/2\ Co \rightarrow 1/2\ Co_3Sn_2$

where Co_3Sn_2 contributes a heat of formation of 2.7 kcal/g atom[6], quite enough to tip the balance. This latter consideration applies equally to ternary compound formation and even to solid solution formation, if the heat of solution is so large as to be a deciding factor. The latter may well be the case in the Ag_2Te-PbTe system[7] where one finds relatively strong thermal effects at the eutectoidal temperature.

In conclusion, one might well say that considering all sources of error such as uncertainty in the estimation of the electronegativity, neglect of entropy changes, secondary reactions, assumption of ionic behavior of all tellurides concerned (with Te^{2-}), the simplified method of estimation presented here is remarkably accurate.

2. Estimation of the Reactivity Alloys

A useful and necessary extension of the method should be to estimate the reactivity of alloys in order to provide sensible guidelines for selection of these. However, it is necessary to introduce some further assumptions here, increasing the sources of error. These are as follows:

(a) Activity is equal to mole fraction.
(b) Heat of solution is zero.

It is believed that neglect in the case of these two factors is justified, particularly if one deals with homogeneous solid solution alloys which constitute the major group of engineering alloys.

As an example, estimations of the reactivity of three commercial alloys are carried out. First the heats of formation of the various compounds involved are calculated according to:

$$\Delta H\ (calc) = 23.7 \times (E_M - 2.1)^2/N\ kcal/g\ atom$$

where x = number of bonds broken, E_M = Electronegativity of Metal according to Table I, and N = Number of atoms in the compound. (The number of bonds broken equals 2 for every Te-atom in the Formula, an original assumption.) (2. 1 is the electronegativity of Te from Table I).

From the total contribution of each constituent to a heat of reaction of the respective tellurides, it has to be concluded that only 347 stainless steel would be nonreactive towards PbTe; for the other two alloys, reaction is predicted (Table II).

These results are presented as examples for the reaction calculations and the use of the concepts given. Experimental verification of the reaction behavior of three alloys was not tried as yet.

D. Conclusions

1. Introduction

The thoughts to be presented in this section are not merely specialized conclusions arising from the previously discussed experimentation. It is felt that a general discussion of the subject of compatibility is in order here so that the cited investigations be put in the proper perspective.

2. Materials Compatibility

Compatibility is a favored term at the present time, not only in thermoelectrics. But, despite this fact, it is a term of rather varied meanings and uses. Therefore, the possibilities for misunderstanding the term are numerous.

In thermoelectrics and, more particularly, in junction terminology, a compatible system is defined as a system which does not cause undue changes in the electrical properties over a specified period of time. This, to a systems user, is quite meaningful. To an engineering researcher who is trying to find the causes for undue changes in electrical properties, it is utterly meaningless. For instance, the information that a certain metallic alloy in contact with a commercial lead telluride degrades electrical properties of the latter to a serious degree affords no means of rectifying the fault or even knowing what causes it.

Heats of Formation Calculated from Electronegativities

We obtain:	ΔH (calc.) kcal/g atom		AH (calc.)
$Si + Te_2 \rightarrow SiTe_2$	2.75	Ta + Te → TaTe	11.30
Fe+Te → FeTe	3.69	Ti + Te → TiTe	11.30
Ni+Te → NiTe	5.77		
Pb+Te → PbTe	5.77		
$Mo+Te_2 \rightarrow MoTe_2$	7.69		
Mn+Te → MnTe	11.30		
Cr+Te → CrTe	11.30		

The three materials selected are 347 stainless steel, 329 stainless steel and incoloy 901
Their compositions (nominal) in weight % and atom fractions are as follows:

347 Stainless Steel	Fe	Mn	Si	Cr	Ni	Mo	Ta	Ti	C
wt%	63.92	2.00	1.00	19.00	13.00	--	1.00	--	0.08
atom fraction	0.6307	0.0198	0.0198	0.2012	0.1218	--	0.003	--	0.004
Contribution to ΔH reaction XTe kcal (calc)	2.33	0.22	0.05	2.27	0.70	--	0.03	--	

Total 5.60 kcal/g atom

Incoloy 901									
wt%	37.45	0.5	0.5	13.00	40.00	6.00	--	2.5	0.05
atom fraction	0.3839	0.0050	0.0100	0.1430	0.3890	0.0360	--	0.0297	0.002
Contribution to ΔH reaction XTe kcal (calc)	1.42	0.06	0.03	1.62	2.24	0.28	--	0.34	

Total 5.99 kcal/ g atom

329 Stainless Steel									
wt%	64.58	0.6	0.5	27.50	4.50	2.25	--	--	0.07
atom fraction	0.6142	0.0058	0.0100	0.3146	0.0409	0.0122	--	--	0.0026
Contribution to ΔH reaction XTe kcal (calc)	2.27	0.07	0.03	3.55	0.24	0.09	--	--	

Total 6.25 kcal/ g atom

Therefore, from a basic materials viewpoint, different criteria for the selection of contacting alloys or other materials of construction in contact with lead telluride or its vapor have to be found. These criteria have been stated in detail already by Fritts in 1959[8]; it is rather difficult to improve on his clear expressions of the physical function of the electrodes, as well as the chemical criteria to be met by it.

He comes to the conclusion that, "In practice, the necessity of using a chemically stable electrode is the most difficult condition to satisfy." He then goes on to cite the five major forms of chemical interaction to be concerned about:

(1) Alloying and formation of low melting eutectic.
(2) Diffusion under formation of a second phase of high conductivity thus short circuiting the element.
(3) Reaction between electrode and thermoelectric material.
(4) Diffusion of electrode material into the thermoelectric material, altering the doping level.
(5) Diffusion of dopant out of the thermoelectric material, altering the doping level.

For each of these mechanisms, some examples are cited. (Some of these examples are in error, but that does not distract from the truth of the basic statements!) For others, remedies are given. Furthermore, it is clearly stated that although all of these interactions are dangerous, some are so time- and temperature-dependent that in specific systems they may practically not be very important. With respect to (3.)-reaction-, it is stated that thermochemical data can be used to predict such reactivity by considering the relative free energy changes of the reactions involved.

Unfortunately, the free energies or any other thermochemical properties of the materials of concern here are not readily available. Thus, the investigation, reported in conclusion here, was designed to fill this gap in the shortest possible time and by the most efficient method possible.

3. Phase Equilibrium Investigations and Compatibility

Considering the aforementioned problem, it becomes quite clear that measurements concerning the thermodynamic properties of all the metals and alloys potentially involved in the construction of thermoelectric systems, as well as their tellurides, plumbides and stannides would be a substantial undertaking.

Therefore, a program of abbreviated phase equilibrium investigations which, hopefully, could be generalized in the end, was considered a reasonable solution to the problem.

It should be recognized here that, after all, phase diagrams are consequences of thermodynamic behavior and that they furthermore can yield accurate and quantitative thermodynamic information[9, 10, 11, 12], which in the present case is not even required.

Furthermore, in the course of the investigations, it becomes apparent whether low melting eutectics form (point 1 of Fritts) or whether material diffuses into the thermoelectric material (point 2).

Additional factors are that phases formed can be identified by microscopy, X-ray or microprobe investigations. Thus, if formed in an actual junction they can be recognized in post-mortem tests. Finally, at least a qualitative feeling is usually acquired regarding the speeds of the reactions investigated.

Thus, phase investigations contribute substantially towards solving problems of compatibility associated with eutectic formation, second phase formation and reaction. Such investigations do not provide information on whether a eutectic of a specific melting point, a second phase with particular properties, or a certain thickness of reaction layer is tolerable. Such decisions have to be made from case to case, considering operating parameters, electrical specifications, and use of each thermoelectric system.

Another point to be stressed is that phase investigations a priori do not concern themselves with the degradation mechanisms cited under 4 and 5. Although solid solubility may be detected, electrical influences are not investigated in the normal cases of phase investigation. Indeed,

solubilities of the order of doping concentrations may not even be detected by the usual methods. Thus, phase investigations are only one facet, albeit an important one, of compatibility.

4. Practical Compatibility Testing

If complex alloys are used as conductors and equally complex material formulations as thermoelectric elements, the establishing of particular phase equilibria may be time consuming and tedious. Thus, "poisoning" investigations using mixtures of thermoelectric powders with the respective metal powders have been used in screening type compatibility testing.

It is suggested that this method is grossly misleading, and of no real use.

First, this method and its results are extremely dependent on the amounts used (volume fractions) and the grain sizes of the powders mixed. Furthermore, the method is dependent on the type of reaction mechanism operative in a specific case. It may produce results which are erroneous in both directions in that it may find perfectly acceptable materials incompatible and unacceptable materials compatible.

A few thought experiments may demonstrate this. It is well known that homogeneous mixing of powders is difficult. Thus, if the metal in the thermoelectric material is segregated such as to form a conductive path, the material will be short circuited and the thermoelectric properties may entirely disappear. The metal does not have to react or diffuse at all in such a case. This situation gets worse if increased temperatures are applied and grain boundary eutectics can form. In an investigation in this laboratory concerning gold and lead telluride, it was found that employing 2-4 at % Au and heating it above the eutectic PbTe-Au temperature, caused all grain boundaries to be filled with metallic conducting Au-PbTe, thus short circuiting the PbTe effectively. The Seebeck coefficient decreased to very low values and the electrical conductivity to high ones as a consequence of this. Therefore, although Au is perfectly safe to use with PbTe (no reaction, no

electrically effective diffusion!) only a decrease of Au concentrations below 1% for the grain size used could prove this fact, since no influence on the electrical properties was found either by annealing in the solid state or above the eutectic temperature.

On the other hand, this same concentration of metal, (1%) reacting to a high resistance telluride would have only minimal influences on the thermoelectric properties of the powder compact, since most conduction would occur through the PbTe. A planar layer of such a high resistance telluride deposited in the junction would, however, be quite disastrous.

Therefore, it is suggested that a normal diffusion couple arrangement is much more advantageous. Such arrangements are widely used in metallurgy to study complex phase interactions initially. Besides, this configuration is close to the working configuration. A diffusion couple will yield more information in the same time as the powder mixture does and will yield it more reproducibly. This has been proven by the many experiments where isothermal testing of actual junctions was conducted.

Sectioning of a diffusion couple will yield information on the phases formed and the soundness of the junction, i.e. Kirkendall effect, mechanical cracking, etc. Electrical measurements will yield the actual resistance. Hot probe Seebeck measurements will give qualitative information on the electrical homogeneity of the junction material. After removing the junction components, Seebeck output measurements vs. temperature with an increasing temperature gradient will reveal changes of carrier concentration in the thermoelectric material. The latter method is particularly effective if the thermoelectric material which has been adjacent to the junction is made the hot side in one measurement of total Seebeck output and the cold side in another one. Also, electron microprobe analysis can be employed to reveal the chemical composition of the phases formed, if these cannot be identified by comparison with microphotographs obtained from phase equilibrium investigations.

Thus, it seems that the diffusion couple method now used by some investigators should be the sole method of compatibility testing. The method of mixing powders should not be used nor should the results of that method be made the basis for decisions of compatibility between metals and thermoelectric materials.

III. BONDING STUDIES

Experimental bonding studies have been concentrated mainly with improving the contact resistance of bonds between 3P PbSnTe thermoelements and tungsten. The effects of high quality surface finish of electrodes and elements were studied. These studies were an integral part of the definition of a suitable process for simultaneous bonding of p and n legs to a common W strap.

A. Surface Finish Effect on Bonding

Six runs were made using tungsten electrodes lapped to dimensional tolerances of 0.0001 inch parallelism of faces and 0.001 perpendicularity of faces and sides. The contact surfaces were lapped to a one micro inch (rms) finish. Two of the six runs were made with both electrode and element contact surfaces lapped to 1 micro inch.

The elements in the other four runs were lapped to an 1800 grit surface (approximately 50 micro inches rms). The first column of Table III lists the average results of these six runs. The second column shows the results of three runs made under identical conditions in which both element and electrode surfaces were lapped to 1800 grit. The third column lists the results of six runs made with electrodes which were precision-lapped and subsequently lapped to give an 1800 grit contact surface prior to bonding. The element contact surfaces were also lapped to 1800 grit.

Comparison of the results of these bonding trials in Table III indicates clearly that insignificant improvement is made in the effectiveness of the bonding process when high quality surfaces are provided on the electrodes and elements. It is, however, important that the gross flatness of the contact surfaces be maintained within limits of the order of 0.0001 inches.

TABLE III

Summary of Results of Bonding Runs with Varying Contact Surface Finishes

Surface Preparation	Elements and Electrodes Precision Finished	Elements and Electrodes 1800 grit	Elements 1800 grit Electrodes Finished and 1800 grit
No. of elements	53	27	51
No. bonds	86	54	86
% bonded	81	100	95
Ov'l. ave. C. R.	229	250	152
No. < 100 $\mu\Omega$	41	44	45
%	38	81	50
Ave. C. R.	69	56	79
No. < 60 $\mu\Omega$	14	31	9
%	13	57	10
Ave. C. R.	39	50	57

B. Hydrogen Treatment of 3P Elements

To test the possibility of reducing the oxygen content of 3P elements, a group of elements was hydrogen annealed just prior to bonding. Nine elements were held for twelve hours at 550°C in flowing hydrogen. Two elements were sealed in an evacuated ampoule, as were two untreated elements of the same lot, and sent for oxygen analysis. Results of the oxygen analysis indicated no effect of the hydrogen anneal on the oxygen

content. The average oxygen content of the untreated elements was 380 ppm; of the treated elements, 390 ppm. This indicates that the oxygen present is not lead oxide (PbO), which should be readily reduced by hydrogen at 550°C. Tin oxide (SnO_2) and tellurium oxide (TeO_2) should be only slightly reduced under these conditions, and MnO not at all.

The conditions of the oxygen measurement technique – carbon saturated Cu-Ni bath at 1250°C – are such that tin and tellurium oxide(s) would be easily reduced; however, MnO would be only very slightly reduced. Since our values for the oxygen content are in agreement with those found by other investigators using neutron activation analysis[13], it would appear that the major part of the oxygen present is not associated with Mn. This is also borne out by the fact that the average total Mn content is several times the average oxygen content. Thus, it seems that the largest part of the oxygen content of 3P material is probably associated with tin and/or tellurium. In this case, appreciable reduction of the oxygen level could be achieved by hydrogen treatment in the vicinity of 700-800°C. Time of treatment in this temperature range must be balanced against the possibility of substantial loss of material by evaporation. Investigators at Westinghouse[14] found substantial decreases in oxygen content of 3P material with hydrogen treatment "above 600°C."

The results of bonding to the hydrogen-treated elements were more or less normal. Seven contacts (50%) were below 100 $\mu\Omega$; their average was 78 $\mu\Omega$. The over-all average for nine bonds was 155 $\mu\Omega$.

In the course of establishing the conditions for bonding of couples, some p-type legs, which had failed to bond satisfactorily, were re-run Their contact resistances improved after the second processing. The n-type legs which were also re-run did not bond at all. From these results it was inferred that a pre-treatment of the p-type elements and subsequent simultaneous bonding of both types would yield the best results. P-type elements were run in the bonding jig for 45 minutes at 825°-830°C in hydrogen. The contact surfaces were relapped and the two types of elements

were bonded at the same time. The first run in which this was done gave an average p-type contact resistance of 40μ ohm for all eight contacts. The average n-type contact resistance was 70 μ ohm, with six out of the eight below 100μ ohm, and an average resistance of 60$\mu\Omega$.

This indicates that high temperature treatment of the 3P material in hydrogen is beneficial to the tungsten diffusion bonding process. Measurements of the oxygen content of elements treated in hydrogen at 825° have not been made yet.

C. Plasma Spraying of W on 3P

An initial evaluation was made of an alternative process for W bonding to PbTe materials. The plasma spraying process consists of injecting metal powder into a jet of ionized inert gas (the plasma). The metal particles are melted in the extremely high temperature plasma and propelled at high velocity against the surface to be metallized, where they solidify in a dense deposit. This process appeared to be a possible method of applying thin tungsten electrodes directly to the thermoelectric elements. It was anticipated that the molten W droplets might literally "bore" their way into the PbTe by locally melting and evaporating the PbTe. This would then yield a structure in which the W would be locked into the bulk material of the element.

Five 3P elements were plasma sprayed with tungsten on the end faces by an outside firm (Metco, Inc., Westbury, L. I., New York). The elements were all more or less badly cracked due to thermal shock. This made a reliable measurement of contact resistance difficult; however, measurements on two specimens indicated (local) contact resistances of a very low order, probably about 10$\mu\Omega$-cm^2.

Photomicrographs are shown of the tungsten deposit (Fig. 14) and interfaces between the W and 3P material (Figs. 15 and 16). These initial findings indicate that further exploration of this technique of contacting PbTe materials is worthwhile. The initial process conditions would seem to require careful preheating of the elements to 300°-400°C and some variation in the plasma temperature so that greater penetration of the initial layers of tungsten particles might be achieved.

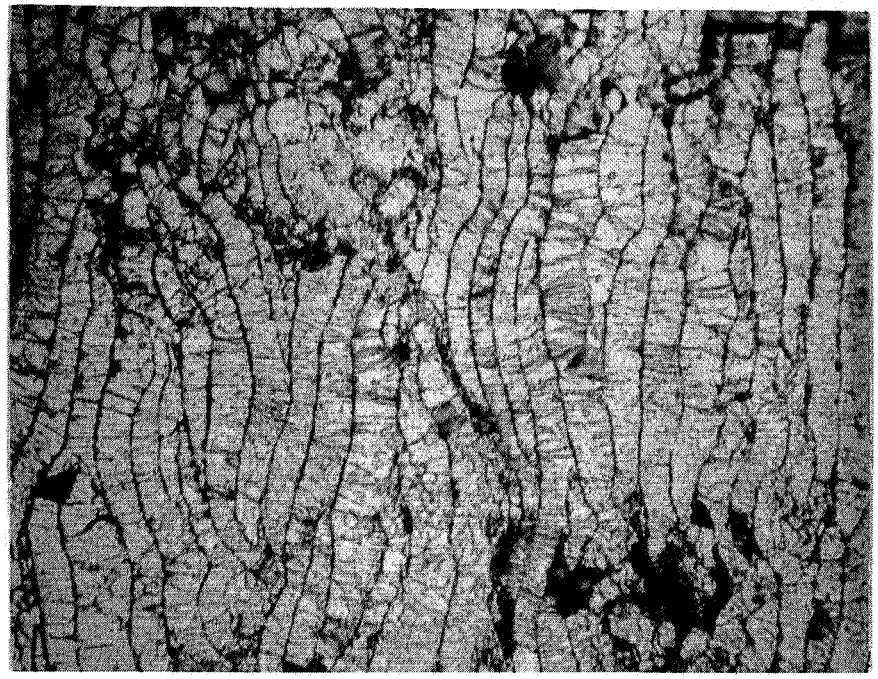

Fig. 14 Plasma-sprayed tungsten. Spraying direction from left to right. Dilute Murikami etchant. 750 X

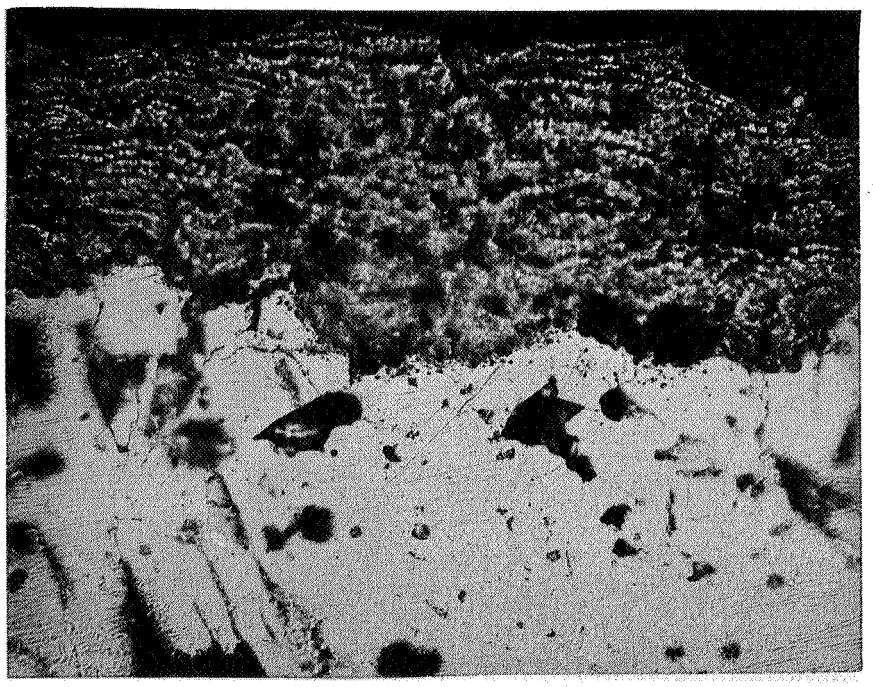

(a)

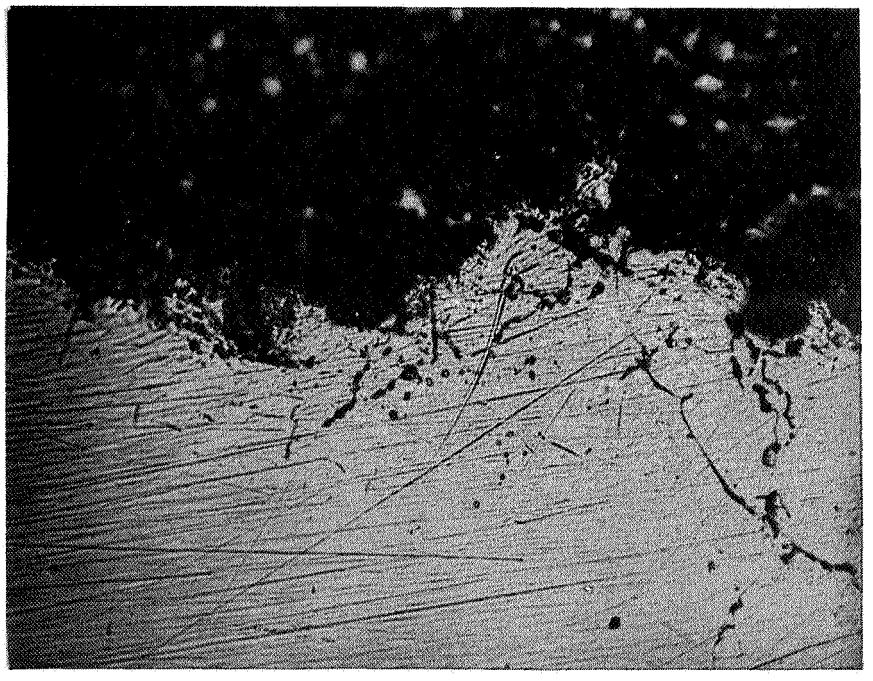

(b)

Fig. 15 Interface of plasma-sprayed W with 3P PbSnTe. Tungsten at top.
a. 250 X b. 750 X

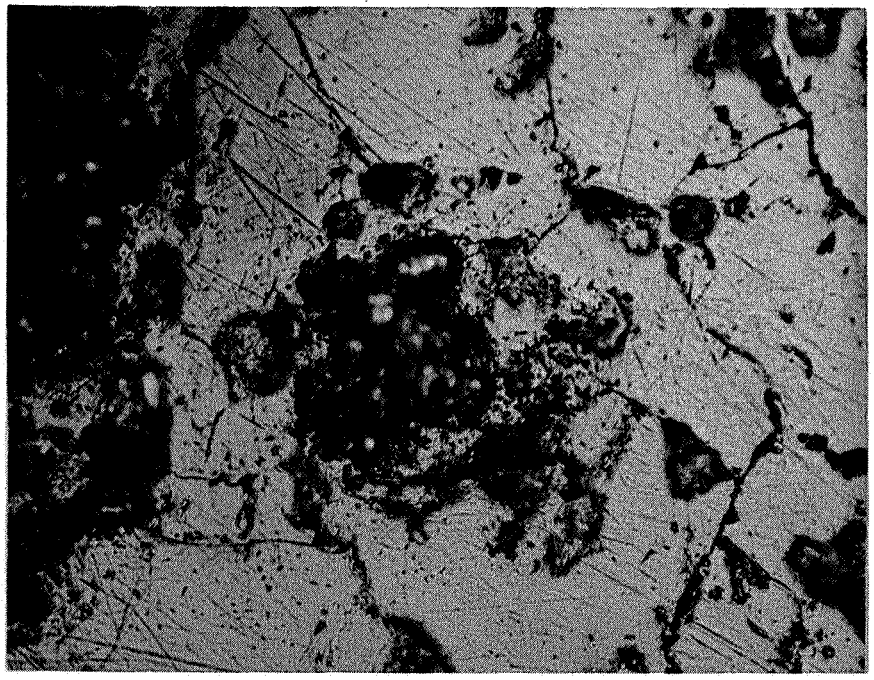

Fig. 16 Plasma-sprayed tungsten imbedded in 3P. Junction was sectioned at a slight angle from the plane of the junction. 750 X

D. The Tungsten Diffusion Bond

Microprobing of the W-PbTe junction of a Si-Ge-PbTe element revealed an interesting piece of information. X-ray photographs of the bond region showed significant interpenetration of W and Pb over a region approximately 2 microns or more wide. In this region Te is essentially completely absent. These photographs are shown in Fig. 17. The center line (vertical line with small divisions) coincides with the edge of the W electrode. The major divisions (each square) represent 10 microns. This evidence lends some support to the hypothesis that the bond is actually comprised of a Pb-W-O compound.

Several other junctions of 3N and 3P elements with tungsten have been prepared for examination by a similar technique and also by direct examination for oxygen. Results of these investigation have not yet been received, however.

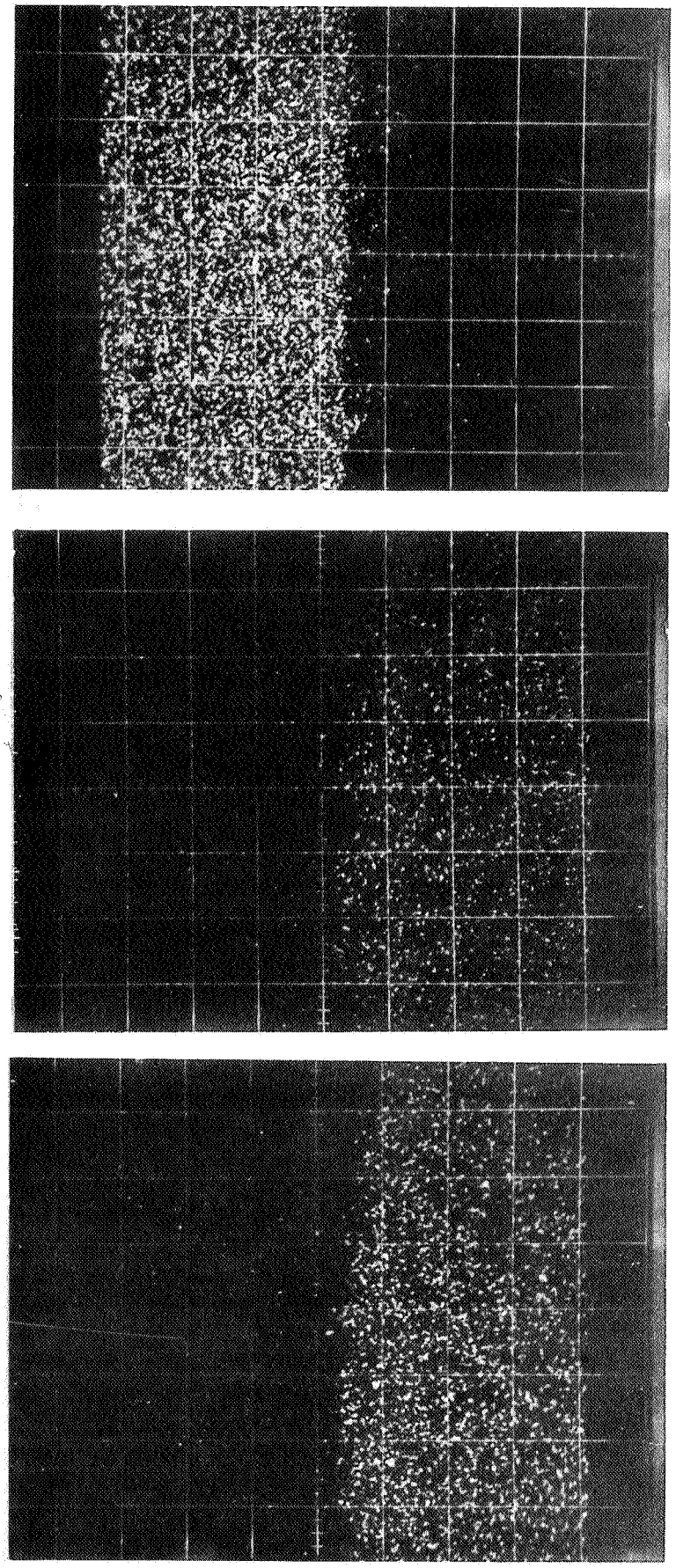

Fig. 17 X-ray photographs of W - 3N junction. Top - W, middle - Pb, bottom - Te. Major divisions, 10 microns.

IV. COUPLE DESIGN, PREPARATION, AND TESTING

Two types of couples have been designed. One is comprised solely of PbTe alloys (3N and 3P); the other is a segmented Si-Ge-PbTe couple. Optimization techniques have been applied to both couple designs to yield maximum efficiency. While this is not particularly important for the PbTe couples which are to be life-tested under operational conditions, the segmented couples are to be used for measurements of conversion efficiency. Thus it is important to design them properly in order that predictions of increased efficiency from segmenting may be tested.

A. 1. Segmented Si-Ge-PbTe Couples

The questions of the efficiency benefits of segmenting have been dealt with at length Swanson, Somers, and Heikes[15]; Ure and Heikes[16]; Moore[17]; and others. Ure and Heikes demonstrate that the efficiency of a segmented generator can never be greater than a cascaded device of the same materials operating over the same temperature intervals. The main problem in calculating the theoretical efficiency of segmented generators and in optimizing their design is the variation in properties between segments. In order to achieve optimum efficiency for the entire generator, it is necessary that the current flowing in each segment be optimum for the segment. This condition is not likely to be realized in general, unless the materials are quite similar in properties. A complete and exact solution to achieve the optimum shape ratios is a complex problem requiring the use of machine computation. It is necessary to achieve optimum balance between heat and current flow, and in the case of large discontinuities between segment properties, the Thomson effect must also be considered. Moore treats this problem at length[18]. A fairly reliable approximate method consists of treating the heat flow at the segment boundaries at zero current, then using the calculated shape ratios to calculate average values of ρ and K for the two legs. The efficiency is then calculated as if the legs were single materials, using the equations

$$Z^* = \frac{(\bar{\alpha}_p + \bar{\alpha}_n)^2}{[(\bar{\rho}_p \cdot \bar{K}_p)^{1/2} + (\bar{\rho}_n \cdot \bar{K}_n)^{1/2}]^2} \quad (1)$$

$$M = (1 + Z^* T_{av})^{1/2} \quad (2)$$

$$\eta = \frac{T_H - T_C}{T_H} \quad \frac{M - 1}{M + \frac{Tc}{T_H}} \quad (3)$$

Figure 18 shows the variation of theoretical thermal efficiency for PbTe (3N and 3P), Si-Ge, and segmented Si-Ge-PbTe calculated by this approach, asuming an intermediate temperature of 500°C.

The latter was the approach used to design a segmented Si-Ge-PbTe couple for testing. Average properties for the segments were determined exactly by graphical integration of the curves of properties vs. temperature[18]. A drawing of the couple is shown in Fig. 19. The Si-Ge elements used are the SNAP 10A type, double-bonded with W shoes. A section has been cut off the p-leg to provide proper matching of the legs.

According to calculations of the type discussed above, the maximum theoretical efficiency for segmented Si-Ge-PbTe working between 800° and 50°C is 9.85%. The intermediate junction temperature is 500°C. The power output of the couple illustrated to a matched load of 9.9 mΩ is 2.64 watts at 16.4 amps with a thermal efficiency of 8.97%. The thermal input (adiabatic) is thus 29.4 watts. Maximum thermal efficiency is 9.04%, with 2.61 watts delivered to an optimum load of 12 mΩ at 14.8 amps. The thermal input in this case is 28.9 watts. The maximum efficiency predicted for the couples to be tested, 9.04%, is almost 92% of the theoretical efficiency.

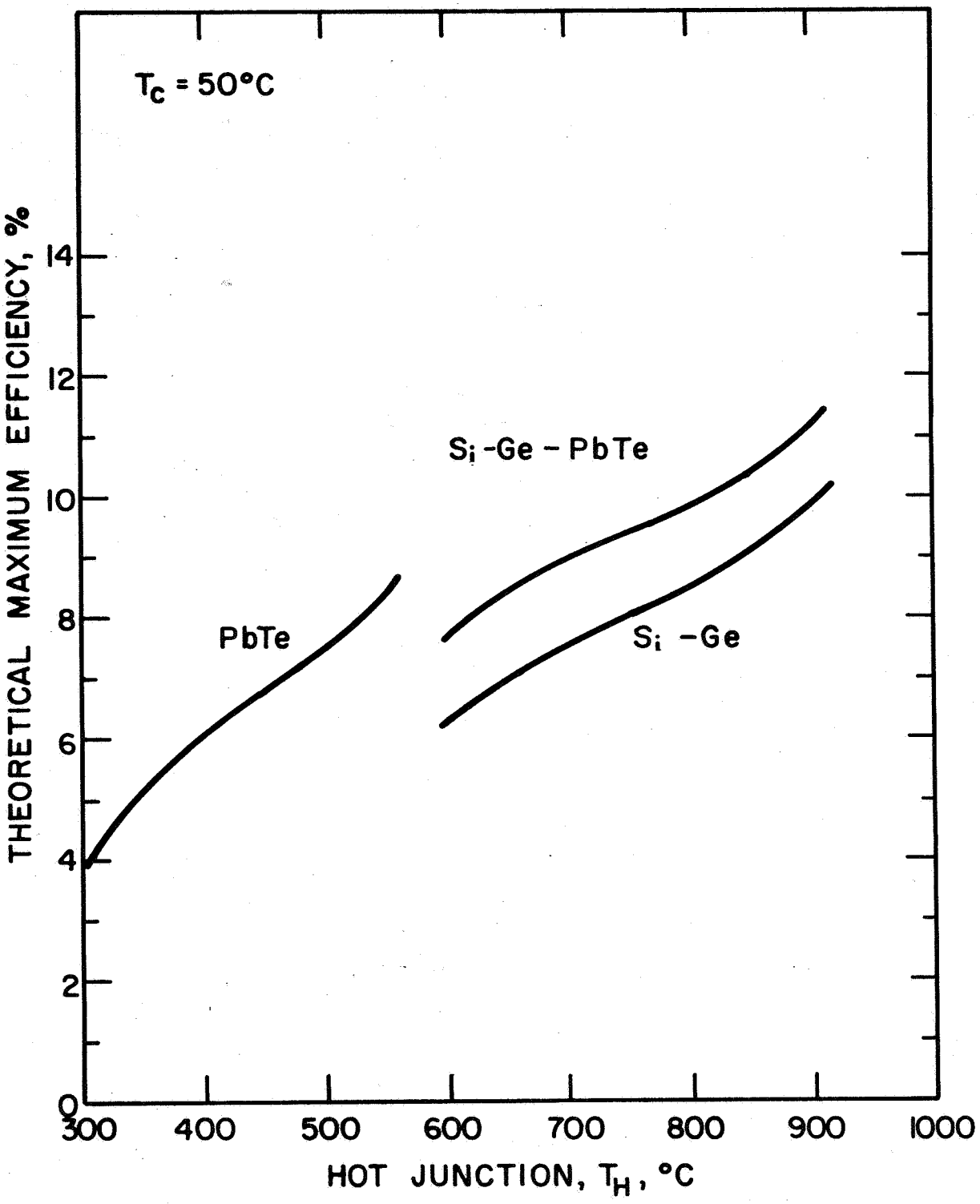

Fig. 18 Variation of theoretical maximum efficiency with hot junction temperature for PbTe (3N and 3P), Si-Ge, and segmented Si-Ge-PbTe.

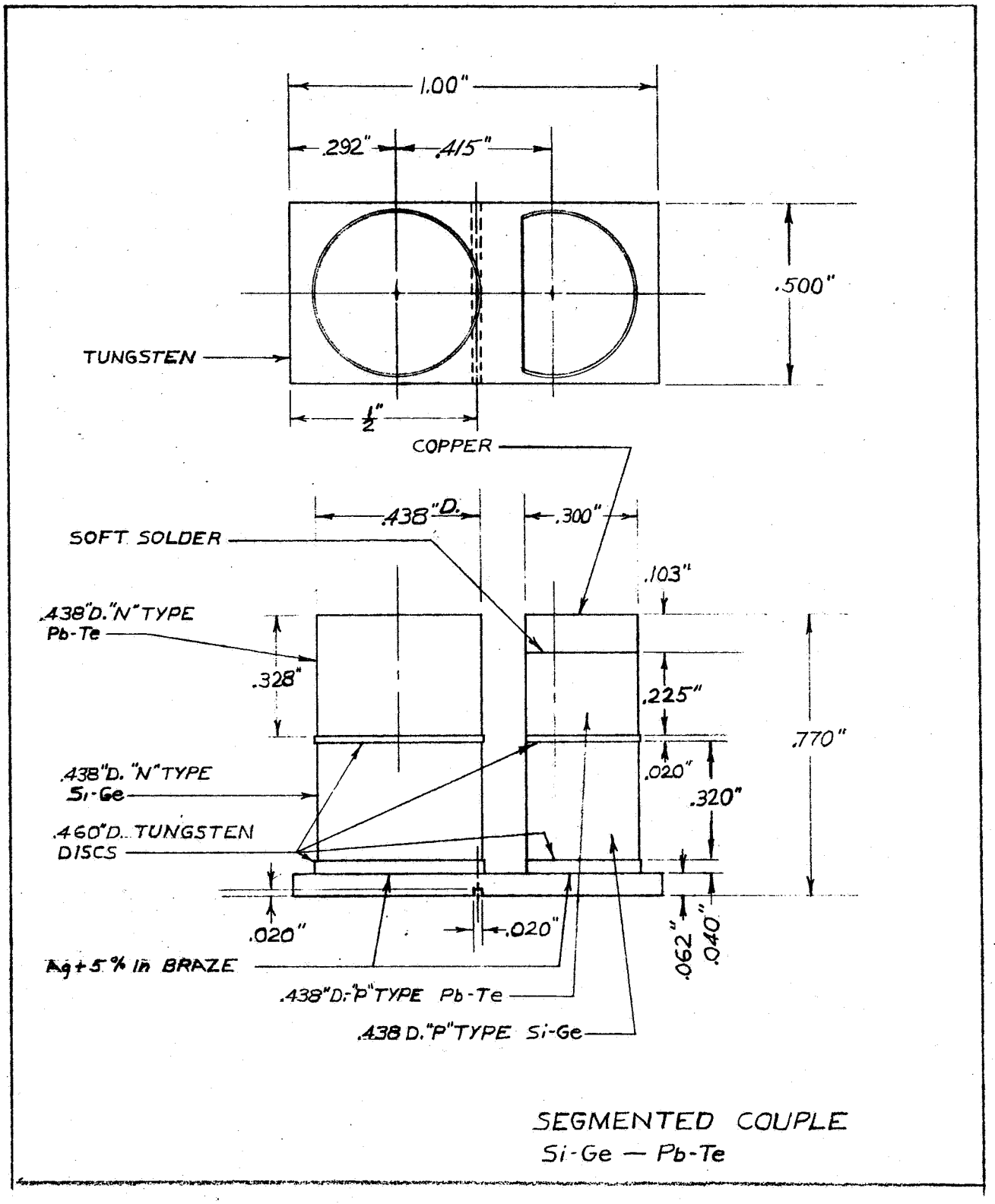

Fig. 19 Optimized Si-GePbTe couple for testing and performance measurements.

A. 2. Segmented Couple Preparation

The segmented couples are prepared by bonding the PbTe segments to the tungsten shoes of the Si-Ge by the ordinary diffusion process. The semicircular p-leg is bonded in this configuration. After bonding, the PbTe segments are ground and lapped to the correct lengths. The W hot shoes of the Si-Ge segments are then brazed to the W hot strap. The hot strap is placed on a flat graphite pedestal; the couples legs are set on the strap with flat pieces of braze and flux in the joint. The pedestal is rf heated until the braze melts and flows (900°C). The brazed couple is then cooled slowly. The brazing process is performed under an argon atmosphere; however, experiments showed that a standard silver solder flux was necessary for wetting of the tungsten surfaces by the silver-5% indium braze.

Two of the optimized segmented couples are shown in Fig. 20. Both legs are provided with copper shoes on the cold ends. These shoes are soft-soldered to the PbTe after nickel plating of the thermoelectric material to promote wetting by the solder. Initial experiments with the segmented couple measurement device using a segmented couple with equal length PbTe segments demonstrated that a copper-copper contact provided the lowest resistance electrical and thermal path of a number of different combinations.

Measurements have been made on segmented Si-Ge-PbTe couples in the configuration shown in Fig. 19. Open circuit voltage, internal resistance, and output power to resistive loads have been measured. Some difficulty has been experienced in measuring the Si-Ge hot junction temperature accurately and in determining the heat flow through the couple proper.

The method of determining the heat flow through the couple has been to simulate the segmented couple with a pair of Min-K blocks of the same dimensions as the couple legs, with a tungsten strap at the hot side. The heater power to achieve a given hot strap temperature was measured. This power was then subtracted from the heater power necessary to achieve

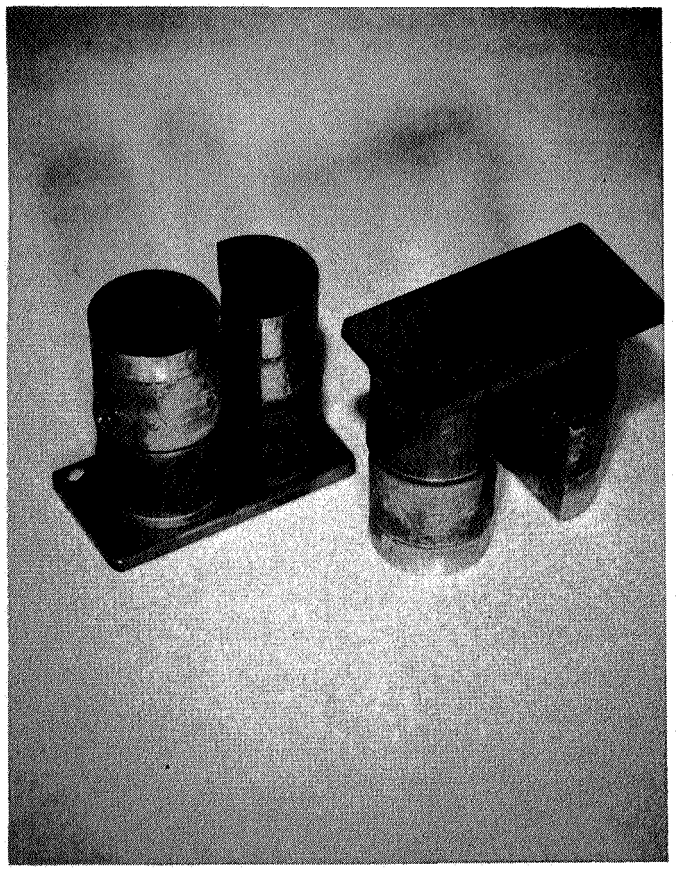

Fig. 20 Segmented Si-Ge-PbTe couples with PbTe segments diffusion bonded to W electrodes of Si-Ge. The bottom segments are copper shoes soft-soldered to the PbTe segments.

the same temperature with the actual couple in place. The difference was taken to represent the heat conducted through the couple (and lost by radiation from the legs of the couple).

The hot junction temperature has been measured by means of a thermocouple spring-loaded against the upper surface of the W-hot strap and a thermocouple cemented in a groove in the under side of the hot strap. Neither method has been completely satisfactory. The cemented thermocouples have consistently measured low temperatures, apparently because of the high emissivity of the cement. The upper thermocouple gave erratic readings and generally appeared much higher in temperature than the open circuit voltage of the segmented couples would indicate. Measurements with a micro-optical pyrometer showed that a 40°-50° difference existed between the junction of the Si-Ge with its W electrode and the indicated upper thermocouple temperature when the Si-Ge junction temperature was 800°C. The 800° level is the minimum at which optical pyrometry may be used with any degree of reliability; thus a correction could not be established for the lower temperatures.

The determination of the heat flow into the couple gave fairly regular results up to an indicated hot side temperature of 800°; above this the results were very erratic. The general approach was too imprecise to provide a differentiation between maximum efficiency and maximum power.

Results of averaging the measurements made on four couples in the configuration shown in Fig. 18 are presented in Table IV. The data have been adjusted for the discrepancy in temperature by plotting the experimental points versus indicated hot side temperature, drawing the best-fitting line, then subsequently adjusting the temperature axis to coincide with the points established by optical measurement. The values for internal resistance and open circuit voltage seem to indicate that the measurement of the hot side temperature is still substantially in error; that is, the values of 850°-900° are most typical of the design values for resistance and open circuit voltage at 800°. This is not felt to be the case. Although errors in the temperature measurement may still remain, it is not expected that their magnitude is the 50° or more indicated. The cold junction temperatures

TABLE IV

Experimental Values of Maximum Power Output and Efficiency for Segmented Si-Ge-PbTe Couples

T_H	T_c	R_I	V_{oc}	P_{max}	Q_{in}	Efficiency
°C	°C	mΩ	mv	watts	watts	%
650	50	8.25	208	1.31	21	6.24
700	65	8.55	230	1.545	24	6.43
750	65	8.80	255	1.845	26	7.10
800	71	9.07	277	2.110	28	7.55
850	80	9.35	305	2.500	30	8.35
900	90	9.65	327	2.77	32	8.75

have run somewhat higher than the design value of 50°C. The 20°-30° decrease in over-all ΔT can only account for a 9 to 13 mv decrease in the open circuit voltage.

The main deficiency in the couples tested thus far has been too low an open circuit voltage (at a specified ΔT). This has resulted in too low a power output and efficiency. Thus, the thermal input is somewhat low in relation to the junction temperature as well; (approximately 29.5 watts are expected at 800°). However, the experimental values of the input heat are the least reliable numbers of those measured. It is felt that the major source of discrepancy between the predicted values and those measured is the neglect of the Thomson effect in the original design calculations. The Thomson heats may have changed the temperature distribution in the couple legs sufficiently to have reduced the open circuit

voltage. When the Thomson effect is included in the input heat, the predicted input at 800° increases to 31.5 watts and the efficiency decreases to 8.35 percent for the maximum power condition.

Two steps will be taken to improve the reliability of the measurements on the segmented couples. Further measurements will be made using the same set-up and technique, except for completely insulating the couple with a block of "Min-K" and using a similarly sized block of "Min-K" for the blank-off measurements of heat losses. After this, the equipment will be modified to provide for measurement of the heat in and out of the couple by measuring the temperature drops in materials of known conductivity. The hot junction temperature will be measured optically.

B. PbTe Couples

The PbTe couples to be used for life-testing represent no essential change from those made originally on an experimental basis. (See Interim Summary Report.) Figure 21 shows the dimensions of the optimized couple. The area ratios are based on maximum efficiency, while the actual dimensions were dictated mainly by a need for a reasonably high internal resistance for measurement purposes. The couples can be expected to have an internal resistance of approximately 11.3 mΩ when operated between 500° and 25°C. The contact resistance will add approximately 0.5 mΩ. Open circuit voltage will be approximately 0.178 volts. The current and power to a matched load will be approximately 7.6 amps and 0.67 watts. The thermal efficiency at the maximum power condition will be approximately 7.7%. The maximum efficiency is 7.76% with 0.665 watts delivered to a load of 13.9 mΩ at 6.9 amps.

The couples were prepared by bonding both legs at the same time to the W hot strap. The p-type legs were prerun in hydrogen at 825°C for improved bonding performance as discussed in section III. Figure 22 shows the graphite bonding fixture used for the preparation of the couples. The copper caps are provided on the cold ends to insure good thermal and

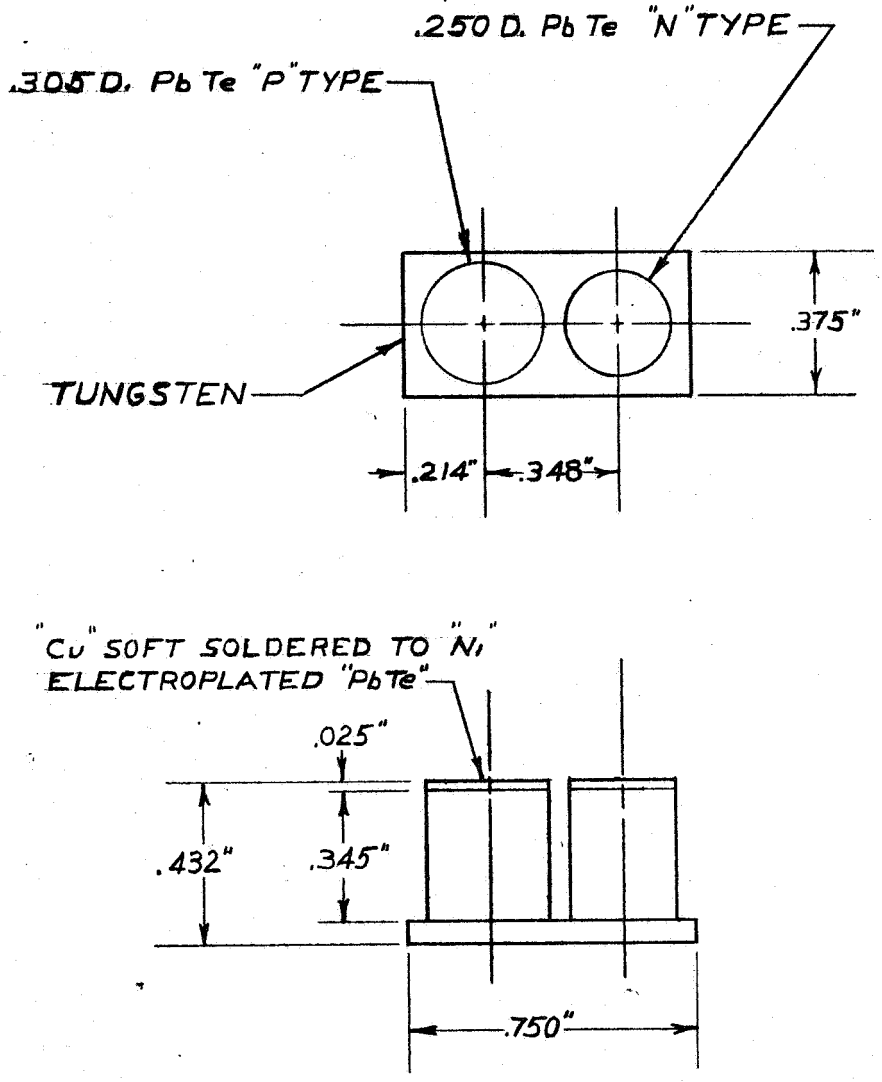

Fig. 21 "Pb Te" COUPLE FOR COUPLE LIFE TESTER

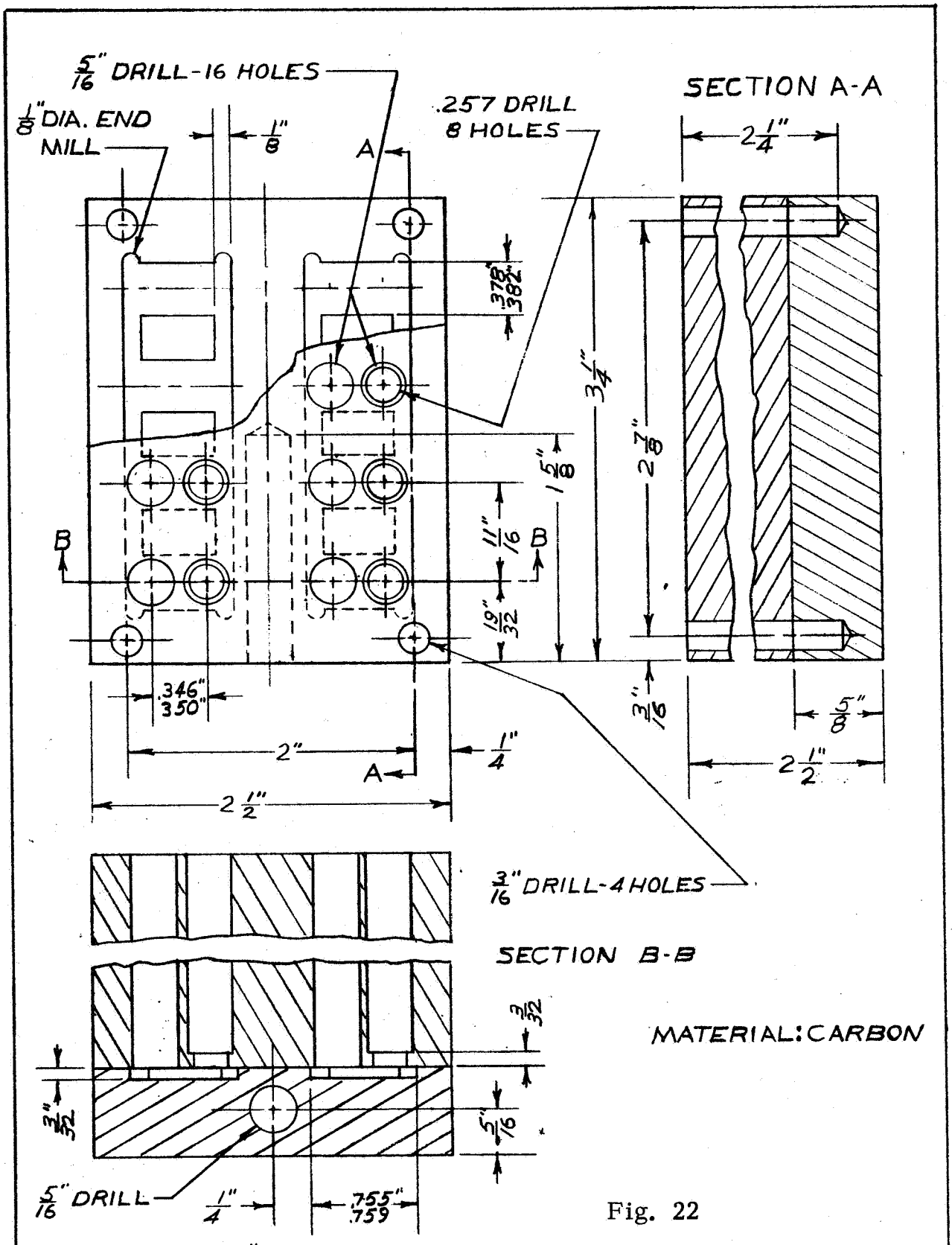

Fig. 22

"PbTe" TO "W" COUPLE BONDING FIXTURE

electrical contact with the cold sinks of the life tester. The ends of the couple legs are lapped, cleaned, and nickel plated. The copper caps are presoldered and the solder ground to a thickness of 0.005 inches. Soldering is accomplished in the fixture shown in Fig. 23. The couples and caps are heated to 200°C under an argon atmosphere, then cooled. Two couples with the cold end caps are shown in Fig. 24.

The room temperature resistance of the bonded and capped couples averaged 3.28 mΩ. The W strap, PbTe to W bonds, and cold end contacts add approximately 0.25 mΩ to the resistance of the PbTe legs. Initial operating characteristics of these couples are reported in section V (B).

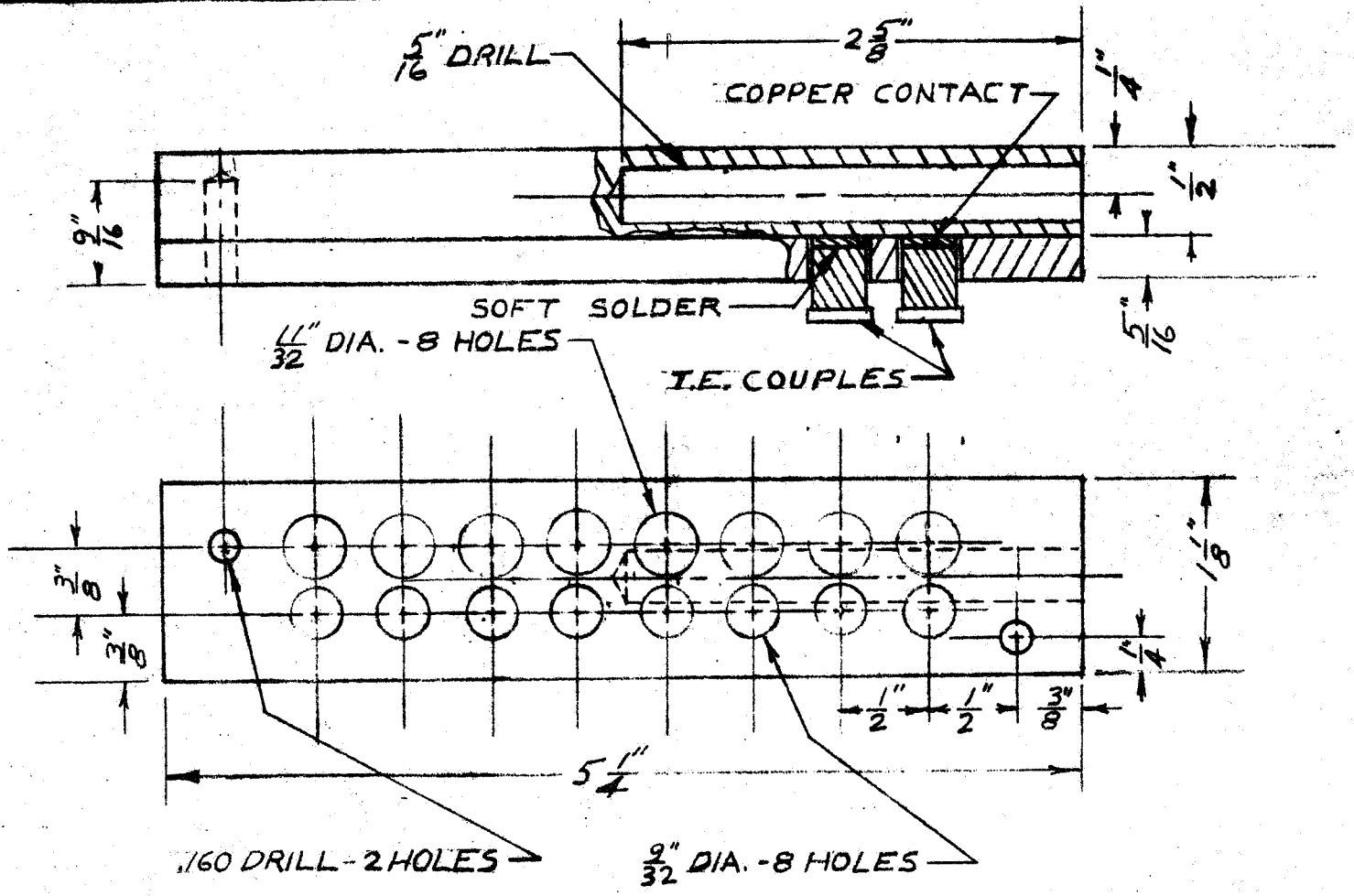

MATERIAL: CARBON
PCS. REQ'D: 1

Fig. 23 COLD END CONTACT BONDING FIXTURE

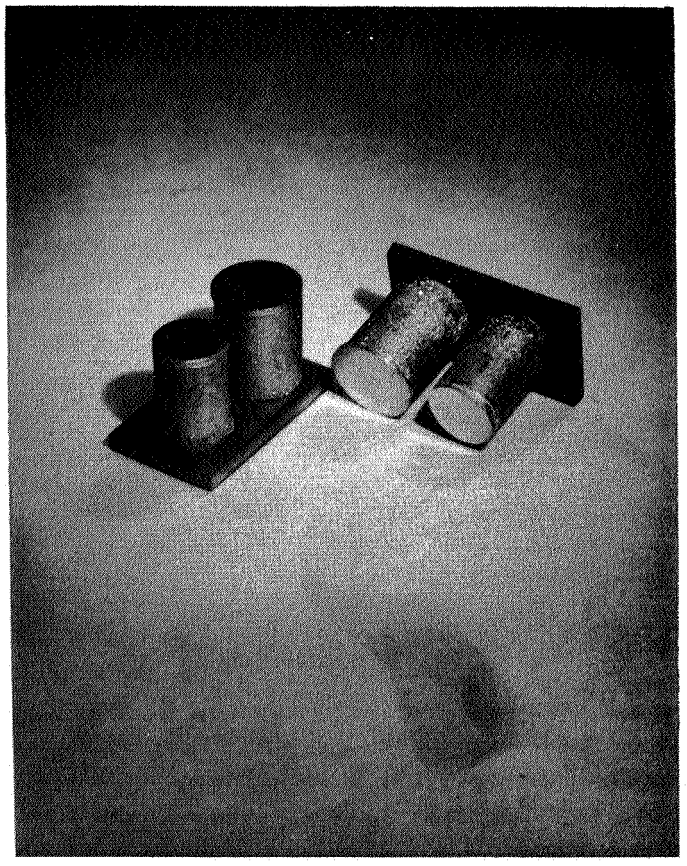

Fig. 24 Tungsten bonded 3N-3P PbTe couples for life-testing. Note copper cold end caps which are soft-soldered to couple legs. 1.3 X

V. TEST DEVICES

A. Segmented Si-Ge-PbTe Couple Tester

A device was built to measure the electrical characteristics of segmented Si-Ge-PbTe couples. The segmented couple tester is basically a single station from the sixteen station PbTe couple tester. (The couple tester is described in detail in the next section.) A cross section of a single station is shown in Fig. 25. The heater insulator, 7 , in the segmented couple tester consists of a block of Min-K approximately 3" x 3" x 2". Figure 26 is a photograph of the segmented couple tester and heater power supply and couple load circuit box. A schematic of these circuits is shown in Fig. 27.

The use of this apparatus in the measurement of the conversion efficiency of segmented couples has been discussed in section IV. Its operation is quite simple. The couple is positioned on the cold sink, 4 in Fig. 25, and the heater, 7, is clamped against the hot strap by compressing the spring, 29. The bell jar is evacuated, or evacuated and back filled with Argon.

Measurements are taken by allowing the couple to come to thermal equilibrium at some value of the load resistance, usually about 12 or 13 mΩ . The small box in front of the power supply in Fig. 26 provides for switching of the thermocouple outputs (hot junction, cold junctions and mid-junctions) to a potentiometer. Values of load voltage and current are read, the circuit is then opened and the open circuit voltage read immediately.

When the internal resistance and power output are calculated from these measurements, correction must be made for the connection and lead cable resistance. Thus:

$$R_I = \frac{V_{oc} - V_L}{I_L} - R_C$$

and

$$P = I_L V_L + R_C I_L^2 .$$

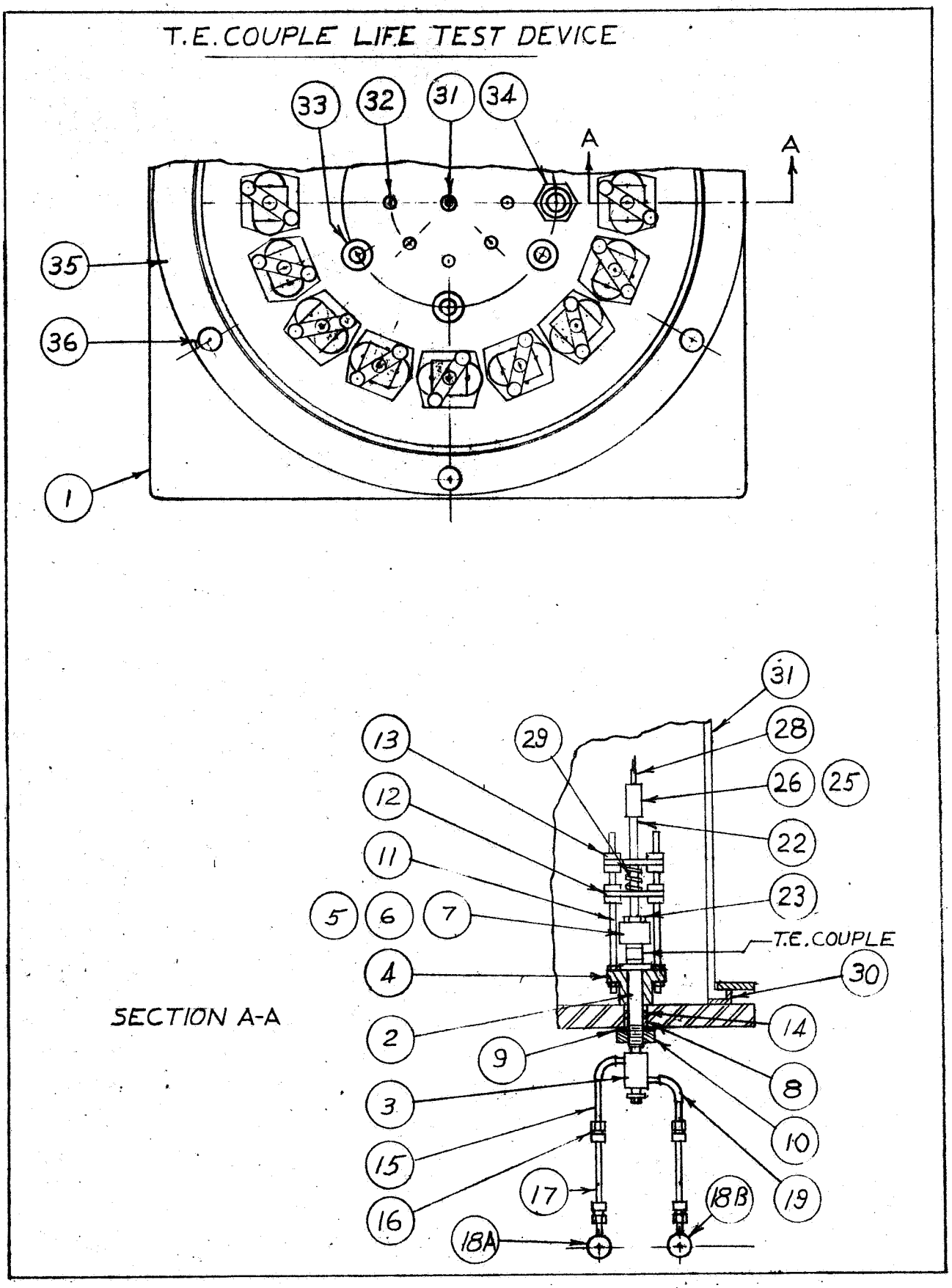

Fig. 25 **Plan view and section through one station of PbTe couple life test device.**

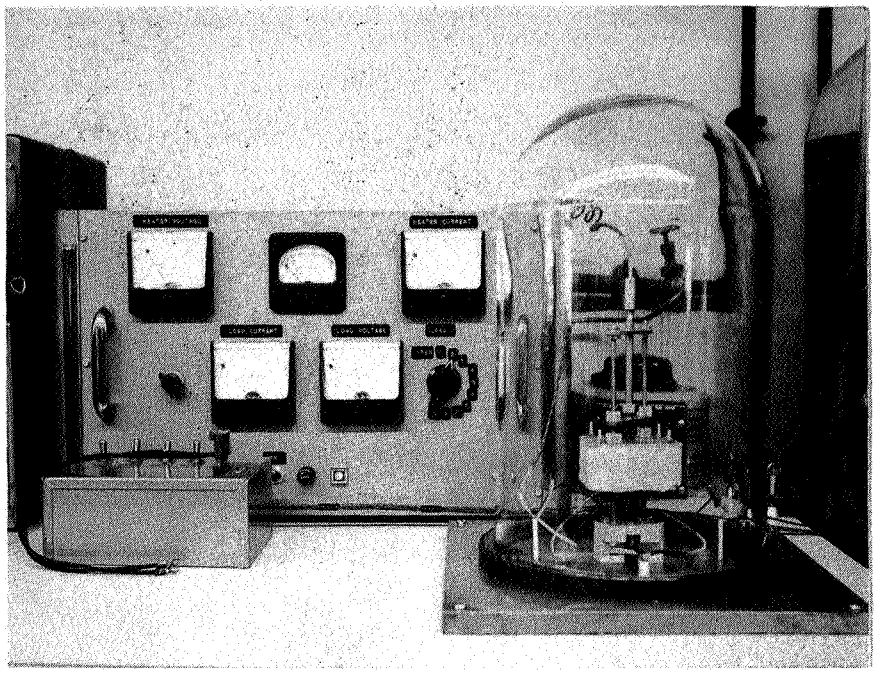

Fig. 26 Apparatus for electrical characterization of segmented Si-Ge-PbTe thermoelectric couples.

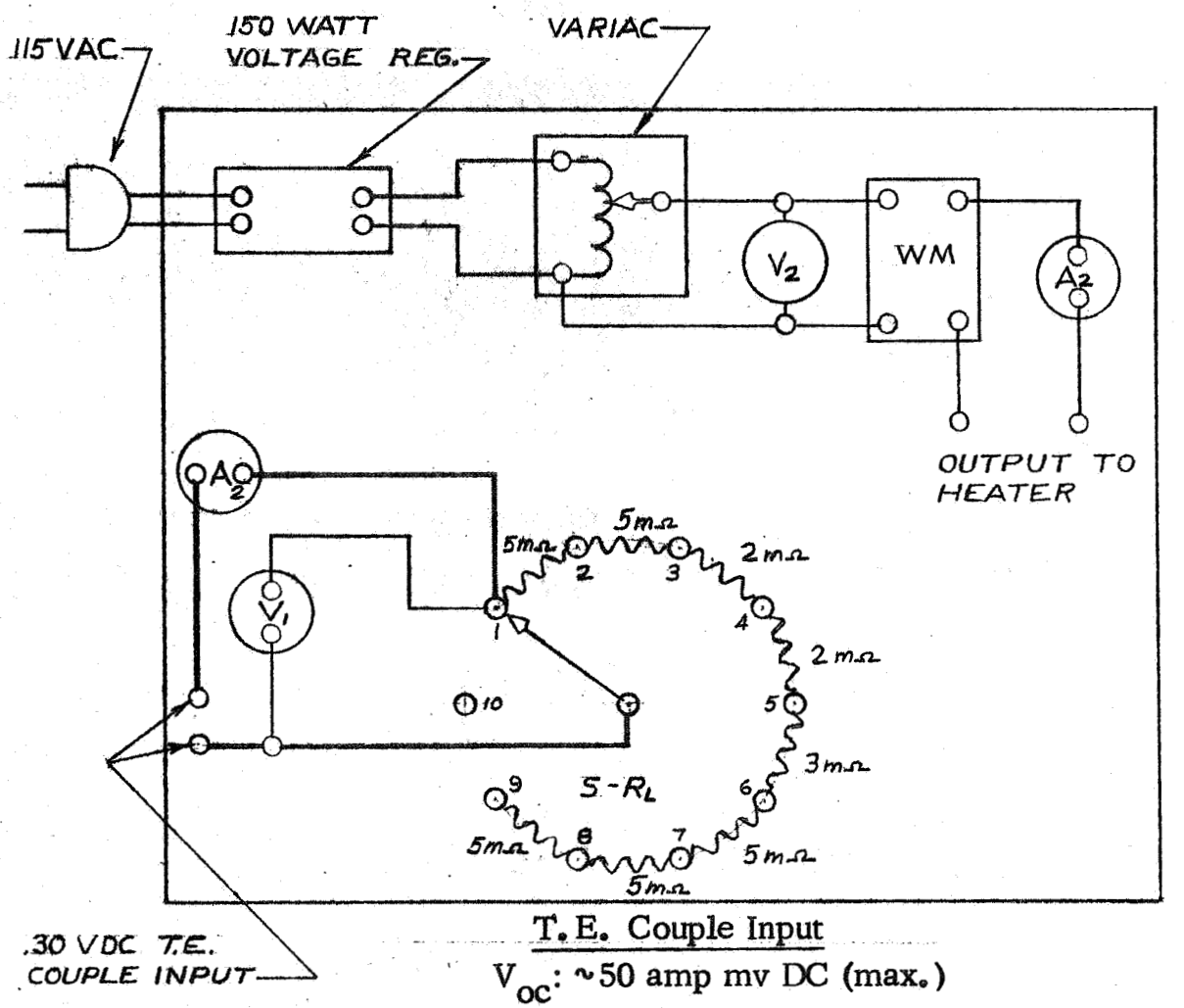

T. E. Couple Input

V_{oc}: ~50 amp mv DC (max.)

$R_{int.}$: ~10.5 m Ω

I : ~35 amps

Parts Ident.	Description
A_1	0-50 amp ammeter (DC)
V_1	0-500 mv millivoltmeter (DC)
S	Rotary, hi-current switch
RL	Load resistor 8 steps of 5, 5, 2, 2, 3, 5
	5, 5 mΩ
V_2	0-150 VAC voltmeter
WM	0-150 watt wattmeter
A_2	0-10 amps AC ammeter

Fig. 27 Segmented Couple Heater Power Supply and Load Circuit

This is the result of the cables having a fairly significant resistance in comparison with the internal resistance of the couple (3.9 mΩ to approximately 10 mΩ for the couple) and of the load voltmeter's being connected across the load only. That is, the measured voltage drop is not the total drop external to the couple.

Results of measurements on the optimized segmented couples are discussed in section IV.

B. PbTe Couple Life-Tester

A sixteen-station test device for life testing of W-bonded PbTe couples was designed and constructed under this contract. The tester is designed to produce information on the degradation of bonded PbTe couples under operational condition. The couples run continuously under a temperature gradient while operating into a matched load resistance. Hot and cold junction temperatures and the voltage drop across the load resistor are recorded automatically. Periodically, the open circuit voltage is determined manually; short circuit and varying load characteristics can also be determined manually. These measurements can be used to calculate the power output and internal resistance of the operating couple.

Photographs of the entire system and the mechanical portion, showing five stations are presented in Figs. 28 and 29.

Figure 25 shows a plan view of the arrangement of the stations in the couple life tester. A section through one station is also shown. (Drawings of the components and a complete parts list are included in Appendix 2.) This design represents a considerable change from the bonded element life tester. (See Interim Summary Report, section VII.) The changes are the result of our experience with the element tester more than the difference between the types of devices being tested. The major changes involve the use of individual heaters and the external cooling system. The heater, 7, is positioned against the couple hot strap by spring loading. The hot junction thermocouple, 28, runs through the heater and is also spring-loaded. The heat sink, 2, runs through the base-plate and is electrically isolated by a Teflon sleeve and washer, 8 and 9. Cooling of the sink is provided by water

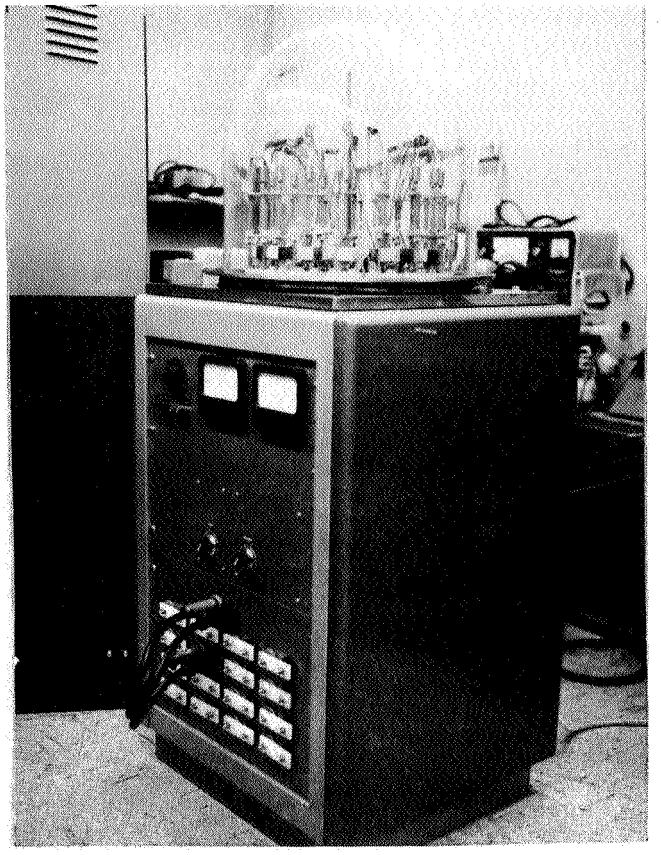

Fig. 28 Sixteen station PbTe couple life tester.

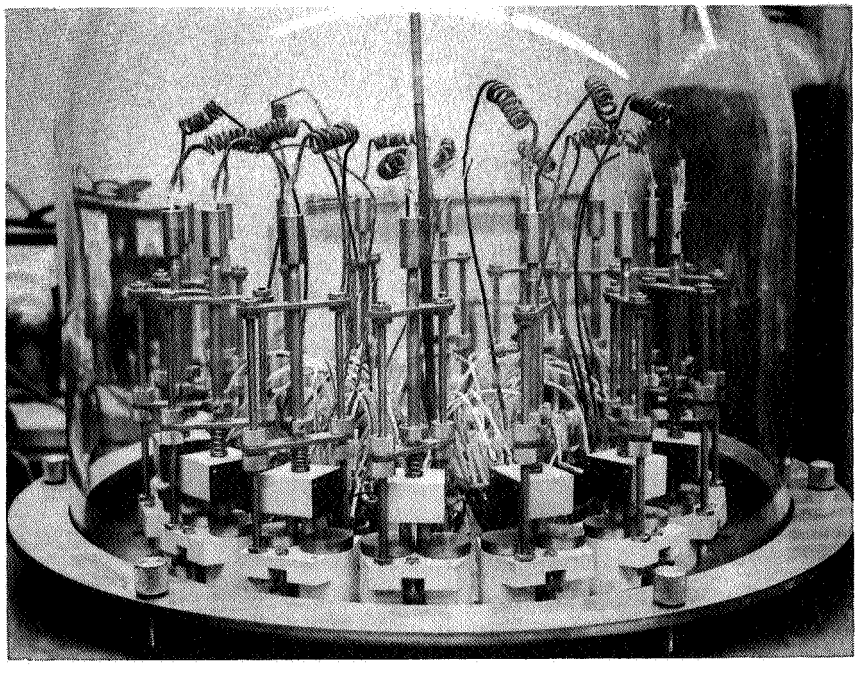

Fig. 29 Mechanical portion of couple life tester with couples in position.

circulating through a jacket, 3, around the heat sink rod. Electrical isolation of the water jacket from the manifolds, 18A and 18B, is provided by polyethylene tubing, 17. Electrical connection to the couple is made at the bottom of the heat sink of each leg, immediately under the water jacket, 3.

The use of individual heaters followed more or less by necessity from the configuration of the heat sinks with external cooling. A single ring heater would not allow for any variation in the length of the couples, since the cold ends are already fixed in place. A large, continuous heater also produces a large amount of waste heat inside the bell jar, i.e., heat not conducted through the couples. Individual heaters sharply reduce this problem. The heaters are essentially flat plates and draw about eight volts and four amps. A single electronic temperature controller is used to control the output of silicon rectifiers. Four variacs are used to adjust for differences among the four sets of heaters. The circuit diagram of the temperature controller is included in Appendix 2.

A schematic of the manual measurement circuit of the couple tester is shown in Fig. 30. The input to the measurement circuit comes through the plug board which can be seen in Fig. 28. Welding cable connects the copper heat sinks to the plug-in connectors from which any couple may be further connected to the manual measurement circuit. The resistances of the various connecting cables have been measured in order that corrections may be made to measurements of output power and internal resistance. In determining the power output, the voltage drop across a known (load) resistance is recorded. From this, the current in the circuit is calculated. The power is then calculated as the sum of the two I^2R terms. The voltage drop across the constant load resistor is measured at the terminals of the plug-in connectors, into which the loads are plugged. The voltmeter of the manual measurement circuit measures the drop across the variable resistance switch; thus a different value for the cable resistance is used in correcting measurements of power and internal resistance made from this point.

In initial tests with the system using the couple designed for life-testing, we obtained the results shown in Table V. The couples were

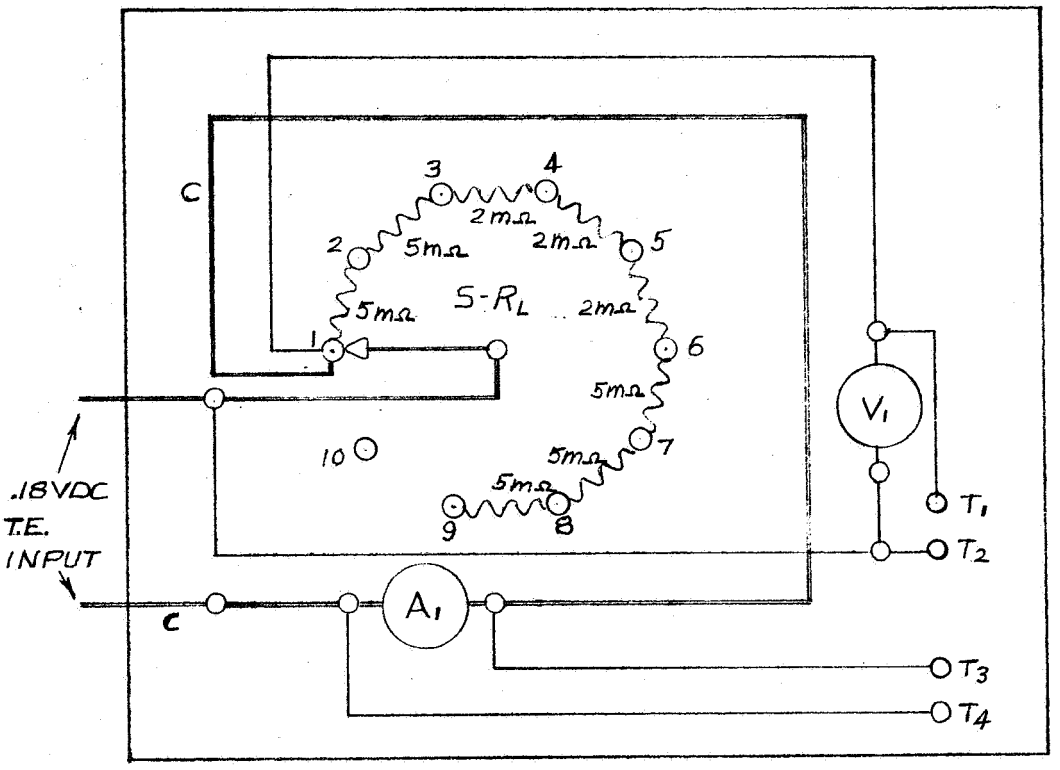

T. E. Couple Input

V_{oc}: ~180 mv

$R_{int.}$: ~12 mΩ

I_{se}: ~15 amps

Parts Ident.	Description
S	10 position rotary hi current
RL	Load resistor, 8 steps of 5, 5, 2, 2, 2, 5,
	5 and 5 mΩ
V_1	0-300 mv DC millivoltmeter
A_1	0-25 amps DC ammeter
T_1-T_2	Banana jacks
T_3-T_4	Banana jacks
C	Braided 1/0 welding cable
	R = .1 mΩ/ Ft.

Fig. 30 Thermoelectric Couple Load and Measurement Circuit for PbTe Couple Life Test Device.

stationed one within each group of four heaters. The heaters were powered at this time by a single variac, thus the differences in hot junction temperatures.

Table V

Initial Operating Characteristics of PbTe Couples in Couple Life Testing Device

Station	T_H °C	T_{C_N} °C	T_{C_P} °C	ΔT °C	V_{oc} mv	R_I m Ω	P_{max} watts
3	523	37	37	486	155	11.2	0.54
7	485	35	36	450	154	10.0	0.593
11	499	36	36	463	155	9.6	0.625
15	520	36	39	482	159	12.6	0.505

The predicted performance for these couples has been described in section IV. An open circuit voltage of 178 mv was predicted for 500° to 25°. These couples fall somewhat short of this. It would appear that this is due to the indicated hot side temperature's being higher than the hot junction temperature. That is, there is an appreciable temperature drop across the tungsten strap. The higher cold junction temperature also contributes somewhat to the lower output, although the average apparent ΔT for the couples listed is 470°. The average resistance is lower than predicted, as well - 10.9 mΩ versus 11.8 mΩ - lending further support to the possibility of a lower hot junction temperature.

Testing of couples will be done at a hot junction temperature of 520° to 525°C.

C. Element Tester Water Safety Control System

The failure of element life-tester in March revealed a number of inadequacies in the system of pressure switches and valves for the maintenance of cooling water in the tester. (See Interim Summary Report.) A schematic diagram of the revised system now in use is shown in Fig. 31. The water supply and safety control system operates to protect the life test device against the type of failure which has occurred previously. In both cases the cooling water has been lost temporarily; the residual heat in the system has caused failure of a joint in the water system inside the device. Recovery of the water supply then caused water to be released inside the device, a minor amount in one case and complete flooding in the most recent.

The system operates as follows. Both water supplies are maintained on. The check valves, C1 and C2 , provide for the supply with the higher pressure to maintain the cooling water flow. This is generally the city supply. The pressure switch, S1, senses the water pressure being supplied to the device. If this pressure, whatever its source, drops below 5 psi, the switch opens the relay, R1, which interrupts the power to the heater. This relay will also open with any interruption in electrical power. The relay must be manually reset.

Inside the upper portion of the life test device a mercury switch (WDS), activated by a float, serves to detect gross amounts of water inside the system in the case of a leak. The switch, working through the relay R2, closes the solenoid valve, S1, to prevent any further water flow. The closing of the solenoid valve drops the pressure sensed by the pressure switch; this in turn opens the relay R1 and thus interrupts the power to heater.

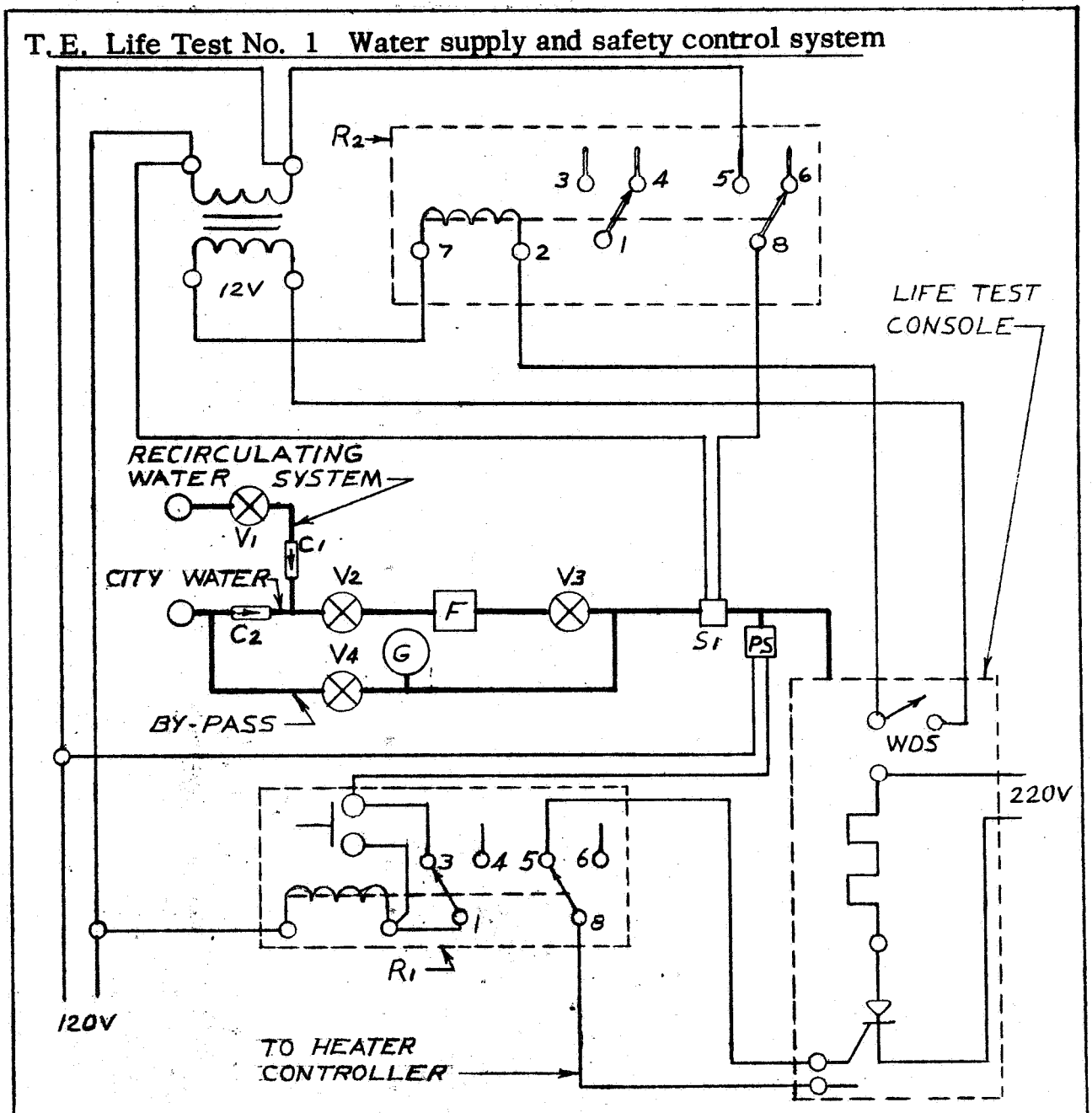

Symbol	Description
S1	Solenoid valve - (Closed when energized)
C1, C2	Check valves
V1, V2, V3, V4	Globe shut off valves
F	Water filter
PS	Pressure switch
R1, R2	Relays
G	Pressure guage
WDS	Water detector switch

Fig. 31 Schematic diagram of element tester water supply and safety control system.

VI. LIFE TESTING

The results of gradient and isothermal tests of W-bonded 3P and 3N thermoelements are reported in this section. The gradient tests were of 800 and 2600 hours duration at an average hot junction temperature of 510°C. Isothermal test results are reported for 4700 hours at 600°C and 1000, 2000, and 3000 hours at 525°C. Some of the general findings of these various tests are discussed here. Most of the results and discussion relate to W bonds to 3P material.

One finding from these tests, which was quite contrary to expectations, is that the initial resistance of a bond, within the range of contact resistances tested, is not a reliable indicator of how the bond will perform when tested. It had been expected that the lower the initial resistance of a bond, the longer it would last or the lower it would remain in comparison to a bond of higher resistance. This has not been borne out. This result led us to an examination of the data for some other factor which might account for differences in behavior among contacts. The only significant finding from this examination of the test data was a strong indication of markedly different behavior between two lots of p-type material. This was also an unexpected result, although we had previously found that occasionally a batch of material would be received which could not be bonded by the normal process. However, the existence of differences in the material which may not affect the bonding performance but will ultimately affect the longevity of the contacts is a more serious problem, requiring some method of detecting the factor or factors responsible.

A. 1. Gradient Life Test III

During this period one test of approximately 870 hours duration was made. (Another test is described in section A. 2.) The test began on 26 January and ended on 3-4 March due to a failure of the test device. Fifteen elements were tested: seven W-bonded 3N type and eight W-bonded 3P-type. The data for total element resistance, Seebeck voltage, and hot junction temperature were averaged for the two groups of elements. The

resistance and Seebeck values were then corrected, where necessary, to provide values at a uniform hot junction temperature. For n-types this was 500°C, and for p-types the hot junction was corrected to 510°C. The average deviation of average hot junction temperatures from these values was ± 8°C. The initial values of junction and element resistances at room temperature are listed in Table VI.

The data for resistance and Seebeck voltage are shown as a function of time in Fig. 32. The most significant change occurs in the resistance of the p-type elements. Both parameters for the n-type elements appear to be level near the end of the test. The p-type Seebeck voltage also seems to be nearly level, while the resistance is still slowly increasing. The open points near the curves for p-type properties represent the average values from the five lowest p-elements of the eight. (One element was read only occasionally because of a poor connection or intermittent ground. It behaved the same as the five low resistance.) The higher average curve is the result of two elements which showed considerable increases in total resistance. That these increases are due to increases in contact resistance is indicated by the minor difference in average Seebeck between the five low elements and the average of all seven.

From inspection of the initial properties of the p-type elements there was no obvious difference in the two elements which showed large increases in resistance from the other six elements.

Table VII lists the values of resistance and Seebeck voltage taken from Fig. 32 at 100 hour intervals. These values are also combined to give a maximum power output (for one couple) according to

$$P_{max} = \frac{Voc^2}{4\ R_i} \quad .$$

TABLE VI

Initial Values of Contact and Element Resistance
Of Elements Tested Under Gradient Conditions
(Life Test III)

Element	Hot Junction Resistance $\mu\Omega$	Cold Junction Resistance $\mu\Omega$	Element Resistance m Ω
4Y6 P19	70	70	1.460
4Y12 P19	90	250	1.460
5B1 P19	55	80	1.520
5H2 P20	100	50	1.500
5B5 P19	65	60	1.480
5Q2 P21	25	55	1.620
5C2 P19	55	80	1.320
5C9 P19	80	55	1.370
2Y3 N9	35	45	.505
2Y7 N9	30	25	.574
2Y8 N9	35	35	.522
2Y9 N9	30	30	.544
2Y11 N9	30	25	.557
2Y14 N9	30	35	.544
2Y15 N9	25	35	.521

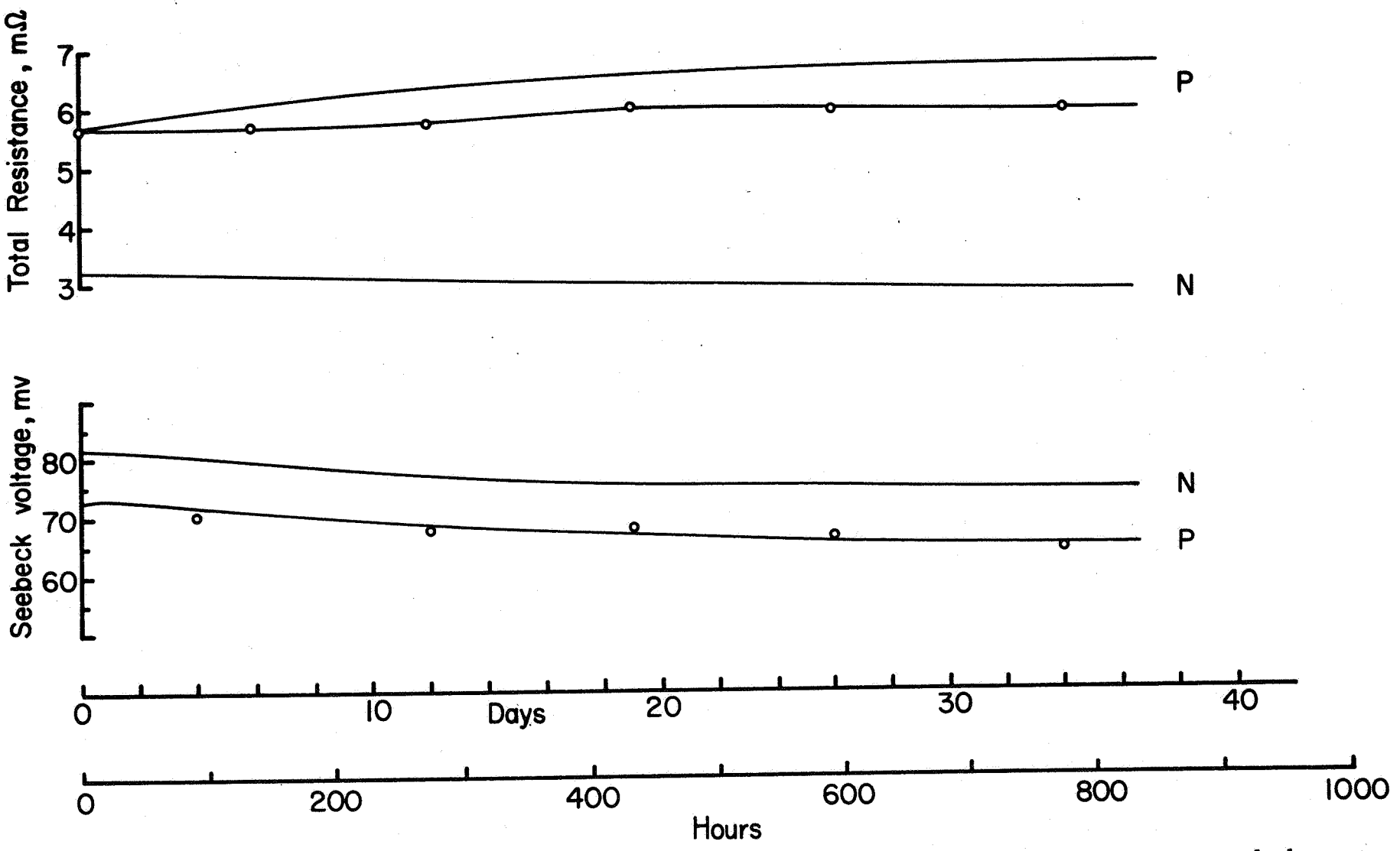

Fig. 32 Results of gradient life testing of W-bonded 3N and 3P elements. Average total element resistance and Seebeck voltage as a function of time. Values corrected to a uniform hot junction temperature of 510° for p-type and 500° for n-type. Open circles represent low resistance p-type elements.

TABLE VII

Average Values of Electrical Parameters and Calculated Power of a Simulated Couple

Time hours	$\bar{R}_p$ mΩ	$\bar{R}_n$ mΩ	$\bar{S}_p$ mv	$\bar{S}_n$ mv	V_{oc} mv	R_i mΩ	P_{max} watts	P/Po
0	5.80	3.15	72.5	82.	154.5	8.95	0.666	1
100	5.85	3.15	71.5	81.5	153.	9.00	0.650	0.975
200	6.10	3.10	69.	78.	147.	9.20	0.587	0.882
300	6.35	3.10	68.	76.	144.	9.45	0.548	0.823
400	6.50	3.05	67.	76.	143.	9.55	0.536	0.805
500	6.55	3.00	65.5	75.	140.5	9.55	0.517	0.777
600	6.60	2.95	65.5	74.5	140.	9.55	0.513	0.770
700	6.65	2.85	65.	74.5	139.5	9.50	0.512	0.769
800	6.70	2.85	64.5	75.	139.5	9.55	0.510	0.765

Figure 33 shows the power output from a (simulated) couple as a function of time in terms of the actual power and normalized to the initial output. The open points on the normalized curve represent the results obtained using p-type resistances typical of the low resistance group, rather than the average value.

The over-all behavior of the elements tested here is similar to that observed by other investigators in both systems and experimental studies. The degradation of power occurs fairly rapidly early in the tests and then levels out. The main source of power degradation is an increase in resistance (of the device) which can be mainly attributed to the contact with the p-type material. In the case of the elements gradient tested here, the other source of degradation is a gradual decrease in the Seebeck voltage of both n- and p-type elements. This behavior has been seen in isothermally tested W-bonded elements. However, in the previous gradient-test for 550 hours (see Sixth Quarterly Report) the bonded n-types showed an increase in Seebeck voltage, while the unbonded n-types showed a decrease. P-type elements both bonded and unbonded, showed a decrease in Seebeck voltage. Table VIII indicates the magnitude of the decreases in Seebeck voltage for the elements most recently tested. As can also be seen in Fig. 32, the n-type elements seem to have stabilized at approximately 91% of the initial voltage, while the p-type elements had not apparently leveled off at this time.

This test was terminated unexpectedly by a failure of the tester which resulted in the interior of the system being flooded with water.

A. 2. Gradient Life-Test IV

A gradient life-test of bonded and unbonded 3P elements was started on 12 April. The loading consisted of three unbonded elements, eight singly bonded elements (bond at hot junction), and four doubly bonded elements. The initial values of room temperature element and contact resistance are listed in Table IX. The average hot junction temperature for this test was 510°C. Cold junction temperatures varied among the groups

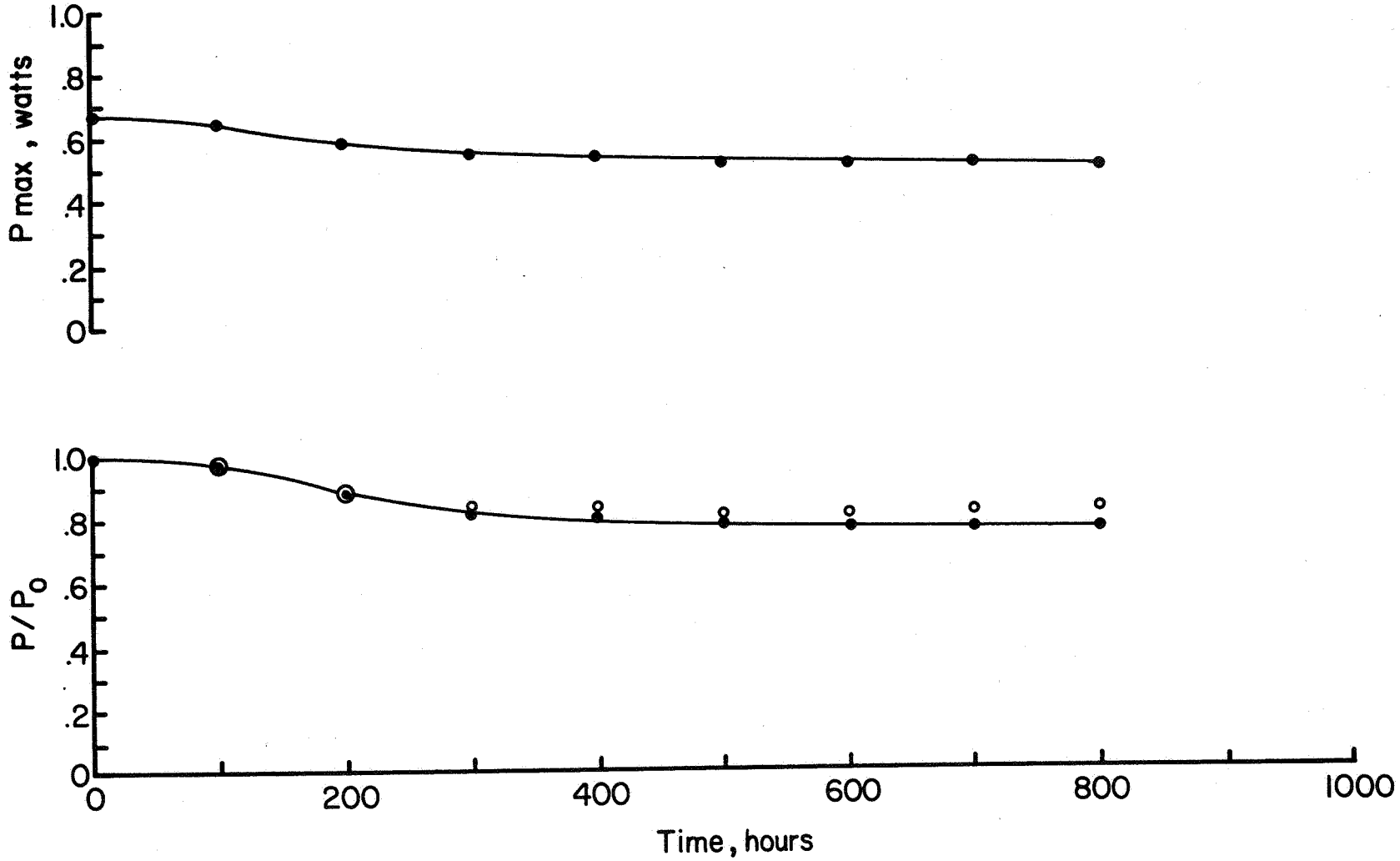

Fig. 33 Variation of power output as a function of time from a simulated couple using the average properties shown in Fig. 34. Open circles in normalized curve represent values obtained using low resistance p-type values.

TABLE VIII

Ratio of Seebeck Voltage to Initial Voltage for Gradient Tested 3N and 3P W-Bonded Elements

Time	S/So-3N	S/So-3P
0	1.	1.
100	.993	.987
200	.952	.952
300	.927	.938
400	.927	.924
500	.914	.903
600	.908	.903
700	.908	.896
800	.914	.890

TABLE IX

Initial Values of Contact and Element Resistance
of Elements Tested Under Gradient Condition (Life Test IV)

Element	Hot Junction Resistance $\mu\Omega$	Cold Junction Resistance $\mu\Omega$	Element Resistance m Ω
Unbonded			
P24 #1	---	---	1.345
P24 #2	---	---	1.490
P24 #3	---	---	1.630
Singly Bonded			
6B2P24	95	---	1.97
6A3P24	100	---	1.35
6B1P24	80	---	1.555
6H3P24	45	---	1.665
2Z10P9	100	---	1.320
6B6P24	75	---	1.440
6H2P24	55	---	1.955
4K7P17	80	---	1.220
Doubly Bonded			
2Z16P19	100	100	1.250
6H4P24	80	120	1.600
6B5P24	105	195	1.640
4I10P15	90	90	1.420

of elements. Initially, the unbonded elements had an average cold junction temperature of 60°, the singly bonded elements averaged 50° at the cold end (not due to a 10° drop across the hot side electrode, but rather to the increased distance between the exposed portion of the cold sink and the hot side stud and insulation), and the doubly bonded elements ran at a cold junction temperature of 22°. The cold junction temperatures increased as the test progressed due to the increasing temperature of the cooling water. This effect can be seen in the variation of ΔT with time for all three groups of elements.

Results of the test have been plotted to 2600 hours in Figs. 34, 35, and 36. Resistance values are shown for the unbonded elements and for three singly bonded elements which remained fairly low in resistance. Average Seebeck voltage data for all elements are plotted in Fig. 36 (and Fig. 34). It was felt that graphical presentation of the resistance data which would consist of decreasing numbers of elements would be both confusing and misleading. Thus the figures include only those elements with resistance below 10.2 mΩ at 2600 hours. Table X lists the initial individual element resistances and the time to reach a resistance of 10.2 mΩ; (the measurement system cannot read a resistance greater than 10.2 mΩ).

In discussing the results shown in Figs. 34-36, it should be noted that the apparent correlation between decreasing Seebeck voltage and decreasing ΔT is false. The change in ΔT will account for, at most, a 0.2 mv decrease in the Seebeck voltage. The major part of the decrease for the unbonded and bonded elements occurs within the first 1000 hours. Table XI lists the changes in Seebeck voltage at 1000 hours and 2500 hours. The average decrease in Seebeck voltage at 2500 hours for all elements in this test, 8.9%, is less than the 11% experienced by the p-type elements of the previous gradient life-test in 800 hours.

The behavior of the W-bonded elements in this test is such as to suggest that the major source of increasing resistance is the bond. The Seebeck voltages of bonded and unbonded elements behave similarly. The

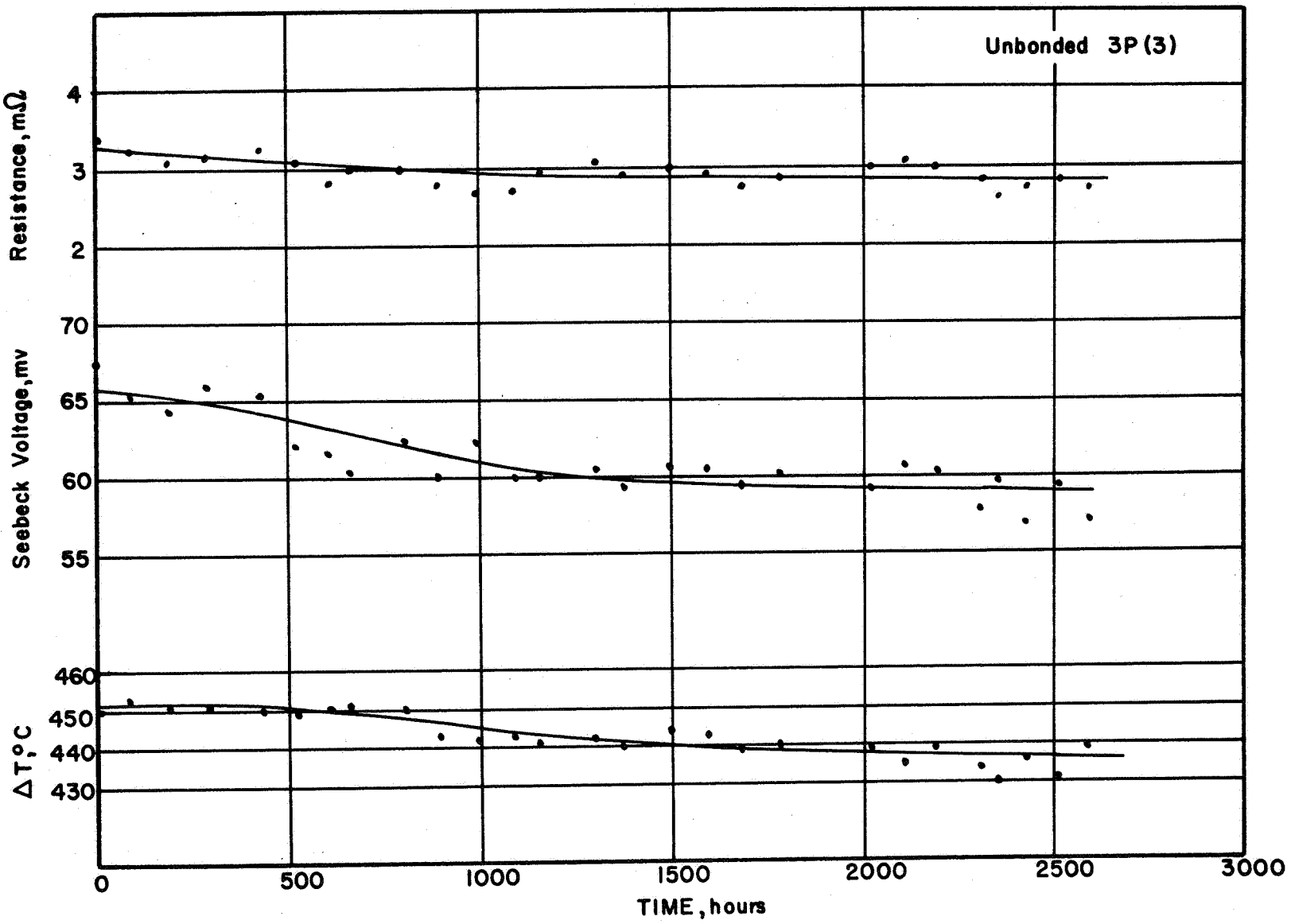

Fig. 34 Change with time of resistance, Seebeck voltage, and ΔT for unbonded 3P elements (average of three)

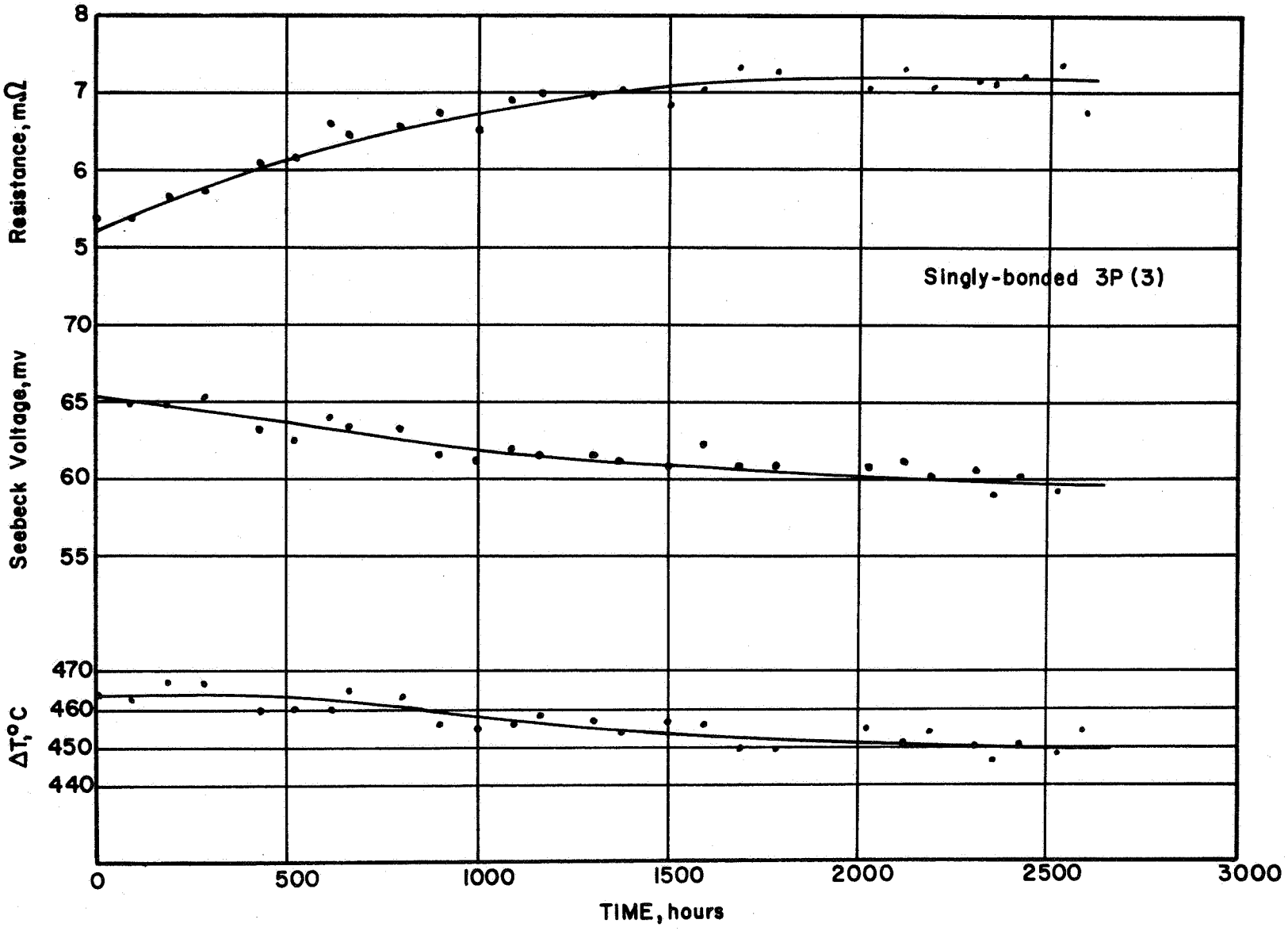

Fig. 35 Change with time of resistance, Seebeck voltage, and ΔT for W-bonded 3P elements (average of three)

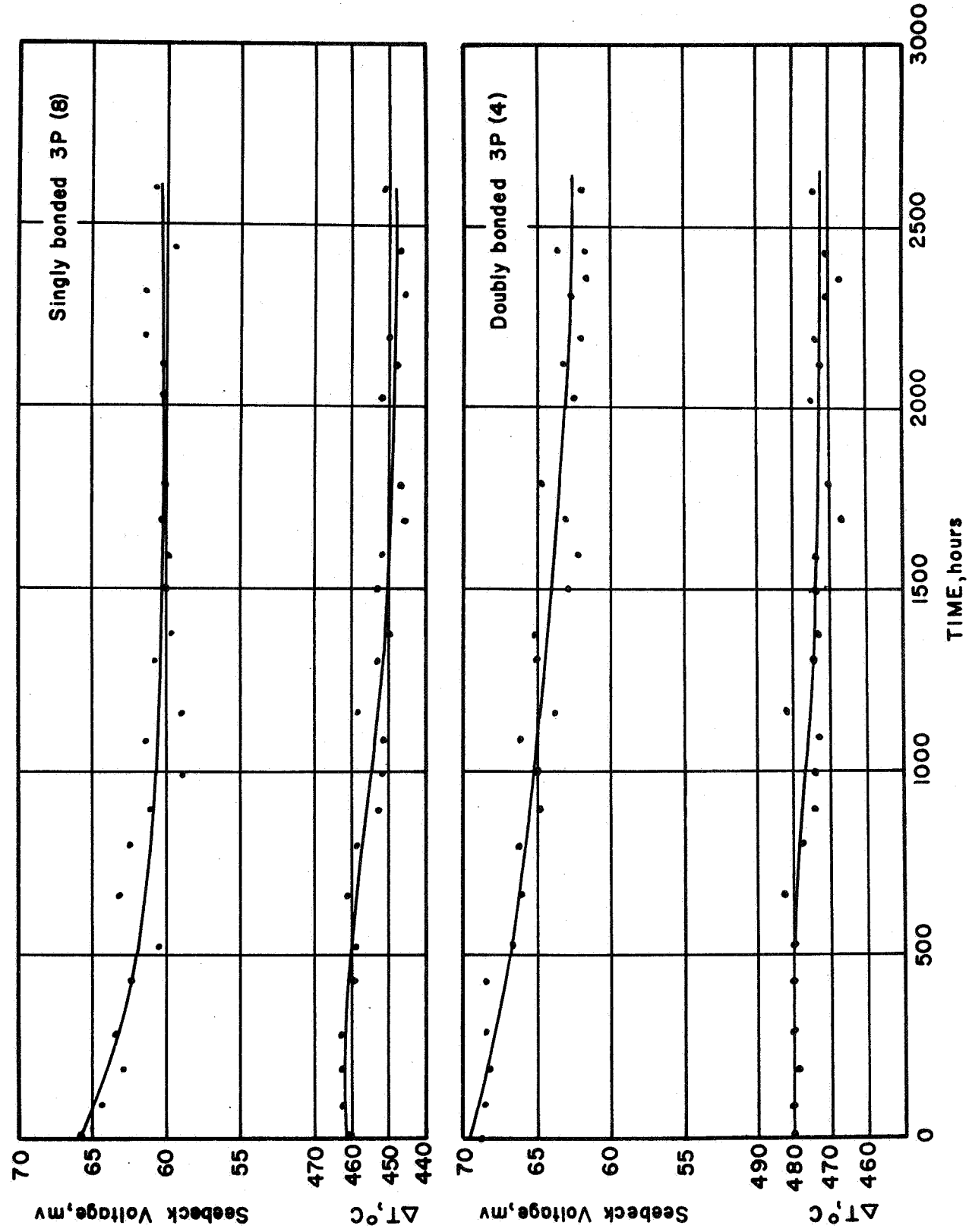

Fig. 36 Variation of Seebeck voltage and ΔT for doubly bonded (W) 3P elements (bottom) and singly bonded (top)

TABLE X

Initial Resistance and Time to Reach 10.2 mΩ Resistance for W-bond 3P Elements (Life-Test IV)

Element	Initial Resistance (510° - Tc) mΩ	Time to 10.2 mΩ hours
Singly bonded		
6B2P24	5.29	> 2600
6A3P24	5.72	1850
6B1P24	5.27	> 2600
6H3P24	5.43	> 2600
2Z10P9	6.02	1200
6B6P24	4.92	500
6H2P24	8.01	300
4K7P17	5.94	300
Doubly bonded		
2Z16P9	5.47	2200
6H4P24	5.68	2200
6B5P24	7.25	1900
4I10P15	6.04	1350

TABLE XI

Changes in Seebeck Voltage of Gradient Tested
3P Elements (Life Test IV)

	Initial Voltage mv	Voltage at 100 hrs * mv	%	Voltage at 2500 hrs * mv	%
Unbonded (3)	66 *	61	7.6	59.2	10.3
Singly-bonded (8)	66	60.8	7.9	60.7	8
Singly-bonded (3)	65.5	62	5.3	59.7	8.9
Doubly-bonded (4)	69.5	65.0	6.5	62.7	9.8

* Corrected for decrease in ΔT from initial value.

resistance of the unbonded elements went down, while that of the bonded elements went up substantially. Since it is known that there is no potential for chemical interaction between the electrodes and elements, it must be considered that the bonded elements behave in approximately the same manner as do the unbonded.

The assumption that the bonding to W takes place by formation of a substoichiometric lead tungstate (a lead tungsten bronze) may serve as an aid to understanding the behavior of the bonded elements. If oxygen diffuses to the hot contact in sufficient amounts to make up the oxygen deficiency in the lead tungsten bronze, then the junction will become highly resistive, since the stoichiometric lead tungstate, $PbWO_4$, is an insulator. Tables IX and X show that there is no apparent feature to distinguish elements which remain low in resistance from those which increase rapidly.

It must be kept in mind that the results of this test should not be regarded as typical. Life test III was terminated by a failure which flooded the interior of the system with water while the system was still at a temperature of 200-300°. The system was heated to a 600° hot side temperature under argon, power to the heater was shut off, and the system evacuated. This was repeated five times. (Heat-up under vacuum is not possible because the heater operates at a too high temperature in vacuum to produce the 600° hot junction.) It is somewhat questionable whether this treatment was sufficient to restore the water vapor level to what it had been previous to the flooding of the system. The presence of water vapor (i.e. oxygen) is believed to have a pronounced effect on the W-diffusion bonds. And indeed when the results of life test III are compared with those of the first 1000 hours of life test IV this would seem to be borne out.

The initial average resistance of the twelve bonded elements of life test IV was 5.95 mΩ. At 800 hours, the minimum average resistance was 8.30 mΩ. This is assuming that the three elements which were over 10.2 mΩ at this time were only 11 mΩ. This to be compared with an increase from 5.70 mΩ to 6.70 mΩ in 800 hours for the P elements of life test III.

B. Isothermal Life Testing

1. Testing of W-Bonded 3N and 3P at 600°

During this period an isothermal life-test of 4700 hours at 600°C was concluded. Twelve bonded n-type elements, ten bonded p-type elements, two Si-Ge-PbTe segmented n-type elements, and two p-type Si-Ge-PbSnTe elements were tested.

Tables XII and XIII show the initial and final contact resistances of the n and p-type elements respectively. Seven out of the original twenty-six n-type bonds failed; only one of the original fifteen low-resistance p-type bonds remained bonded. All of the p-type elements and electrodes showed considerable oxidation, while a few of the n-type elements had light tan or purple oxide films on the electrodes.

The average values of the n-type contact resistances are listed at the bottom of Table XII, excluding the two segmented elements. While the averages show an approximate doubling of contact resistance, it should be noted that five contacts remained virtually the same or even decreased slightly in resistance.

The bulk element resistances and Seebeck voltages of the tested n-type elements are listed in Table XIV. Average values of these parameters are shown in Table XV. Elements which lost one or more bonds during testing appeared to have lower resistances after testing. The average values for both groups are shown, as well as the over-all averages for all the elements from the same runs (2X, 2Y, 3G, 3H, and 3I).

There is a definite indication, in any case, of a decrease in element resistance and a slight increase in Seebeck voltage. On the average, the effect of this period of life testing on the n-type elements with bonds that remained intact was to change the total resistance (including contacts) from 0.708 mΩ to 0.688 mΩ and the Seebeck voltage from about 78 mv to about 82 mv (T_n = 500°, T_c = 25°, versus copper).

Table XVI lists the individual element resistances and Seebeck voltages of the life-tested p-type elements. The average values for the tested elements and a control group of elements from the same bonding

TABLE XII

Contact Resistances of N-Type Elements
Life-tested at 600°C

	Initial		4700 hours	
Element	Top	Bottom	Top	Bottom
	μ Ω	μ Ω	μ Ω	μ Ω
2Y19N9	30	60	190	60
2Y18N9	35	50	120	140
2Y17N9	50	40	100	40
2X17N6	55	60	55	160
2X15N6	45	70	175	140
3G9N11	90	40	70	50
3G8N11	60	60	160	--
3H2N11	60	65	---	40
3I4N11	40	40	---	--
3G3N11	40	60	---	--
3T2NI (Si-Ge)	--	10	---	30
3T3NI (Si-Ge)	--	10	---	10
3HIN11	50	80	---	120
3I5N11	40	50	100	280
Average Value:	50	60	120	115

TABLE XIII

Contact Resistance of Life-Tested P-Type Elements

Element	0 hours		4700 hours	
	Top	Bottom	Top	Bottom
	$\mu\Omega$	$\mu\Omega$	$\mu\Omega$	$\mu\Omega$
2Z20P9	60		--	--
2Z15P9		60	--	--
2Z14P9	100	50	--	--
2Z12P9	90	100	--	--
2Z5P9	65	75	--	--
2Z4P9	90		--	--
3E10P11		90	--	--
3E8P11	140	80	--	--
3J5P11	140	80	--	275
3J1P11	70	95	--	--
3M1PI (Si-Ge)	30	---	--	--
3M3PI (Si-Ge)	50	---	--	--

TABLE XIV

Element Resistance and Seebeck Voltage of Life-Tested N-Type Elements

Element	R_e (0 hours)	R_e (4700 hours)	S_{500} (4700 hours)
	mΩ	mΩ	mv
2Y19N9	.538	.510	82
2Y18N9	.541	.530	80
2Y17N9	.543	.540	80.5
2X17N6	.755	.735	80.5
2X15N6	.715	.565	87.5
3G9N11	.590	.610	79
3I5N11	.510	.380	81.5
3G8N11	.520	.290	79
3H2N11	.495	.470	77
3I4N11	.530	.226	81
3G3N11	.540	.320	82.5
3H1N11	.490	.272	79

TABLE XV

Average Values of Element Resistance and Seebeck Voltage for Life-Tested N-Type Elements

Element Type	R_o	R_{4700}	S
	mΩ	mΩ	mv
Bonded-tested	.600	.553	81.6
Bond(s) lost-tested	.515	.316	79.6
All tested	.656	.455	80.8
Bonded-untested	.583	___	77.7

TABLE XVI

Element Resistance and Seebeck Voltage of Life-Tested P-Type Elements

Element	R_e (0 hours)	R_e (4700 hours)	S (4700 hours)
	mΩ	mΩ	mv
2Z20P9	1.370	.393	68.5
2Z15P9	1.420	.417	73.5
2Z14P9	1.420	.408	73.5
2Z12P9	1.410	.920	72
2Z5P9	1.265	.324	74
2Z4P9	1.225	.482	66
3E10P11	1.460	1.575	73
3E8P11	1.280	.582	73.5
3J5P11	1.530	1.920	73
3J1P11	1.485	1.053	73
3J13P11	1.290	.310	75

runs with no testing are shown in Table XVII. The tested elements, in similar fashion to the n-type elements with contacts that failed, show a post-test resistance which is approximately half the original value. Individual control elements are listed in Table XVIII, number in parentheses indicating the number of bonds on the element.

There appears to be a relation between the bonds and the value of resistance measured. It can be seen by comparing elements from the same run in Table XVI and Table XVIII that there is no correspondence in resistance (for example 3E10 and 8 with 3E9 and 3). Subsequent experiments were done with unbonded elements and elements measured with bonds and after removing the bonds. These measurements revealed that resistance measurements of unbonded elements were highly variable. Their average resistance, merely indicated by the measurements on the life-tested elements, tended to be less than half that of similar bonded elements. Resistances of unbonded elements corresponded to bonded elements when dummy (that is nonbonded) tungsten electrodes were placed on the ends of the elements in the measurement jig. Indium disks were used in the interfaces between the element and electrodes, and the tungsten electrodes and the current electrodes of the resistance jig. Measurements were made in the same manner in these experiments as in the measurements of the tested samples; that is, the voltage probes were on the element itself.

This inaccuracy in the resistance measurements of unbonded elements is apparently the result of some peculiarity in the current distribution within the samples when the samples are measured by themselves.

2. Isothermal Testing at 525°C

Life testing of tungsten-bonded 3P elements has been done recently at 525°C. The junctions tested were prepared during this period under what we feel were improved conditions. This is indicated at least, by lower average contact resistances. Three batches of elements

TABLE XVII

Average Values of Element Resistance and Seebeck Voltage of Life-Tested and Control P-Type Elements

Element type	R_o mΩ	R_{4700} mΩ	S mv
All tested	1.378	0.762	72.3
Untested	0.994	-----	71.7

TABLE XVIII

Element Resistance and Seebeck Voltage of Untested P-Type Control Elements

Element	R_o mΩ	S mv
2Z3P9 (2)	1.745	70
2Z17P9 (2)	1.620	66
3E3P11 (1)	0.434	73
3E9P11 (0)	0.493	73
3J2P11 (2)	1.145	73
3J8P11 (1)	0.525	75

have been tested and measured, thus far, for periods of 1000, 2000, and 3000 hours, respectively. The junctions displaying satisfactory contact resistance have all been put back on test to accumulate further time.

Results of these tests are given in summary form in Tables XIX through XXI. Detailed results are tabulated in Appendix 3. The methods employed are the same as those used previously (First Interim Summary Report). Double-wall ampoules are used for all tests over 1000 hours' duration. High vacuum is used for evacuation of the inner ampoule, and high purity argon is backfilled to 400 mm Hg.

The data presented in the above tables have been treated by dividing the elements and junctions according to the post-test value of the contact resistance. Three groupings are used: bonds below 100 $\mu\Omega$; bonds between 100 and 500 $\mu\Omega$; and bonds over 1000 $\mu\Omega$ or those which have failed. Two major points are considered in discussing the data: (1) what was the over-all performance of the bonds and elements under the test conditions; and (2) did the successful bonds (those below 100 $\mu\Omega$) give any indication in their initial properties that they would remain low in resistance. Tables XXII and XXIII contain average values of contact and element resistances calculated from all three batches of elements tested. While it is not entirely legitimate to average elements with 1000 hours and 3000 hours of testing together, comparison of the values from the individual summary tables with these averages shows that there is not a great deal of difference in behavior over this span of testing.

Fifty-nine contacts with thirty-eight elements were tested in this initial series of tests at 525°C. Four intact junctions had to be eliminated because of fracturing of their elements very near the junction. Five elements were eliminated because of cracking. Thus, the averages are based on fifty-five contacts and thirty-three elements. Twenty of the fifty-five junctions remained below 100 $\mu\Omega$ in resistance; an additional sixteen contacts remained below 500 $\mu\Omega$, and nineteen junctions were found to be separated after testing. Tables XIX through XXI show the distribution of

TABLE XIX

Summary of Results of 1000 hour Life-Test at 525°C of W-bonded 3P Elements

Total Bonds Tested	20	
Number < 1000 $\mu\Omega$ (%)	18	(90%)
Number < 100 $\mu\Omega$ (%)	13	(65%)
Ave. Initial C.R., $\mu\Omega$	77	
Post-test Ave. C.R., $\mu\Omega$	98	
Initial C.R. of Bonds < 100 $\mu\Omega$, $\mu\Omega$	73	
Post-test C.R., Bonds < 100 $\mu\Omega$, $\mu\Omega$	78	
Ave. Initial C.R. of Failed Bonds, $\mu\Omega$	--	
Ave. Initial Element Resistance, m Ω	1.785	
Ave. Post-test Element Resistance, m Ω	2.00	
Initial element Resistance for Elements with Bonds < 100 $\mu\Omega$ (post-test), m Ω	1.750	
Post-test Element Resistance of Elements with Bonds < 100 $\mu\Omega$ (post-test), m Ω	2.035	
Post-test Element Resistance of Elements with Bonds > 100 $\mu\Omega$, m Ω	1.97	
Initial Element Resistance for Elements with Bonds > 100 $\mu\Omega$, m Ω	1.76	
Initial Seebeck voltage, 500° - 25°, mv	70	
Post-test Seebeck voltage, mv	70.5	

TABLE XX

Summary of Results of 2000 hour Life-Test
at 525°C of W-bonded 3P Elements

	2000 hours	
Total Bonds Tested	17	
Number < 1000 $\mu\Omega$ (%)	8	(47%)
Number < 100 $\mu\Omega$ (%)	2	(12%)
Ave. Initial C.R., $\mu\Omega$	72	
Post-test Ave. C.R., $\mu\Omega$	295	
Initial C.R. of Bonds < 100 $\mu\Omega$, $\mu\Omega$	87	
Post-test C.R., Bonds < 100 $\mu\Omega$, $\mu\Omega$	80	
Ave. Initial C.R of Failed Bonds, $\mu\Omega$	72	
Ave. Initial Element Resistance, mΩ	1.31	
Ave. Post-test Element Resistance, mΩ	1.65	
Initial element Resistance for Elements with Bonds < 100 $\mu\Omega$ (post-test), mΩ	1.15	
Post-test Element Resistance of Elements with Bonds < 100 $\mu\Omega$ (post-test), mΩ	1.75	
Post-test Resistance of Elements with Bonds > 100 $\mu\Omega$, mΩ	1.50	
Initial Resistanceof Elements with Bonds > 100 $\mu\Omega$. mΩ	1.34	
Initial Seebeck voltage, 500° - 25°, mv	71.5	
Post-test Seebeck voltage, mv	73.5	

TABLE XXI

Summary of Results of 3000 hour Life-Test
at 525°C of W-bonded 3P Elements

	3000 hour	
Total Bonds Tested	22	
Number < 1000 $\mu\Omega$ (%)	10	(45%)
Number < 100 $\mu\Omega$ (%)	5	(23%)
Ave. Initial C.R., $\mu\Omega$	62	
Post-test Ave. C.R., $\mu\Omega$	142	
Initial C.R. of Bonds < 100 $\mu\Omega$, $\mu\Omega$	51	
Post-test C.R., Bonds < 100 $\mu\Omega$, $\mu\Omega$	76	
Ave. Initial C.R. of Failed Bonds, $\mu\Omega$	71	
Ave. Initial Element Resistance, m Ω	1.57	
Ave. Post-test Element Resistance, mΩ	2.05	
Initial element Resistance for Elements with Bonds < 100 $\mu\Omega$ (post-test), mΩ	1.57	
Post-test Element Resistance of Elements with Bonds < 100 $\mu\Omega$ (post-test), mΩ	1.94	
Post-test Resistance of Elements with Bonds > 100 $\mu\Omega$, m Ω	2.21	
Initial Resistance of Elements with Bonds > 100 $\mu\Omega$, mΩ	1.575	
Initial Seebeck voltage, 500° - 25°, mv	74.5	
Post-test Seebeck voltage, mv	73.4	

the numbers of junctions. The 2000 hour test group shows markedly poorer performance than the other two tests. The elements and electrodes of this group showed varying degrees of oxidation, which neither of the other test groups showed. No correlation with three factors within the group of elements — lot of material, bonding run, or single or double encapsulation — could be found. This suggested that oxygen may have intruded during some part of the encapsulation process. The results of this test are therefore somewhat suspect, but are included, nevertheless.

Average element resistances changed upwards considerably in all three tests. The over-all average increase in room temperature resistance was approximately twenty-two percent. Of more interest is that the increases became greater with increased testing. The increases in over-all average element resistance were 12%, 26%, and 30.6% for the 1000, 2000, and 3000 hour groups, respectively.

The Seebeck voltage showed only minor changes in any of the tests — a slight increase in two tests and a decrease in the third. This is in distinct contrast to elements tested under gradient conditions which have shown 10% decreases in Seebeck voltage over periods of 1000 to 2000 hours.

Table XXII indicates that the initial contact resistance cannot be taken as a reliable indicator of performance, under these conditions. While the bonds which remained fairly low in resistance (category II) show a lower initial resistance than those in category III, which increased to over 100 $\mu\Omega$, the bonds which failed (category IV) had exactly the same initial resistance. In fact, those contacts with initial resistances of 60 $\mu\Omega$ or less resulted in behavior comparable to the over-all behavior of the entire group.

The bonded element resistance at room temperature also does not appear to give any indication of the performance of the junctions. Table XXIII shows the average resistances of elements which correspond to categories I, II, and III of Table XXII. The difference in resistance is rather small between elements with contacts that remained below 100 $\mu\Omega$ and those which were greater than 100 $\mu\Omega$. The change in resistance with testing of the two

TABLE XXII

Average Changes in Contact Resistance for
W-3P Bonds Tested at 525°

		$\mu\Omega$	$\frac{CR}{CRo}$
I.	All Contacts		
	Average Initial C.R.	70	1
	Average Post-test C.R. (Bonds < 1000 $\mu\Omega$)	136	1.94
II.	Bonds < 100 $\mu\Omega$ Post-test		
	Average Initial C.R.	67	.96
	Average Post-test C.R.	76	1.09
III.	Bonds < 500 > 100 $\mu\Omega$ Post-test		
	Average Initial C.R.	73	1.04
	Average Post-test C.R.	200	2.86
IV.	Bond Failed or > 1000 $\mu\Omega$ Post-test		
	Average Initial C.R.	68	.96

TABLE XXIII

Average Values of Room Temperature Resistance of
W-Bonded 3P Elements Tested at 525°C for 1000 to 3000 hours

All Elements	m Ω	$\frac{\bar{R}}{Ro}$
Average Initial Element Resitance	1.55	1.0
Average Post-test Element Resistance	1.90	1.22
Elements with Bonds < 100 μ Ω		
Initial Resistance	1.60	1.03
Post-test Resistance	1.95	1.26
Elements with Bonds > 100 μ Ω		
Initial Resistance	1.55	1.00
Post-test Resistance	1.90	1.22

categories of element contacts is equal, 0.35 mΩ. This indicates that the behavior of the contacts is not very closely tied to the behavior of their elements.

Table XXIV illustrates an interesting and important point to be made in connection with the change in resistance of the elements. This table lists the average change with testing for a single contact in the above and below 100 μΩ categories, with the average change in the accompanying element resistance. It is apparent that, in all but one case, the change in the total room temperature element resistance is much larger than the increase in room temperature contact resistance. It has not been established whether this increase in resistance represents an over-all increase in the resistivity of the material which would persist over the entire range of temperature to over 500°, or is merely a distortion of the low temperature variation in resistivity as a result of the high temperature exposure.

Figure 37 is a plot of the percentage variation in contact resistance versus the variation in the element resistance (of the contact) for the 525° isothermally tested elements. These points represent contacts which were below 500 μΩ after testing. There is no apparent relation between the two factors. The 525° test data were then examined for any correlation of behavior of elements and contacts with the bonding run or lor of material. It was found that elements from lot #19 were tested in the 2000 and 3000 hour tests.

The P19 elements in the 2000 hour test showed an average 0.2% increase in element resistance; in the 3000 hour test a 3% increase. The remainder of the elements in the 3000 hour test were from lot P21. Under the same conditions the average increase in element resistance was 35%.

The behavior of the contacts in the 3000 hour test was then compared on the basis of the lot number of the elements. It was found that five out of six contacts to P19 elements increased less than 100%, (only one was this high), while only four out of sixteen contacts to P21 elements increased less than 100%. Eight contacts initially below 100 μΩ either failed or were

TABLE XXIV

Comparison of Changes in Element and Contact Resistance of W-Bonded 3P Elements Tested at 525°C

Test Period	Contacts < 100 μΩ			Contacts < 500 > 100 μΩ		
	Initial	Post-test	Change	Initial	Post-test	Change
1000 hours						
Contacts	.073	.078	.005	.077	.098	.021
Elements	1.750	2.035	.285	1.785	2.020	.235
Total	1.823	2.113		1.862	2.118	
2000 hours						
Contacts	.087	.072	.015	.096	.295	.199
Elements	1.150	1.750	.600	1.1310	1.650	.340
Total	1.237	1.822		1.406	1.945	
3000 hours						
Contacts	.051	.076	.025	.070	.142	.072
Elements	1.570	1.920	.350	1.570	2.050	.480
Total	1.621	1.996		1.640	2.192	

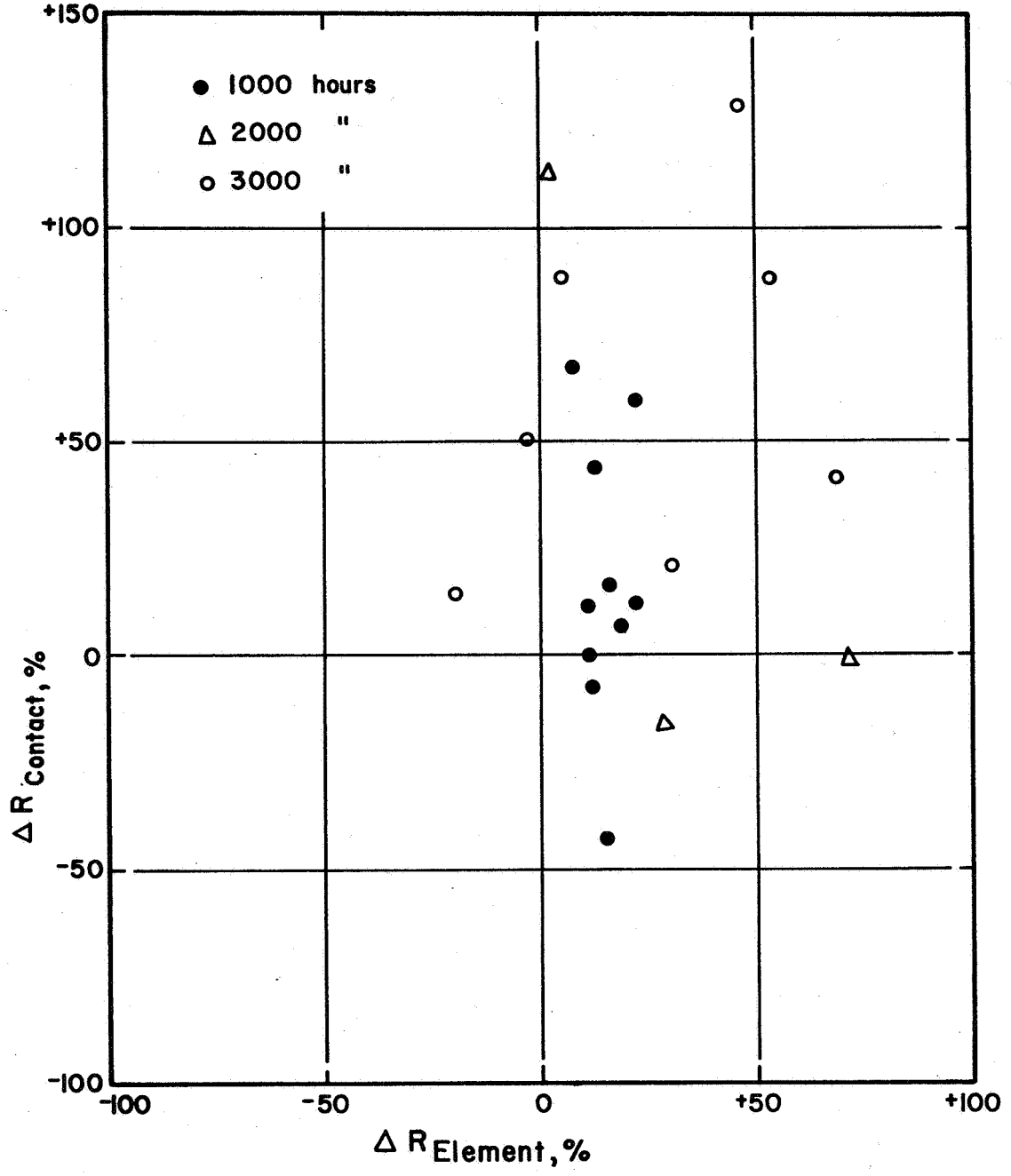

Fig. 37 Variation of change in contact resistance as a function of change in element resistance. Isothermally tested W-bonded 3P elements; 525°C for 1000, 2000, and 3000 hours

over 1000 $\mu\Omega$ after testing. There was no noticeable difference in initial bonding behavior between these lots of material.

Six of the eight bonded p-type elements in gradient life test III were from P19. The five lowest resistance p-type elements were all P19. Since the random probability would favor P19 anyway, it is perhaps more fair to say simply that P19 elements performed fairly well under gradient conditions as well, although they cannot be compared in this case to P21 elements undergoing the same test. What this indicates is that apparently there are differences in the materials which can rather drastically influence the life-time characteristics of the bonded elements. Elements from these two lots, P19 and P21, will be analyzed for over-all composition, impurities, and oxygen content to try to pin-point the significant difference between them. In addition, future testing must be shaped to maintain tests of another variable, the lot of material and its possible effect on life.

VII. REFERENCES

1. M. Weinstein and A. I. Mlavsky, Rev. Sci. Instr. 33, 1119 (1962).

2. H. E. Bates, F. Wald, and M. Weinstein, First Interim Summary Report, Contract NAS9-9149, pp. 76-88.

3. H. E. Bates, F. Wald, and M. Weinstein, Adv. Energy Conv. 7, 183 (1967); (First Interim Summary Report, Contract NAS9-9149, pp. 39-76).

4. I. I. Kornilov, The Chemistry of Metallides (New York: Consultants Bureau, 1966), p. 5.

5. W. Gordy and W. J. O. Thomas, J. Chem. Phys. 24, 439 (1956).

6. G. V. Raynor, "Crystal Structure and Bond Mechanism of Intermetallic Phases," in The Physical Chemistry of Metallic Solutions and Intermetallic Compounds, (New York: Chemical Publishing Co., Inc., 1960), II, 322.

7. F. Wald, "Constitutional Investigations in the Silver-Lead-Tellurium System, J. Less Common Metals, in press, (Seventh Quarterly Report on Contract NAS9-9149).

8. R. W. Fritts, "Lead Telluride Alloys and Junctions," in Thermoelectric Materials and Devices, ed. by I. B. Cadoff and E. Miller, (New York: Reinhold Publishing Corp., 1960), pp. 156-62.

9. L. S. Darken and R. W. Gurry, Physical Chemistry of Metals (New York: McGraw-Hill Book Co., 1953), pp. 206-94.

10. J. H. Hildebrand and R. L. Scott, The Solubility of Nonelectrolytes, 3rd ed. (New York: Dover Publications, Inc., 1964), pp. 320-45.

11. O. Kubaschewski and E. L. L. Evans, Metallurgical Thermochemistry (New York: Pergamon Press, 1958), pp. 32-213.

12. P. S. Rudman, Analysis of Phase Diagrams for Thermodynamic Data, Abstract Bulletin of the Institute of Metals Division, The Metallurgical Society, Fall Meeting, 1967, pp. 66-67.

13. N. Elsner, General Atomics Corp., personal communication.

14. R. L. Novak, Westinghouse Astronuclear Laboratory, personal communication.

15. B. Swanson, E. Somers, and R. Heikes, J. Heat Trans. 83, 77 (1961).

16. R. Ure and R. Heikes, in Thermoelectrocity: Science and Engineering, (New York: Wiley-Interscience, Inc., 1961), p. 491.

17. R. Moore, Adv. Energy Conv. 2, 183 (1962).

18. Data on Si-Ge taken from T. Nystrom, Paper #9, Proc. IEEE/AIAA Thermoelectric Specialists Conf., 1966. PbTe alloy data taken from 3M's data sheets of July 1966.

APPENDIX 1

ABSTRACTS OF PAPERS PUBLISHED IN THE OPEN LITERATURE

(1) Journal of the Less Common Metals 13 (6), 579-590, (1967).

CONSTITUTIONAL INVESTIGATIONS IN THE SILVER-LEAD-TELLURIUM SYSTEM

F. Wald

Tyco Laboratories, Inc.
Waltham, Massachusetts

The phase diagram of the pseudobinary section Ag_2Te-PbTe has been determined. A large eutectoidal region was found on the Ag_2Te side stabilizing the high temperature b. c. c. from of Ag_2Te at temperatures as low as 475°C. Surveys in other areas of the system revealed only one other pseudobinary section, at lower temperatures between Ag_5Te_3 and PbTe.

Electrical measurements showed that alloys of PbTe containing 3-4 mol % of "AgTe" were p-type; along the Ag_2Te-PbTe and Ag_5Te_3-PbTe sections, alloys with similar concentrations of these silver compounds were n-type. Some of the alloys show reasonable thermoelectric properties.

(2) Transactions of the Metallurgical Society of AIME, in press*.

ON THE CONSTITUTION OF THE PSEUDOBINARY SECTION LEAD TELLURIDE-IRON

F. Wald and R. W. Stormont

Tyco Laboratories, Inc.
Waltham, Massachusetts

The phase diagram of the pseudobinary section PbTe-Fe was determined.

It was found to contain both monotectic and eutectic reactions, the latter taking place at 14 at % Fe and 875 $\pm$ 5°C. The solid solubility of Fe in PbTe was found to be 0.3 at % by electronmicroprobe analysis. No solubility of PbTe was detected in Fe.

Slight deviations from true pseudobinary behavior were found to occur in the range of ~ 5-10 at % Fe.

---

* to appear in issue of December 1967.

(3) Transactions of the Metallurgical Society of AIME, in press.

THE PSEUDOBINARY SECTION OF PbTe AND Au

Dennis Mottern
Sandia Corporation
Albuquerque, New Mexico

and

Fritz Wald
Tyco Laboratories, Inc.
Waltham, Massachusetts

The constitution of the pseudobinary section PbTe-Au was determined. The system was found to be a simple eutectic one with a eutectic temperature of 742 $\pm$ 5°C at 42 at % Au, 58 mol % PbTe. No solubility of Au in PbTe was found.

APPENDIX 2

PARTS LIST AND DRAWINGS FOR PbTe AND SEGMENTED COUPLE TESTERS

This appendix contains detailed drawings of all the mechanical components of the sixteen couple life-tester for PbTe couples. Many of these parts are common to the Si-Ge-PbTe segmented couple measurement device, since the segmented couple tester is essentially a single station from the sixteen couple tester. A parts list for the segmented couple tester is included after the drawings. Schematic circuit diagrams of the heater power controller for the couple tester are also included.

PARTS LIST - PbTe COUPLE LIFE TESTER

Dwg. No.	Description
1.	Baseplate
2A.	Heatsink rod, right hand
2B.	Heatsink rod, left hand
3.	Heatsink jacket
4.	Heatsink insulator
5.	Heater bracket plate
6.	Heater assembly
7.	Heater bracket
8.	Insulating sleeve
9A.	Teflon washer
9B.	Steel washer
10.	Heatsink nut
11.	Bearing rod
12.	Bearing plate
13.	Bearing nut
14.	$\frac{1}{2}$" O-ring
15.	$\frac{1}{4}$" O. D. Copper tubing
16.	Plastic to copper compression fitting
17.	Polyethylene tubing
18A.	Inlet manifold
18B.	Outlet manifold
19.	$\frac{1}{4}$" Copper elbow
20.	Thermocouple plate spring
21.	Thermocouple spring rod
22.	Heater pressure rod
23.	Thermocouple rod nut
24.	Heater pivot spring
25.	Thermocouple spring (heater)
26.	Thermocouple cap
27.	Thermocouple insulator plate
28.	Thermocouple insulator
29.	Heater pressure spring
30.	Bell jar gasket
31A.	Outgas fitting
31B	Outgas fitting nut
31C.	Outgas fitting spacer
31D.	Outgas fitting O-ring $\frac{1}{4}$" I. D. (0. 071" diameter)
32A.	Electrical feedthru nut
32B.	Electrical feedthru
32C.	Feedthru insulating washer
32D.	Feedthru insulating sleeve

PARTS LIST - PbTe COUPLE LIFE TESTER Cont' d

Dwg. No.	Description
33.	Thermocouple transducer gland
34A.	Vacuum fitting
34B	Vacuum fitting nut
34C.	O-ring retainer
34D.	O-ring 1" I. D. (0. 071" diameter)
35.	Bell jar ring
36.	Bell jar ring nut
37.	Spring plate

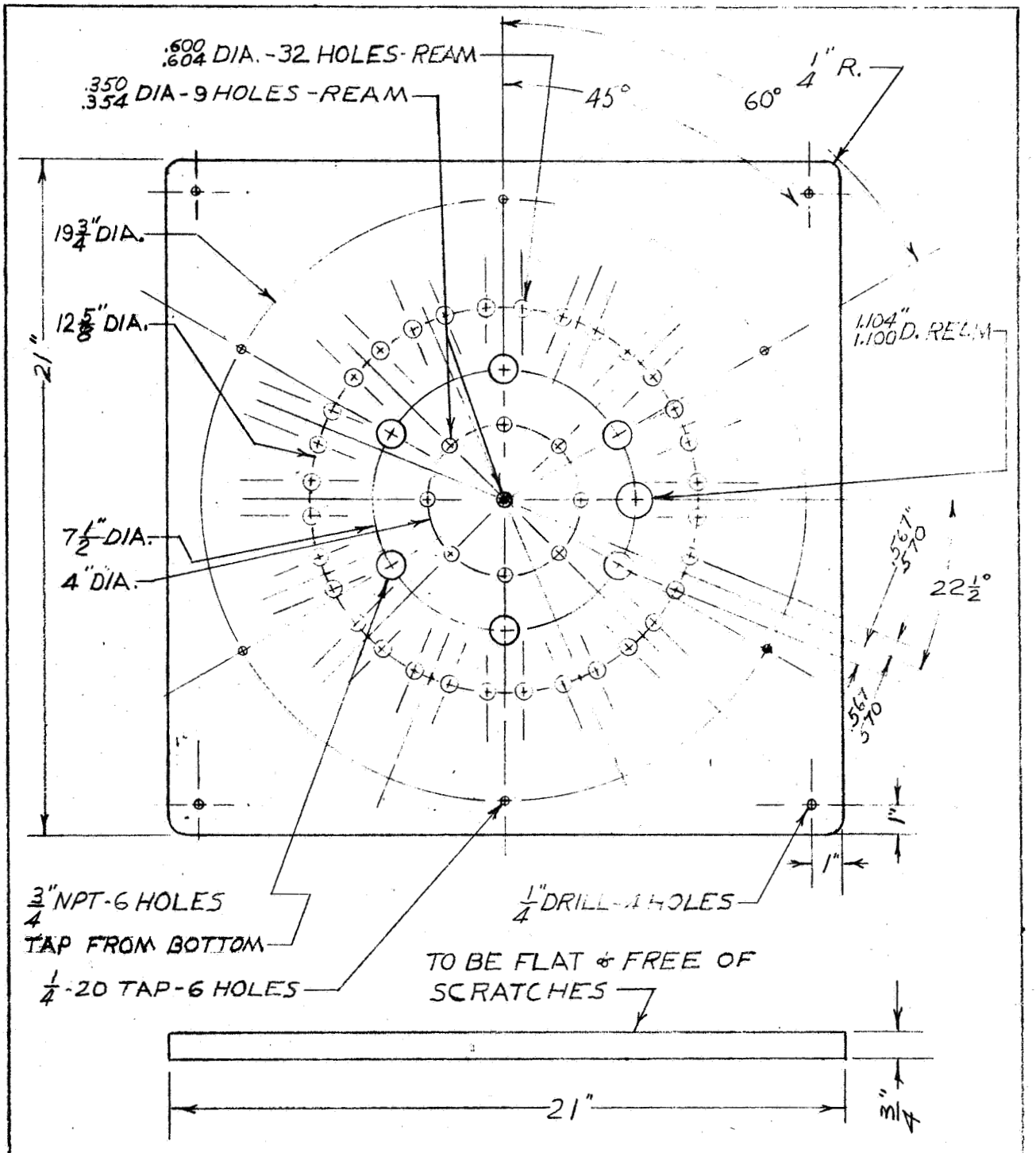
.600 / .604 DIA. - 32 HOLES - REAM
.350 / .354 DIA - 9 HOLES - REAM
45°
60°
1/4" R.
19 3/4" DIA.
12 5/8" DIA.
7 1/2" DIA.
4" DIA.
21"
1.104" / 1.100 D. REAM
.567 / .570
22 1/2°
1"
3/4" NPT - 6 HOLES
TAP FROM BOTTOM
1/4 - 20 TAP - 6 HOLES
1/4" DRILL - 4 HOLES
TO BE FLAT & FREE OF SCRATCHES
21"
MATERIAL: BRASS (YELLOW)
PCS. REQ'D : 1
(1) BASE PLATE

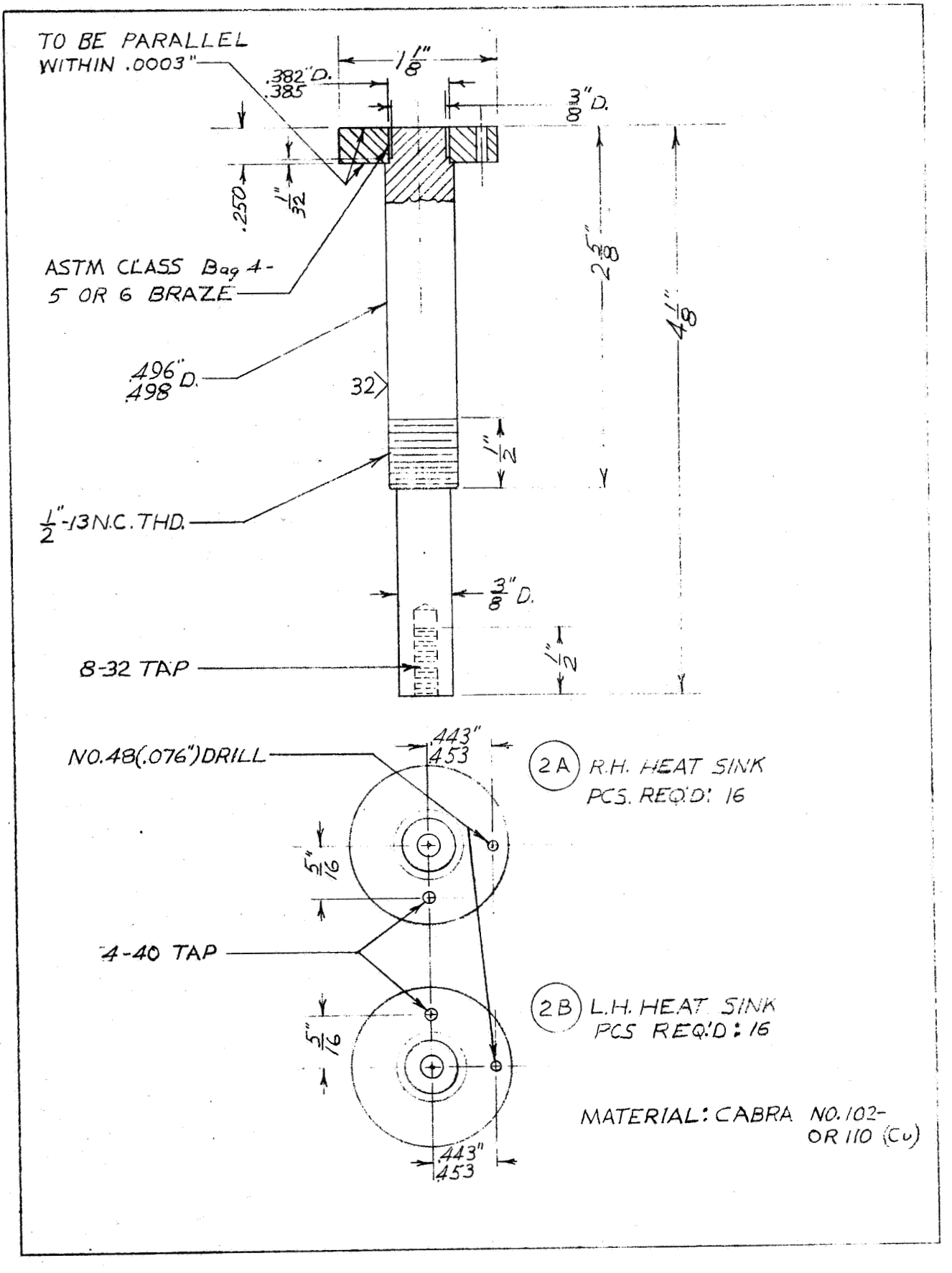
TO BE PARALLEL WITHIN .0003"
1 1/8"
.382" D. .385
.250
1/32"
ASTM CLASS Bag 4-5 OR 6 BRAZE
.496" D. .498
32
1/2"
1/2"-13 N.C. THD.
3/8" D.
8-32 TAP
1/2"
2 5/8"
4 1/8"
NO. 48 (.076") DRILL
.443" .453
5/16"
4-40 TAP
2A R.H. HEAT SINK
PCS. REQ'D: 16
2B L.H. HEAT SINK
PCS REQ'D: 16
MATERIAL: CABRA NO. 102- OR 110 (Cu)

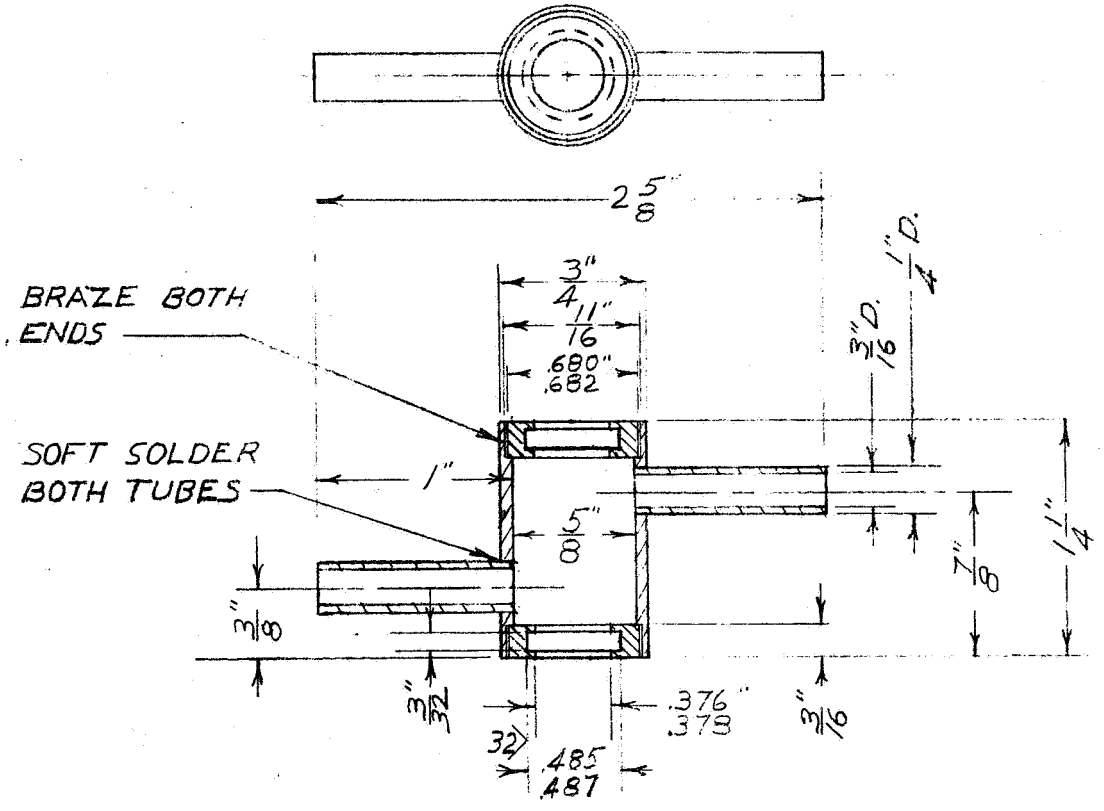

MATERIAL : COPPER
PCS. REQ.'D :32

(3) HEAT SINK JACKET

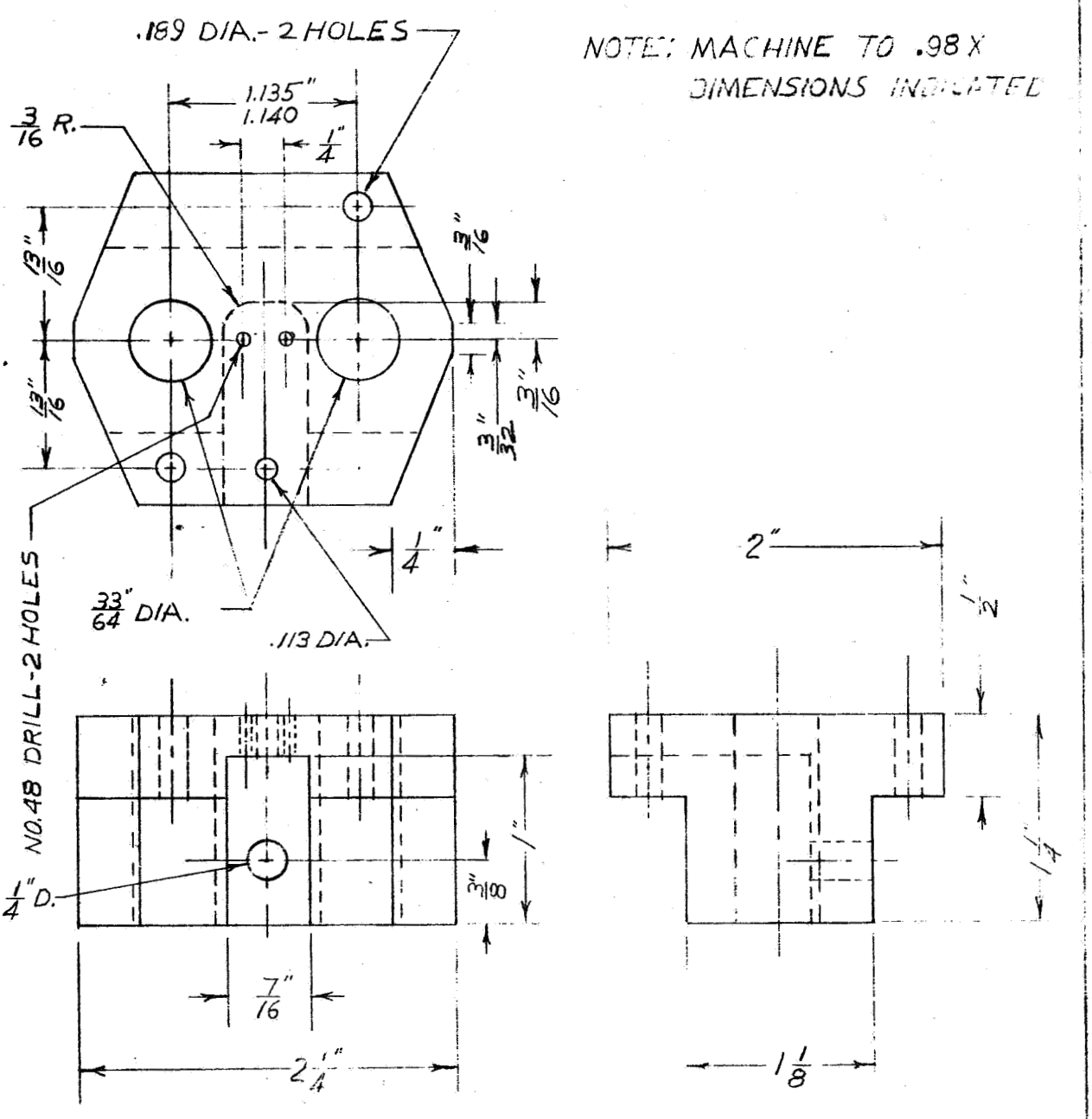

MATERIAL: FIRED LAVA

PCS. REQ'D: 16

(4) HEAT SINK INSULATOR

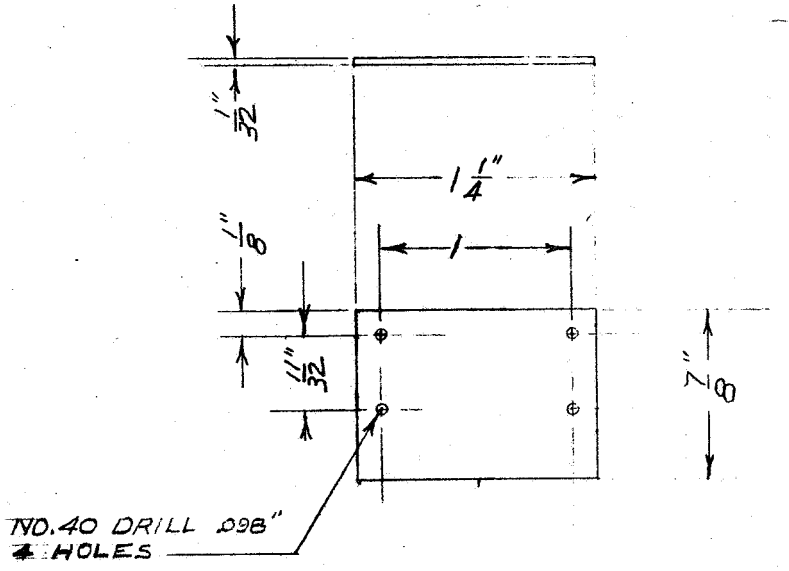

MATERIAL: ST. ST.
PCS. REQ'D: 32

(5) HEATER BKT. PLATE

Pt Rh - 24 GAGE - 20 TURNS
.135" O.D.

NOTE: MACHINE LAVA PARTS TO .98 X DIMENSIONS INDICATED

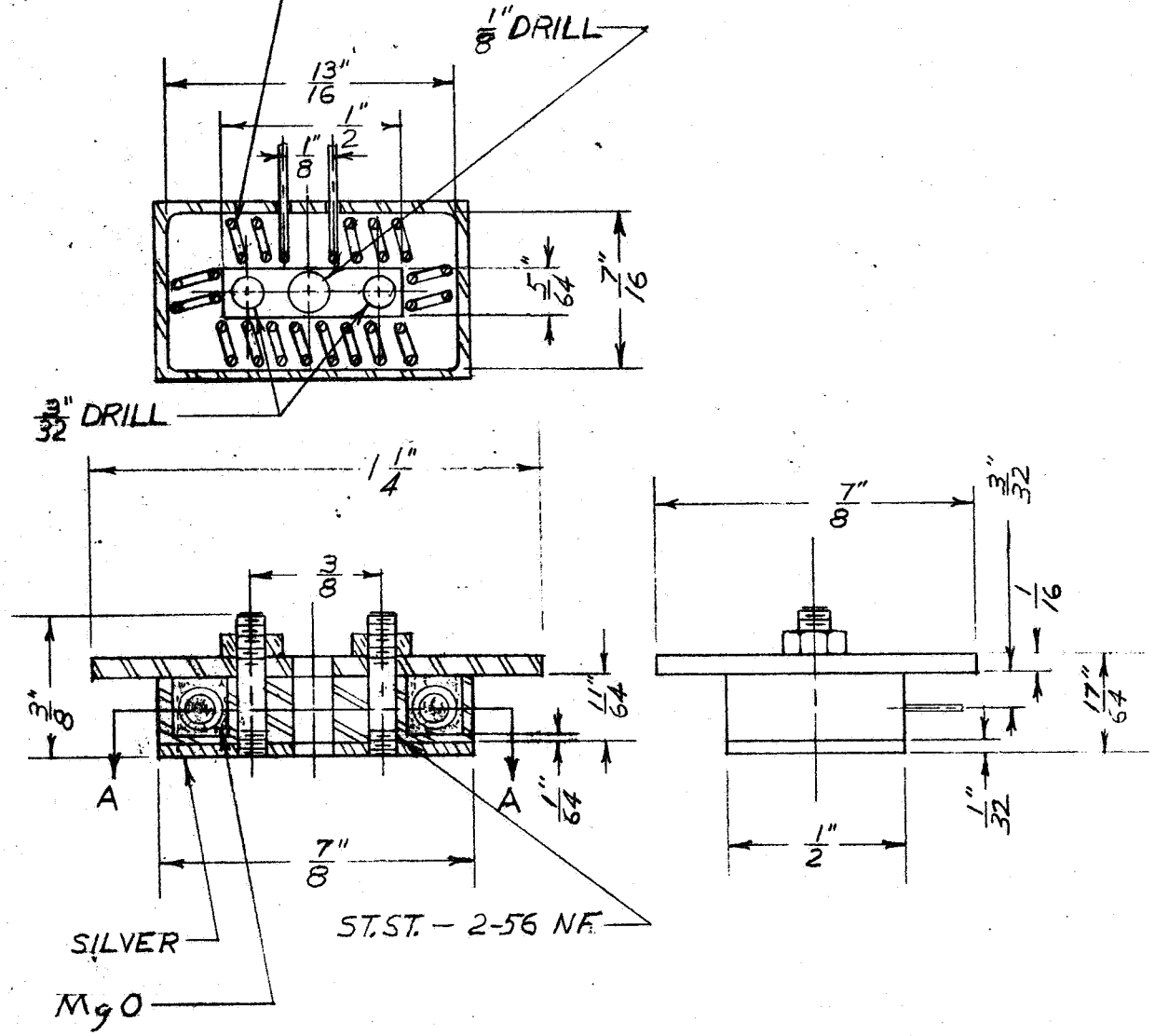

MATERIAL: FIRED LAVA EXCEPT WHERE OTHERWISE INDICATED

PCS. REQ'D: 1

(6) HEATER ASSEM.

NOTE: MACHINE TO .98 X DIMENSIONS INDICATED

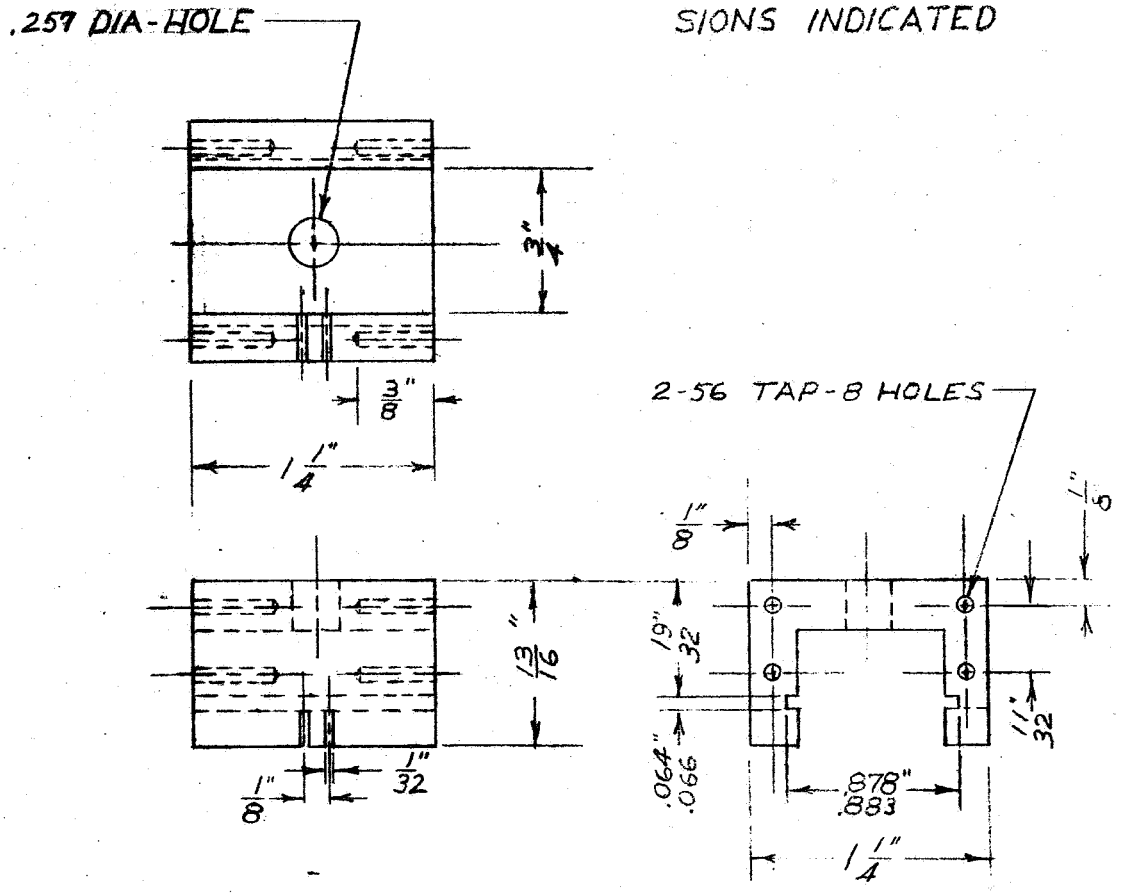

MATERIAL: FIRED LAVA

PCS. REQ'D: 16

(7) HEATER BRACKET

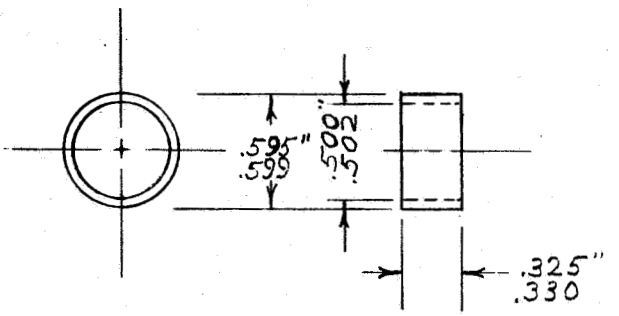

MATERIAL: TEFLON
PCS. REQ'D: 64

(8) INSULATING SLEEVE

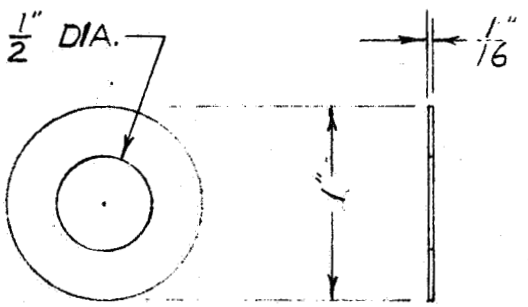

PART NO.	PCS. REQ'D	MAT.
9A	32	TEFLON
9B	32	STEEL

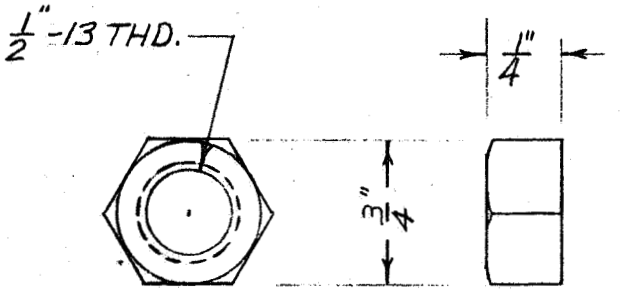

MATERIAL: STEEL
PCS. REQ'D : 32

(10) HEAT SINK NUT

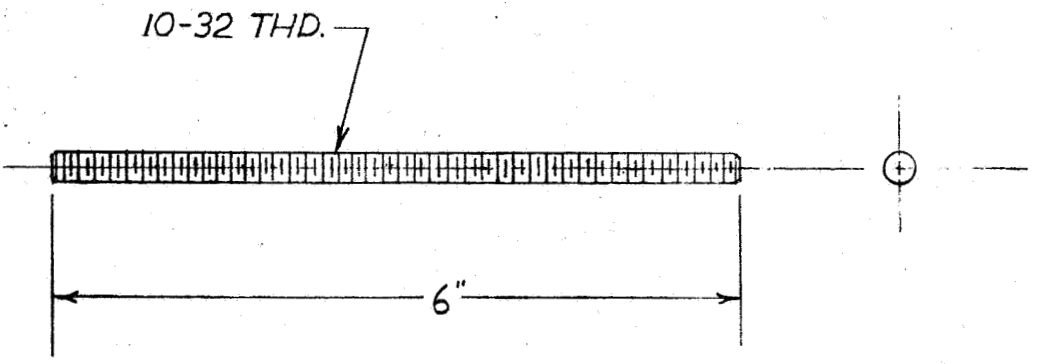

MATERIAL: ST. ST.
PCS. REQ'D: 32

(11) BEARING ROD

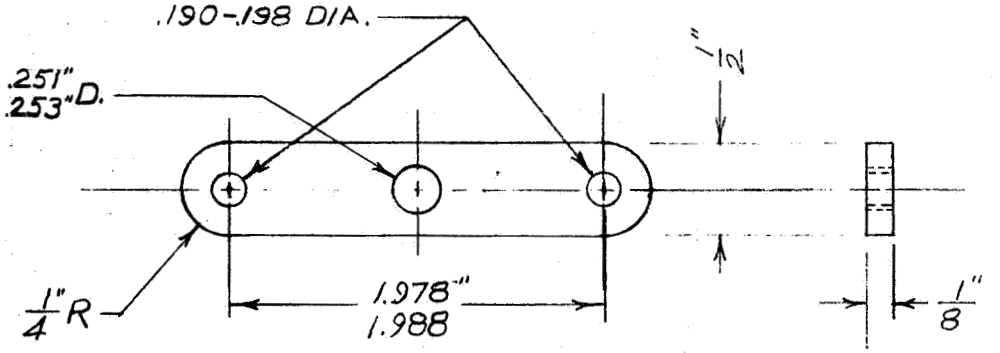

MATERIAL: ST. ST.
PCS. REQ'D: 32

(12) BEARING PLATE

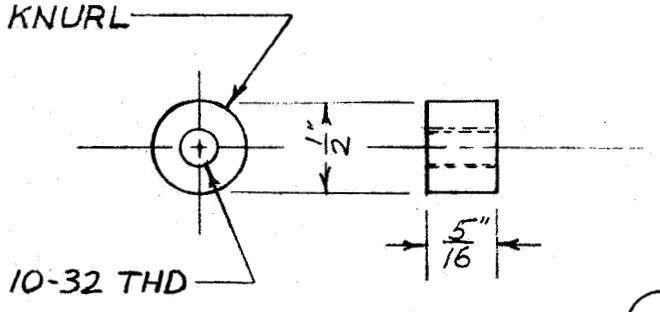

(13) BEARING PLATE NUT

MATERIAL: ST. ST.
PCS. REQ'D: 64

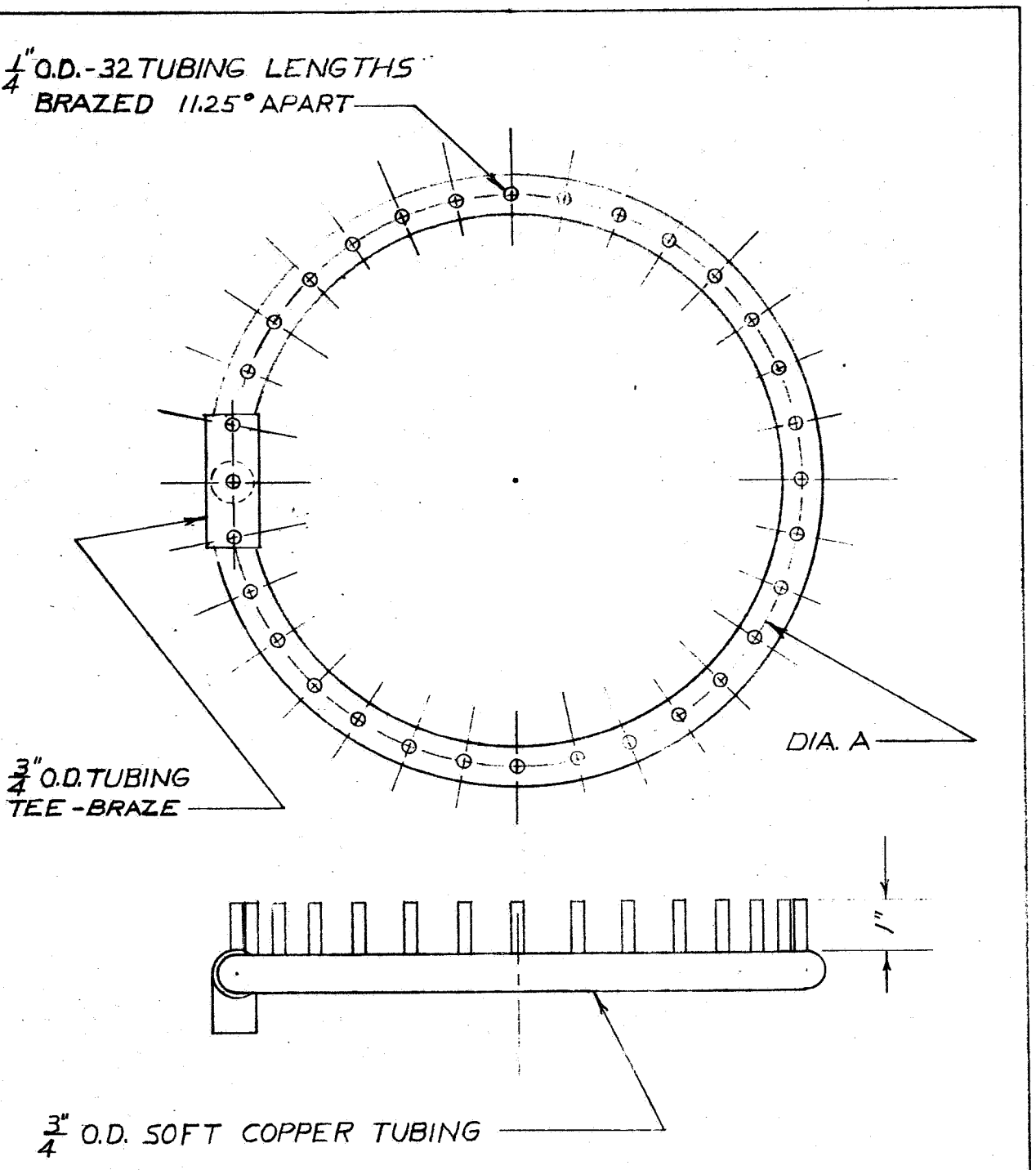

PART NO.	DIA. A	PCS. REQ'D
18 A	10.0"	1
18 B	16.5"	1

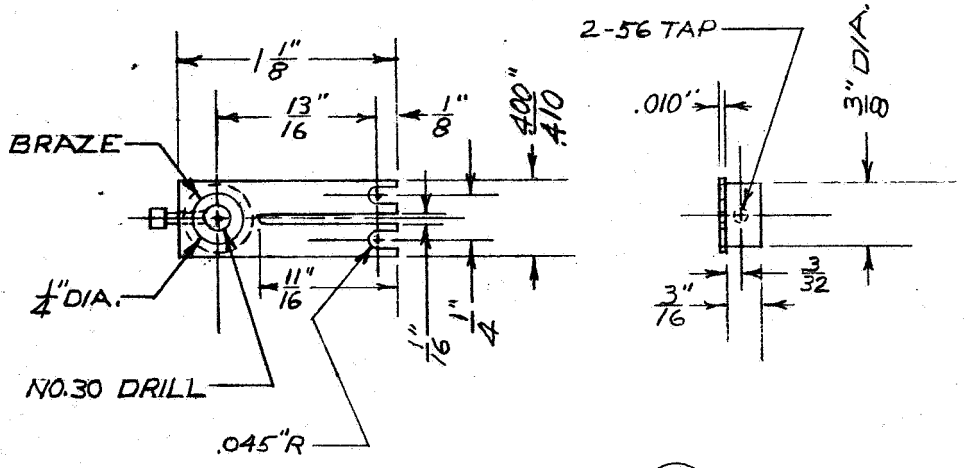

MATERIAL: BERYLIUM COPPER
PCS. REQ'D: 16

(20) T.C. SPRING

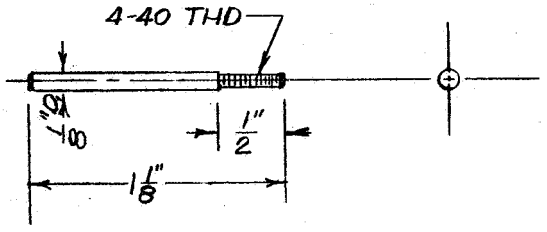

MATERIAL: STEEL
PCS. REQ'D: 16

(21) T.C. SPRING ROD

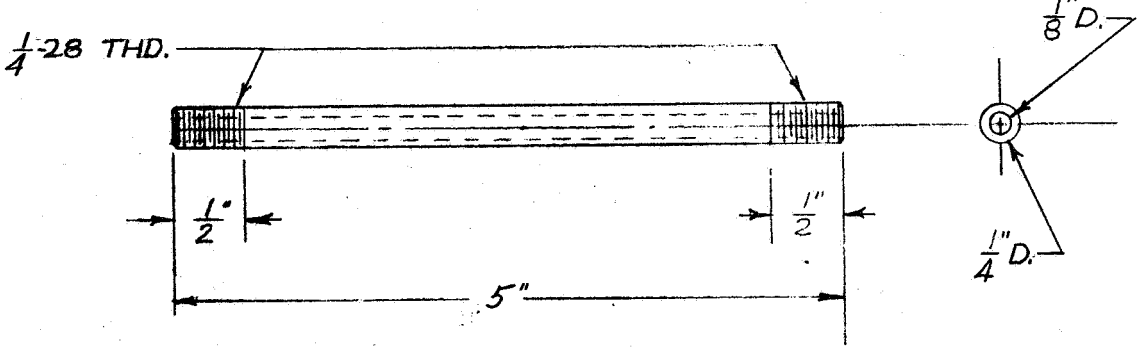

MATERIAL: ST.ST.
PCS. REQ'D: 16

(22) SPRING ROD

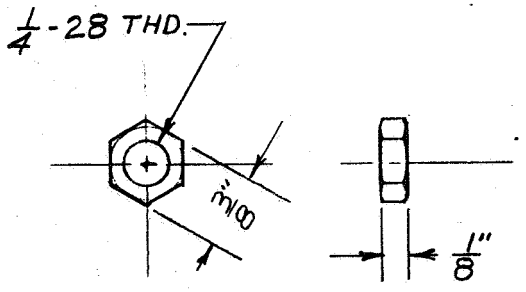

(23) T.C. ROD NUT

MATERIAL: ST. ST.
PCS. REQ'D: 32

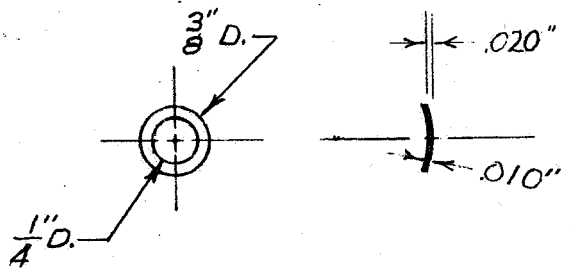

(24) HEATER SPRING

MATERIAL: ST. ST.
PCS. REQ'D: 16

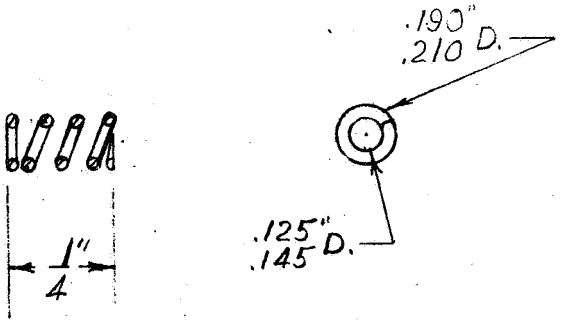

MATERIAL: SPRING STEEL
COMPRESSION: .25 LBS.
PCS. REQ'D: 16

(25) T.C. SPRING

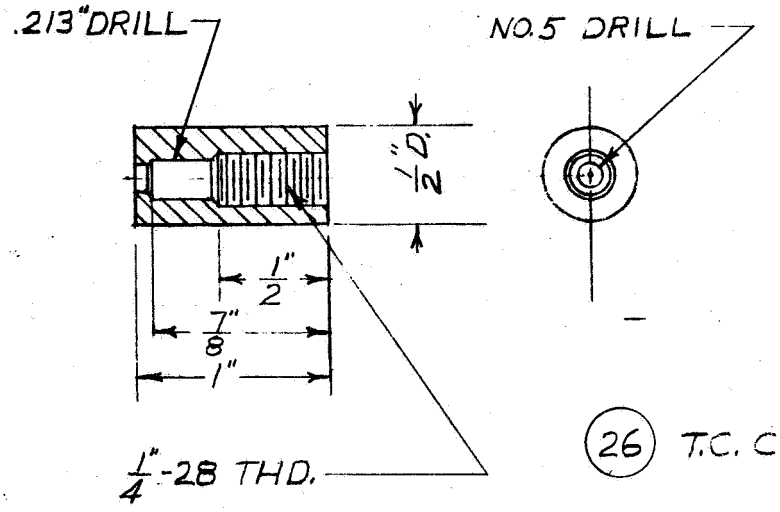

(26) T.C. CAP

MATERIAL: ST. ST.
PCS. REQ'D: 16

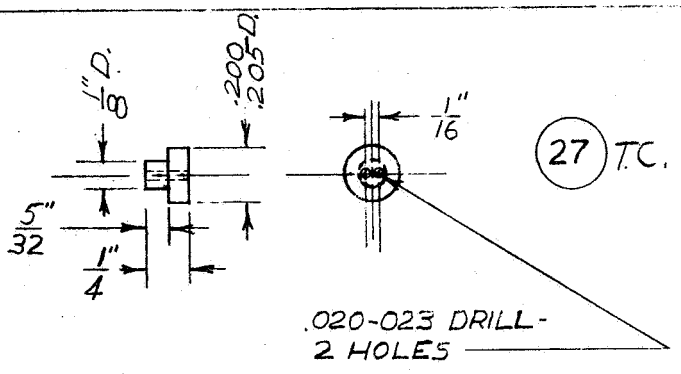

(27) T.C. INSULATOR PLATE

MATERIAL: FIRED LAVA
PCS. REQ'D: 16

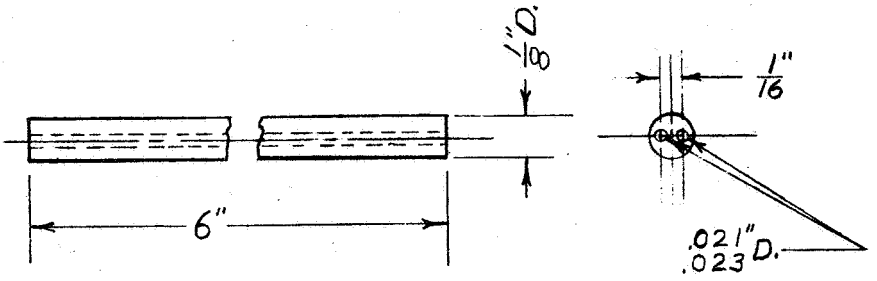

MATERIAL: CERAMIC
PCS. REQ'D: 16

(28) T.C. INSULATOR

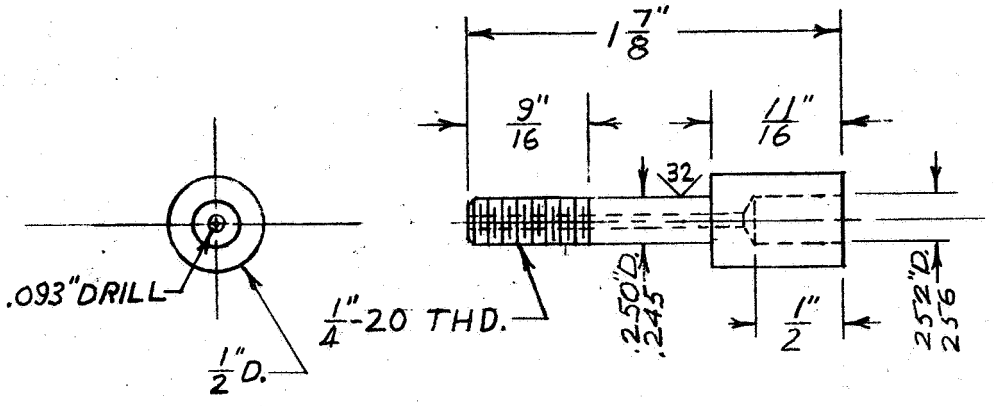

31A OUTGAS FITTING
MATERIAL: BRASS
PCS. REQ'D: 1

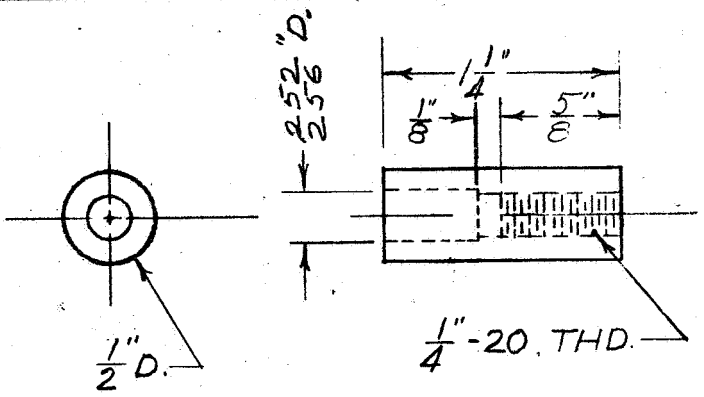

31B OUTGAS FITTING NUT
MATERIAL: BRASS
PCS. REQ'D: 1

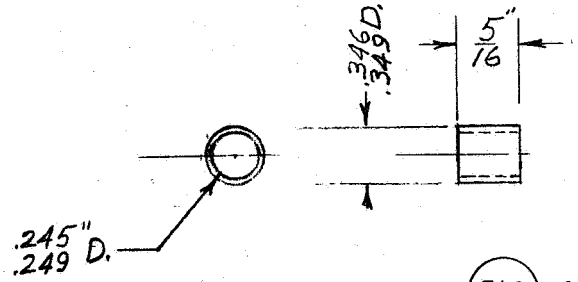

31C O.F. SPACER
MATERIAL: BRASS
PCS. REQ'D: 2

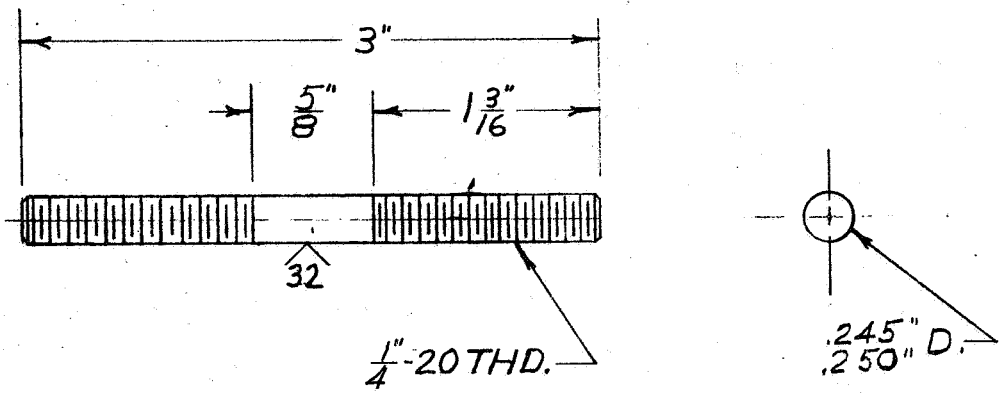

(32A) ELECT. FEED THRU

MATERIAL: COPPER
PCS. REQ'D: 8

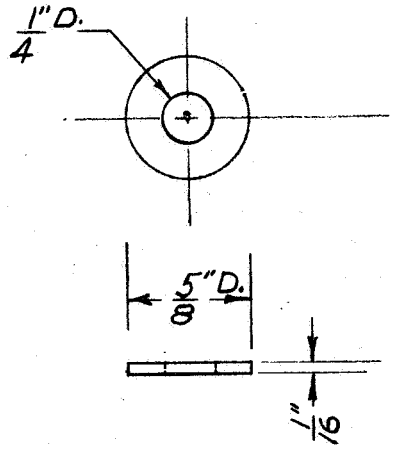

(32B) FEED THRU INSU. WASH.
MATERIAL: TEFLON
PCS. REQ'D: 16

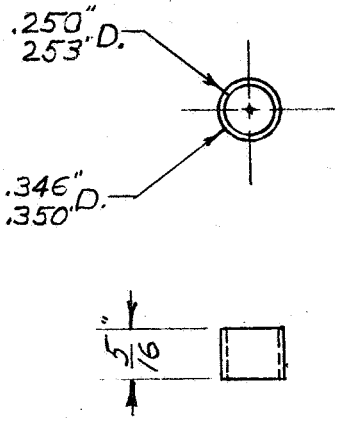

(32C) F.T. INSU. SLEEVE
MATERIAL: TEFLON
PCS. REQ'D: 16

(34A) VACUUM FITTING
MATERIAL: BRASS
PCS. REQ'D: 1

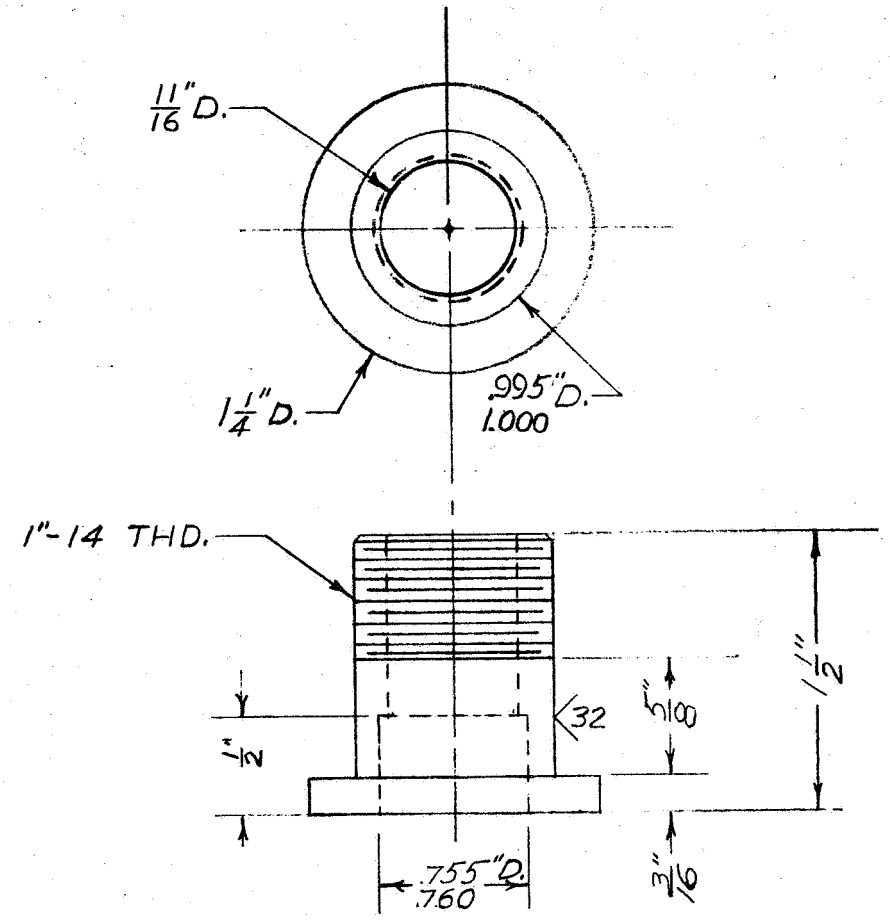

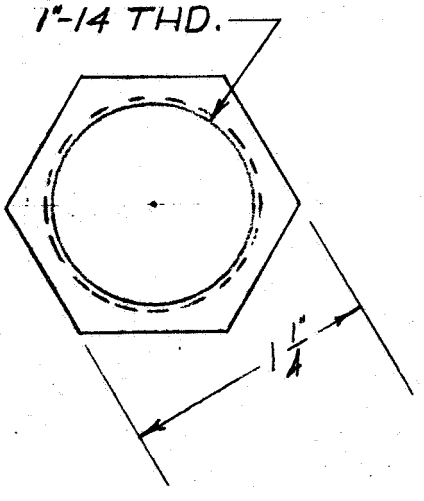

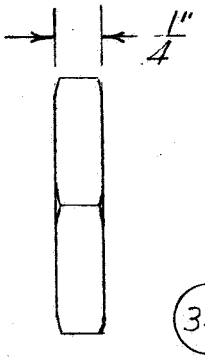

(34B) NUT
MATERIAL: BRASS
PCS. REQ'D: 1

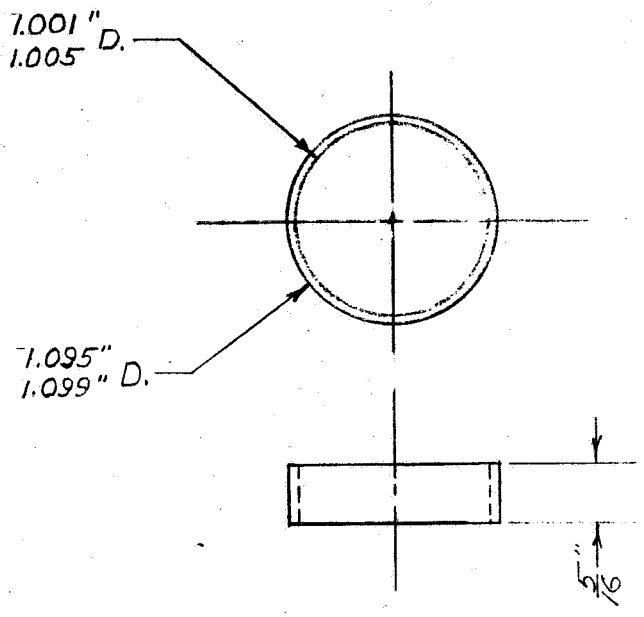

(34C) "O" RING RETAINER
MATERIAL: BRASS
PCS. REQ'D: 2

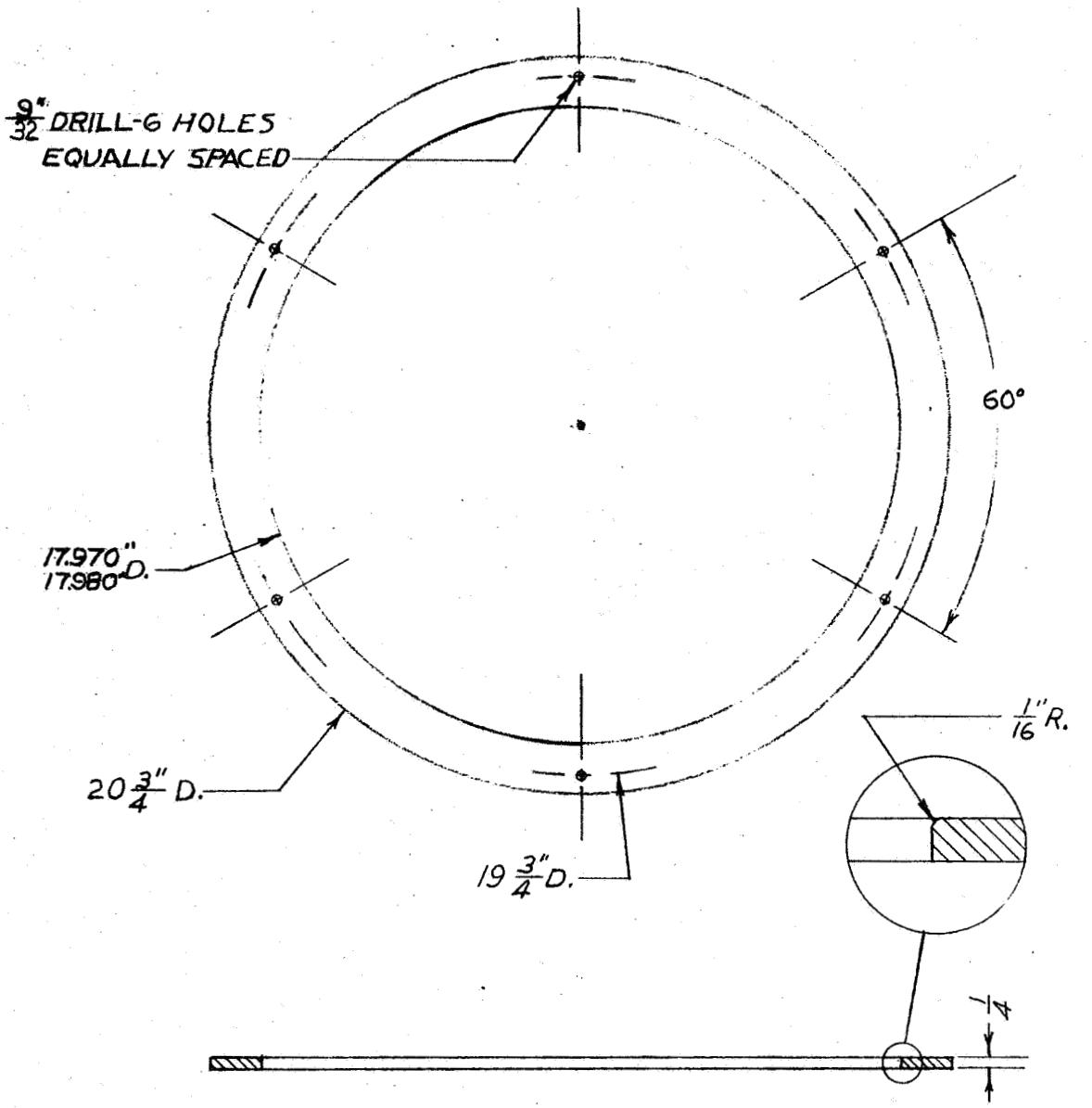

MATERIAL: BRASS
PCS. REQ'D : 1

(35) B.J. CLAMPING RING

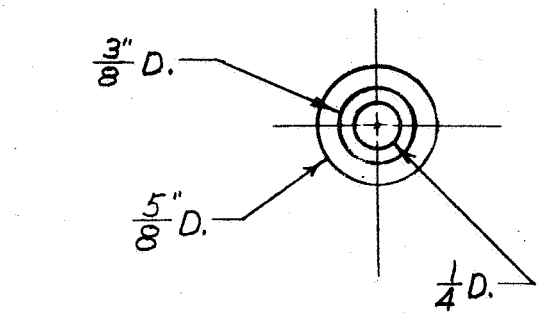

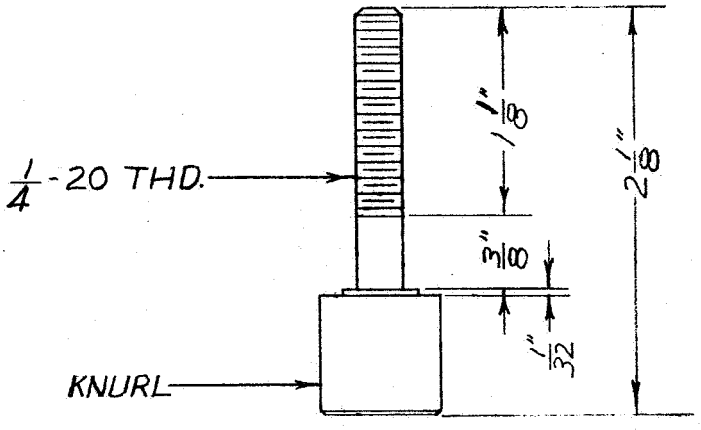

(36) CLAMP RING BOLT
MATERIAL: BRASS
PCS. REQ'D: 6

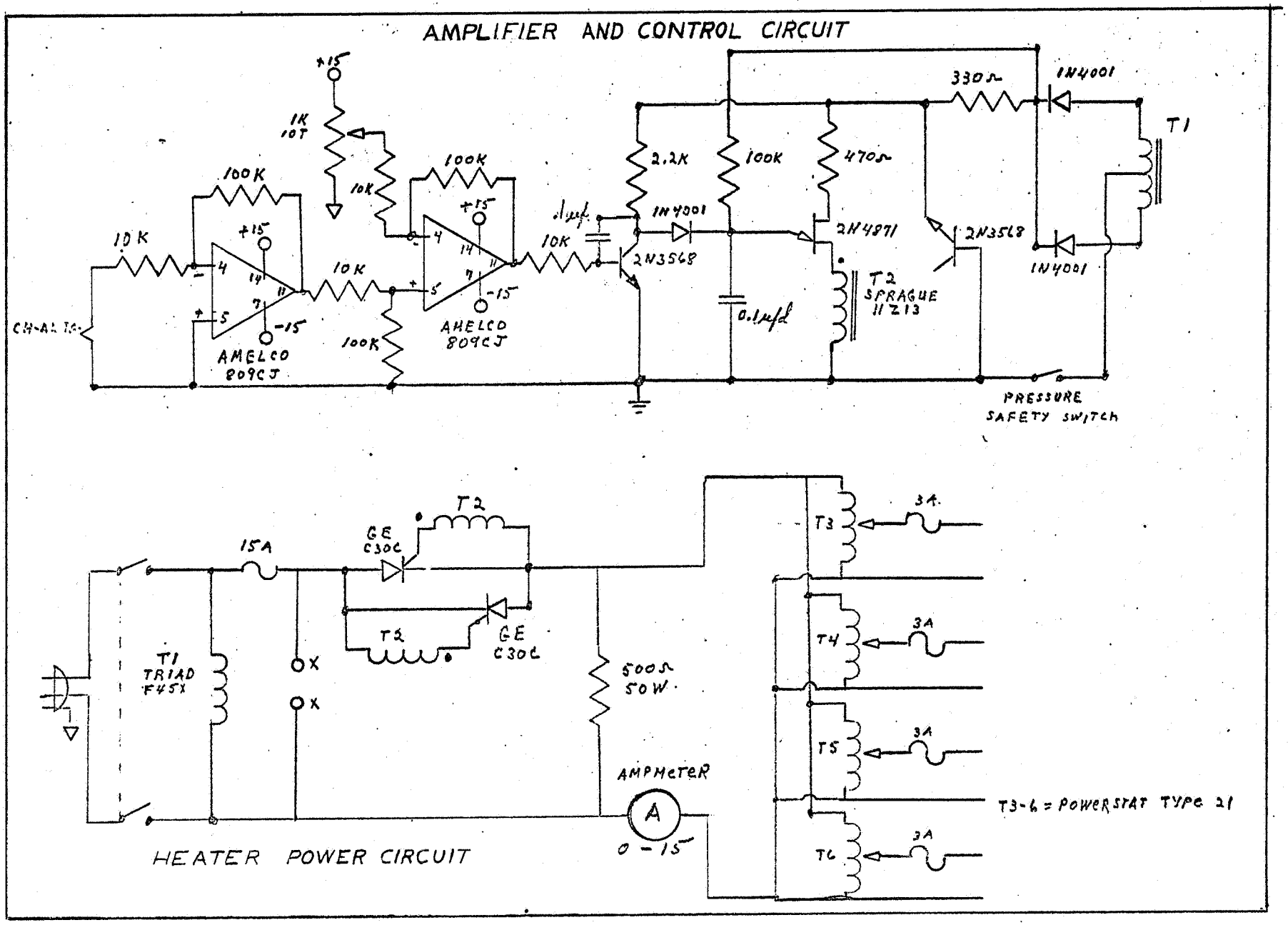
AMPLIFIER AND CONTROL CIRCUIT
+15
1K 10T
10K
100K
100K
10K
+15
4
14
11
7
5
-15
AMELCO 809CJ
10K
100K
10K
+15
4
14
11
7
5
-15
AMELCO 809CJ
.1μf
10K
2N3568
2.2K
100K
470Ω
1N4001
330Ω
1N4001
T1
2N4871
2N3568
1N4001
T2 SPRAGUE 11Z13
0.1μfd
PRESSURE SAFETY SWITCH
T2
GE C30C
15A
T3
3A
T4
3A
T5
3A
T6
3A
T3-6 = POWERSTAT TYPE 21
T1 TRIAD F45X
X
X
T2
GE C30C
500Ω 50W
AMPMETER
A
0 - 15
HEATER POWER CIRCUIT

AMPLIFIER POWER SUPPLY

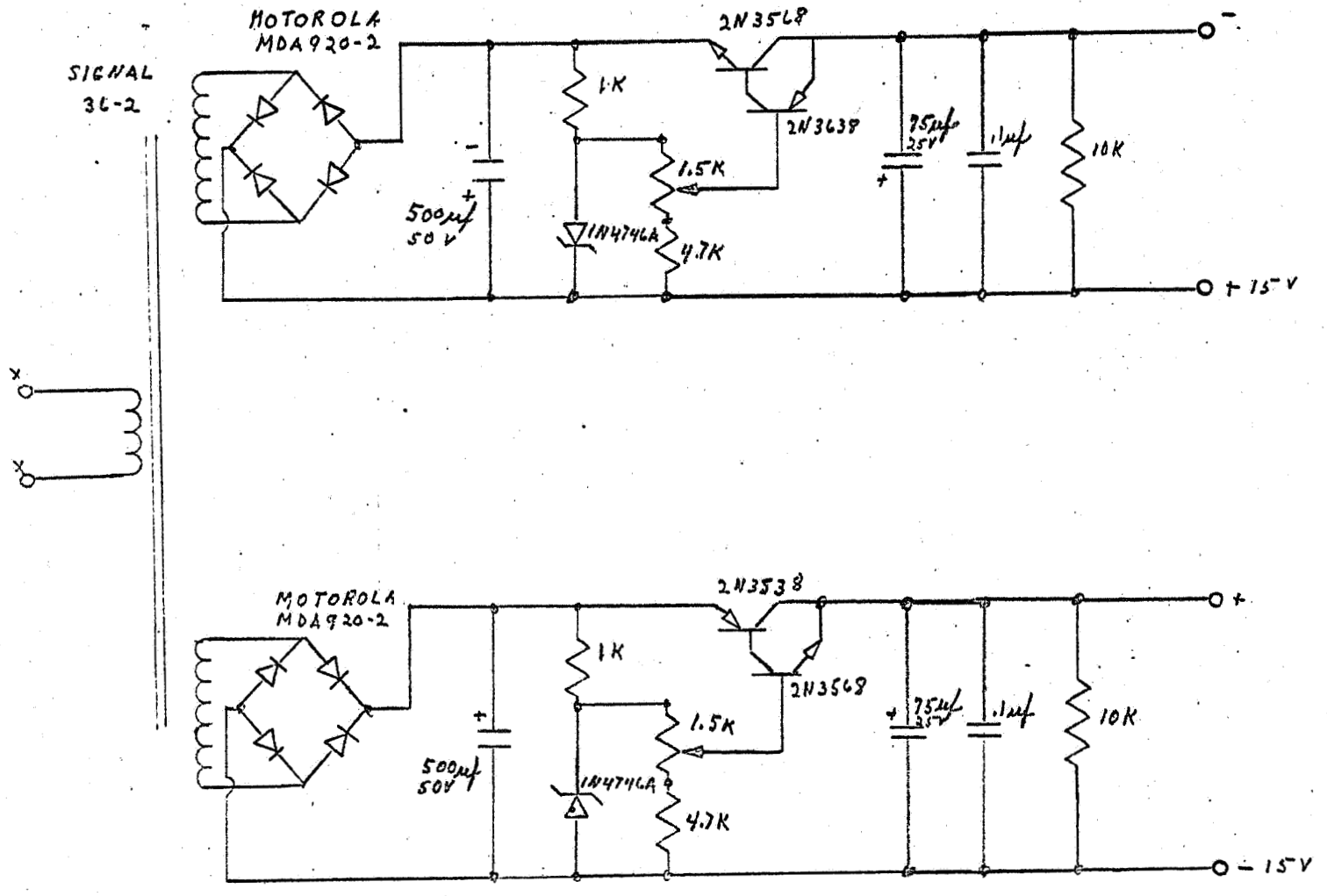

Parts List for Segmented Couple Tester

Drawing No.	Description
1.	Baseplate
2A.	Heatsink rod, right hand
2B.	Heatsink rod, left hand
3.	Heatsink jacket
4.	Heatsink insulator
5.	Heater bracket plate
6.	Heater assembly
7.	Heater bracket
8.	Insulating sleeve
9A.	Teflon washer
9B.	Steel washer
10.	Heatsink nut
11.	Bearing rod
12.	Bearing plate
13.	Bearing nut
14.	$\frac{1}{2}$" O-ring
15.	$\frac{1}{4}$" O. D. copper tubing
16.	Plastinc to copper compression fitting
17.	Polyethylene tubing
19.	$\frac{1}{4}$" Copper elbow
20.	Thermocouple plate spring
21.	Thermocouple spring rod
25.	Thermocouple spring (heater)
26.	Thermocouple cap
27.	Thermocouple insulator plate
28.	Thermocouple insulator
29.	Heater pressure spring

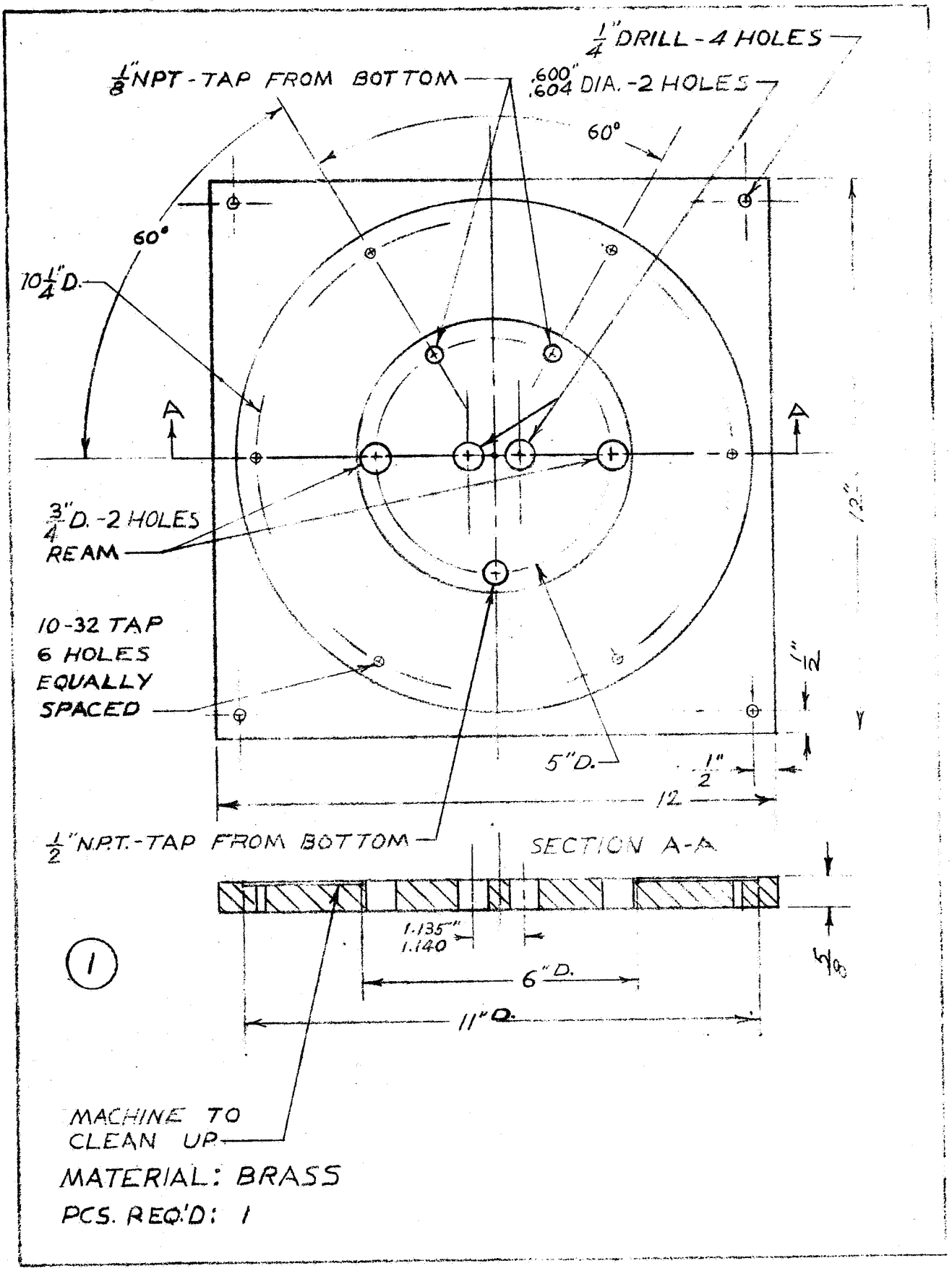
1/4" DRILL - 4 HOLES
1/8" NPT - TAP FROM BOTTOM
.600" .604 DIA. - 2 HOLES
60°
60°
10 1/4" D.
3/4" D. - 2 HOLES REAM
10-32 TAP 6 HOLES EQUALLY SPACED
5" D.
1/2"
12
12"
1" IN
1/2" N.P.T. - TAP FROM BOTTOM
SECTION A-A
1.135" 1.140
6" D.
11" D.
5/8
MACHINE TO CLEAN UP
MATERIAL: BRASS
PCS. REQ'D: 1

APPENDIX 3

(5/26) 525° Isothermal Life Test Data

	Initial Values			1000 Hours		
Element	Top CR	Bottom CR	Element	Top CR	Bottom CR	Element
	μΩ	μΩ	mΩ	μΩ	μΩ	mΩ
6L1P30	85	60	1.755	125	35	2.015
6L3P30	95	60	1.795	145	100	1.935
6L4P30	110	70	1.720	90	75	2.035
6M1P30	95	60	1.795	100	70	2.080
6M2P30	80	55	1.815	90	55	2.015
6M3P30	85	50	1.665	95	80	2.025
6M6P30	90	75	1.735	130	70	1.950
6I1P15	95	75	1.830	200	70	*
6I2P15	75	60	1.870	**	85	*
6I5P30	70	100	1.830	140	**	*
P25-1	--	--	1.690	---	--	1.960
P25-2	--	--	2.050	---	--	1.900

* Element broken - one or more bonds were intact

** Break in element ran into bond; both were intact, but impossible to measure.

(3/9/67) 525° Isothermal Life Test Data

	Initial Values			2000 Hours		
Element	Top CR	Bottom CR	Element	Top CR	Bottom CR	Element
	μΩ	μΩ	mΩ	μΩ	μΩ	mΩ
5C1P19	--	70	1.150	--	---	1.04
5C4P19	50	50	1.400	--	175	1.20
5C5P19	90	70	1.230	--	260	1.41
5C6P19	50	30	1.410	--	1025	2.96*
5K1P19	--	65	1.190	--	---	1.43
5K4P19	105	--	1.390	--	---	1.10
5O7P21	--	100	1.570	--	175	0.93
5X1P24	--	80	1.250	--	450	2.08
5X2P24	--	80	1.250	--	80	2.14
5X3P25	--	75	1.200	--	160	1.23
5X4P24	500	65	1.225	975	---	2.08
5X5P24	--	95	1.060	--	80	1.36
5X6P24	--	75	1.690	--	---	1.04
5X7P24	--	80	1.280	--	---	3.04*

* Element cracked

(2/12/67) 525° Isothermal Life Test Data

	Initial Values			3000 Hours		
Element	Top CR	Bottom CR	Element	Top CR	Bottom CR	Element
	μΩ	μΩ	mΩ	μΩ	μΩ	mΩ
5M6P21	85	60	1.405	1850	320	2.98
5O4P21	215	75	1.570	--	---	2.08
5O1P21	95	60	1.645	**	---	1.98
5O6P21	65	40	1.745	1115	75	2.70
5O2P21	80	25	1.645	--	255	2.08
5O8P21	115	35	1.700	--	190	1.94
5O9P21	40	55	1.755	--	---	1.94
5Q1P21	35	85	1.480	--	120	2.50
5Q9P21	35	--	1.550	80	---	2.28
5D7P19	70	--	1.600	85	---	2.08
5D8P19	30	--	1.630	2700**	---	6.0*
5D4P19	40	--	1.580	60	---	1.53
5C3P19	90	70	1.390	--	80	1.10
4Y13P19	--	80	1.450	--	150	1.53

* Element cracked

** Bond intact, element cracked near junction.